Supporting Information for

Localized Electronic Structure of Nitrogenase FeMoco Revealed by Selenium K-edge High Resolution X-ray Absorption Spectroscopy

Justin T. Henthorn, Renee J. Arias, Sergey Koroidov, Thomas Kroll, Dimosthenis Sokaras, Uwe Bergmann, Douglas C. Rees*, Serena DeBeer*

Contents

Cell Growth: Azotobacter vinelandii

Pre-cultures of *Azotobacter vinelandii* were cultivated in 50 mL of modified Burke's medium containing 10 mM NH_4Cl as a nitrogen source, 20 g/L sucrose, 0.2 mM $FeSO_4 \cdot 7H_2O$, 3 μM $Na_2MoO_4 \cdot 2H_2O$, 1.67 mM $MgSO_4$, 0.9 mM $CaCl_2$, and 10 mM KH_2PO_4/K_2HPO_4 (pH 7.5) at 30º C with shaking at 180 rpm.[1-2] Pre-cultures were grown from frozen glycerol stocks containing 1:1 (v/v) cell stock at an optical density (OD_{600}) between 1.5-2 and 50% glycerol. Main cultures (15 L) were also grown in Burke's medium, except with a depleted source of nitrogen (1.3 mM NH_4Cl) to stimulate nitrogenase expression. The cultures were grown in an Eppendorf BioFlo Bioreactor with a dissolved oxygen (DO) cascade designed to increase agitation to 800 rpm when the dissolved oxygen fell below 80%. Air flow into the media was set to 20 L/hour, and minimum agitation was set to 300 rpm. The temperature was maintained at 30º C via a heat jacket, and excess foam was avoided by injecting 200 uL of sterile anti-foaming agent (polyethylene glycol 1000). Cells were harvested by centrifugation at 8000 rpm and 4º C when the cells reached an OD of 1.5.

Nitrogenase protein activity was assessed via gas chromatography in which 2 mL of whole cells were placed into a sealed 9 mL Wheaton vial. 1 mL of headspace was removed from the vial and replaced with 1 mL of pure acetylene at 1 atm. The vials were allowed to react for 30 min at 30º C with shaking at 180 rpm. Optimal nitrogenase activity was observed at raw peak areas of ethylene of 15- to 25-fold above a water control containing no cells.

Purification of the MoFe- and Fe-proteins

Isolation of the MoFe- and Fe-proteins were performed anaerobically, either on a manifold with argon, or in an anaerobic chamber with 95% argon / 5% hydrogen atmosphere. The purification was modified from Spatzal and Einsle, 2012.[2]

All buffers were degassed using automated argon-vacuum cycles on a custom-made high-vacuum Schlenk line. All liquid lines to the purification system (AKTA) were pre-equilibrated with 5 mM $Na_2S_2O_4$ in degassed purification buffers, and all purification buffers were kept under argon. Cells were homogenized in an anaerobic chamber with 50 mM Tris/HCl (pH 7.5), 150 mM NaCL, and 5 mM $Na_2S_2O_4$. Cells were then lysed using a high-pressure homogenizer (Emulsiflex C5, Avestin), pressurized with argon. The cell lysate was then transferred to centrifuge bottles in the anaerobic chamber, and centrifuged at 14,000 rpm (JA-14 rotor). Supernatant was loaded onto a HiTrap-Q anion exchange column (70 mL, GE-Healthcare), which had been pre-equilibrated with loading buffer (50 mM Tris/HCl, pH 7.5; 150 mM NaCl; 5 mM $Na_2S_2O_4$). A linear NaCl gradient over 300 min was then applied to the column using elution buffer (50 mM Tris/HCl, pH 7.5; 1 M NaCl; 5 mM $Na_2S_2O_4$). MoFe-protein (Av1) eluted at approximately 350 mM NaCl, while Fe-protein (Av2) eluted at approximately 475 mM.

After collection from the anion exchange column, the proteins were each concentrated using an Amicon concentrator pressurized with 5 bar argon in the anaerobic chamber. The MoFe-protein was concentrated to approximately 10 mL with 100,000 kDa MWCO filters (Millipore Ultracell), while the Fe-protein was concentrated to 10 mL with 30,000 MWCO filters. After concentration, each protein was loaded onto a size exclusion column (S200, 26/60, GE Healthcare, 450 mL), which had been pre-equilibrated with size exclusion buffer (50 mM Tris/HCl, pH 7.5; 200 mM NaCl; 5 mM $Na_2S_2O_4$). The pure proteins were then collected and concentrated to less than 2 mL of total volume, for MoFe-protein final concentrations of ~30 mg/mL, and Fe-protein concentrations of ~40 mg/mL. Protein concentrations were determined with UV-vis absorbance at 410 nm, with extinction coefficients of 76 $mM^{-1}cm^{-1}$ for the MoFe-protein and of 9.4 $mM^{-1}cm^{-1}$ for the Fe-protein. Nitrogenase *in vitro* activity was monitored via the acetylene reduction assay (ARA), described in the next section.

Acetylene Reduction Assay

Nitrogenase *in vitro* activity was monitored via the acetylene reduction assay (ARA), in which the reduction of acetylene (HC≡CH) is reduced to ethylene ($H_2C=CH_2$).[3-4] Activity mixtures consist of 20 mM creatine phosphate, 5 mM ATP, 5 mM $MgCl_2$, 25 units/mL phosphocreatine kinase, and 25 mM $Na_2S_2O_4$. The stock solutions for creatine phosphate, ATP, and phosphocreatine kinase were all prepared in 50 mM Tris/HCl (pH 7.5), while the $Na_2S_2O_4$ stock solution was prepared in 500 mM Tris/HCl (pH 7.5). Activity mixtures were dispensed in 1 mL volumes into sealed 9 mL Wheaton vials and degassed via Schlenk line and kept under argon. 1 mL of argon headspace was replaced by 1 mL of acetylene and incubated at 30° C for 4 minutes with shaking at 180 rpm. The reaction was then initiated by addition of the component proteins (MoFe=Av1, Fe=Av2). The optimal component ratio for checking nitrogenase activity was Av2:Av1=2:1, active site ratio 1:1, 0.25 mg Av1 : 0.27 mg Av2. The volumes of the reaction mixtures were kept constant by adding varying amounts of degassed size exclusion buffer (50 mM Tris/HCl, pH 7.5; 200 mM NaCl; 5 mM $Na_2S_2O_4$). Reactions were terminated by addition of 3 M citric acid at varying time points, and ethylene and acetylene were assessed via gas chromatography (activated alumina 60/80 mesh column, flame ionization detector, column temperature at 110° C, detector temperature 150° C, and He carrier) from the headspace of the reaction vials. Peak integration was performed using the Peak Simple software (SRI Instruments), with defined amounts of acetylene in protein-free assay mixtures serving as calibration curves.

Se-Labeling of the FeMo-cofactor of MoFe – Av1Se$_{lo}$ and Av1Se$_{hi}$

Se-incorporated Av1-FeMo-co (Av1-Se) was prepared with slight modifications to methods previously described.[5-6] The activity mixtures are identical to the proton reduction assay mixtures, with added KSeCN in varying concentrations. The KSeCN stock solution was prepared in size exclusion buffer (50 mM Tris/HCl, pH 7.5; 200 mM NaCl; 5 mM $Na_2S_2O_4$). Labeling was assessed by running parallel acetylene reduction assays with the same KSeCN, and observing inhibition of the acetylene reduction to ethylene as evidence of Se-labeling. To generate Av1Se$_{hi}$, 10 mM KSeCN was added to assay solutions, while to generate Av1Se$_{lo}$ 250 μM KSeCN was added to assay solution.

Av1Se$_{hi}$ and Av1Se$_{lo}$ were then isolated from the activity components in the anaerobic chamber by ultrafiltration using a 100 kDa MWCO filter. The mixture was kept on ice to slow any further reactions in the assay mixture, and was washed 2-5 times in cold size exclusion buffer (50 mM Tris/HCl, pH 7.5; 200 mM NaCl; 5 mM $Na_2S_2O_4$). After washing the samples, the protein was loaded onto a size exclusion column (S200, 26/60, GE Healthcare, 450 mL) that had been pre-equilibrated with degassed size exclusion buffer. The protein was then collected and concentrated adjusted to either 20 mg/mL or 200 mg/mL for various experiments. The final protein concentrations were adjusted to 30 mg/mL for crystallography.

CO-Inhibition of the Se-Labeled FeMo-cofactor – Av1SeCO

CO-inhibition of Av1-Se was achieved with methods previously described with some adjustments.[5-7]The assay mixtures were as described in the previous section, with the headspace of the reaction vials replaced with CO. For these reactions, time points were not a factor, so the reaction volumes were scaled up in three-neck round bottom flasks. For crystallography, the reactions were scaled up to be 12 mL total, and for HERFD, the reactions were scaled up to 380 mL. The three-neck flasks were degassed via Schlenk line technique while constantly stirring.

First, Av1-Se was tested for activity using the procedure for the acetylene reduction assay. Protein concentrations were either Av2:Av1=2:1, or to conserve Av2 and slow the reaction, Av2:Av1=1:1. Then the headspaces of the three-neck flasks were replaced by CO, and the assay

mixtures were allowed to react at room temperature with stirring for 20 minutes. The mixtures were then were concentrated by ultrafiltration with 100,000 kDa MWCO filters and washed 3-5 times with cold size exclusion buffer (50 mM Tris/HCl, pH 7.5; 200 mM NaCl; 5 mM $Na_2S_2O_4$) in the anaerobic chamber. CO was regularly bubbled through the solution until flash-frozen for future use. After washing the samples, the protein was loaded onto a size exclusion column (S200, 26/60, GE Healthcare, 450 mL) which had been pre-equilibrated with degassed size exclusion buffer bubbled through with CO. Av1SeCO was constantly bubbled through with CO during the washing steps. For crystallography, Av1SeCO concentration was adjusted to 30 mg/mL. For HERFD, Av1SeCO concentration was adjusted to 200 mg/mL.

Reactivation of Se-labeled, CO-inhibited FeMo-cofactor – $Av1Se_{reac}$

For $Av1Se_{reac}$, the protein was labeled as usual with Se, inhibited with CO as described, above and then reactivated from CO. Reactivation from CO consisted of bubbling a fresh reaction mixture containing all activity components with Ar to replace excess CO. Importantly, a fresh reaction mixture consists of 20 mM creatine phosphate, 5 mM ATP, 5 mM $MgCl_2$, 25 units/mL phosphocreatine kinase, and 25 mM $Na_2S_2O_4$, and newly added Av2 at a ratio of Av2:Av1=1:1. Reactivation was assessed in a parallel assay vials for acetylene reduction activity.Then this reactivated $Av1Se_{reac}$ was concentrated via ultrafiltration as described, and then applied to a cold sizing column. The protein was then collected and the concentration was adjusted to approximately 20 mg/mL. Reactivation from CO of native FeMoco (no Se labeling) has previously been reported,[7] with the reincorporation of S at the 2B position confirmed crystallographically. Additionally, reactivated MoFe was found to exhibit similar N_2 reduction activity as native protein.

Crystallization of MoFe

All Av1-Se samples were crystallized using the sitting drop vapor diffusion method at 21° C in an anaerobic chamber (5% H_2 / 95% Ar), with protein concentration at 30 mg/mL. The reservoir solution consisted of: 24-28% PEG 6000 (v/v), 750-850 mM NaCl, 100 mM imidazole/malic acid (pH 8.0), and 5 mM $Na_2S_2O_4$.[5, 7-8] For CO-inhibited samples, the reservoir solutions were bubbled through with CO before setting the drops. After the drops were set, clear Duck tape was used to seal the reservoirs. The tape was then punctured with a syringe and the wells were quickly filled with an additional 2 mL of CO, and resealed with a second layer of clear Duck tape. A seeding strategy using crushed Av1 crystals was employed to accelerate crystallization and to generate higher quality crystals. Cryo-protection of the crystals before freezing in liquid nitrogen consisted of dipping the crystals into a 5 uL drop of reservoir solution containing 8-12% MPD (v/v).

Preparation of protein samples for XAS

Protein samples used for XAS data collection were concentrated to a final volume of 100 – 150 uL in an anaerobic chamber. The highly concentrated samples (200 mg/mL) required slow dispensation into XAS cuvettes, since capillary action with the highly concentrated sample made it difficult to add to the sample cell all at once. 10 uL of the highly concentrated sample were added to the cuvette at a time, and the sample cell was then centrifuged for 60 seconds at 1000 rpm. This process was repeated until the entire sample had been dispensed into the cuvette. Protein samples were then frozen inside the anaerobic chamber with liquid nitrogen, and kept frozen during every subsequent manipulation and sample measurement. The sample cells used were machined 5 x 5 x 20 mm Delrin cuvettes with a sample measurement window of 38um Kapton tape and a sample volume of approximately 120 uL.

Preparation of non-protein samples for XAS

Seleno-L-cystine was purchased from Sigma Aldrich and used as received. A room temperature saturated solution of seleno-L-cystine in water was prepared by adding 5 mg of the solid to a vial containing 1mL of deionized water. After vigorous agitation for 5 minutes, the mixture was passed through a glass microfiber filter pad to remove undissolved seleno-L-cystine. The filtrate was then added to an XAS solution cell (described above) and frozen in liquid nitrogen.

$[Et_4N]_2[Fe_2Se_2(SPh)_4]$ was prepared according to the published procedure.[9] The crystalline solid was diluted in boron nitride (Sigma Aldrich) to a calculated absorbance of approximately 1. The sample was finely ground together with boron nitride in a nitrogen atmosphere glovebox and pressed into an aluminum sample holder of 1mm path length, which was then sealed with 38um Kapton tape.

Preparation of protein samples for EPR – Av1, Av1Se$_{EPR}$, and Av1SeCO$_{EPR}$

400 uL of Av1 at 100 μM was used in preparation for EPR. 100 uL of Av1 at 100 μM concentration was put aside for EPR measurements.

Se-incorporation was performed on 300 uL of 100 μM Av1 by supplying active enzyme with 10 mM KSeCN. Active enzyme was achieved by anaerobic assay mixtures containing 20 mM creatine phosphate, 5 mM ATP, 5 mM $MgCl_2$, 25 units/mL phosphocreatine kinase, and 25 mM $Na_2S_2O_4$. The stock solutions for creatine phosphate, ATP, and phosphocreatine kinase were all prepared in 50 mM Tris/HCl (pH 7.5), while the $Na_2S_2O_4$ stock solution was prepared in 500 mM Tris/HCl (pH 7.5). Active site rations of Av1:Av2 were 1:1, using concentrations of 0.25 mg/mL Av1 and 0.27 mg/mL Av2. Se-incorporation was monitored by gas chromatography on parallel test assays with acetylene added, following the inhibition of acetylene activity by KSeCN. The activity assay mixture was then concentrated and washed with sizing buffer (50 mM Tris-HCl, pH 7.5) 3-5 times in the anaerobic chamber back to 300 uL. Av1Se$_{EPR}$ was then checked for activity again with new assay mixtures, with the acetylene reduction activity at about 80% of the wild-type activity. The protein was then concentrated back down to 300 uL of 100 μM Av1, washing the mixtures 3-5 times with sizing buffer. 100 uL of Av1Se$_{EPR}$ was put aside for EPR, while 200 uL were used for CO inhibition.

Av1Se was inhibited with CO using assay mixtures which had been prepared with 1 atm of CO. CO-inhibition was monitored by parallel acetylene reduction assays. The resulting assay mixture was then concentrated down to 200 uL of 100 μM Av1 with constant bubbling CO through the solution. 100 uL of 100 μM Av1SeCO$_{EPR}$ was then put aside for EPR.

Quantification of Se-occupancy from Anomalous Data

Se-occupancies within all Av1-Se crystals were calculated using a modified script from reference.[6] Diffraction data were collected at 7110 eV (1.743 Å) and 12662 eV (0.979 Å) at the Stanford Synchrotron Radiation Lightsource (SSRL) beamline 12-2 equipped with a Dectris Pilatus 6M detector. At 12662 eV, an energy experimentally determined by MAD scans to be above the Se K-edge, Fe atoms in the MoFe-protein were assumed to be absorbing at 100%. These atoms were then used as internal standards to estimate Se-occupancy using the relationship:

$$f = f_0 + \Delta f' + i\Delta f''$$

At 12662 eV, the atoms of interest were determined to have experimental scattering factors $f_{Fe}'' = 1.5$, $f_{Se}'' = 4.42$, and $f_S'' = 0.24$. The scattering factor f_{Se}'' at 12662 eV was found to vary by approximately 20% over the protein samples, and therefore the average value was used for all samples. This experimentally observed variation in the scattering factor is attributed to chemical effects at the Se absorption edge. While it is anticipated to affect the absolute Se occupancies, the observed variation in f_{Se}'' should have a negligible effect on the relative Se ratios. The data were indexed, integrated, and scaled using XDS and Aimless.[10-12]Molecular replacement was used to obtain phase information, with the 1.0 Å Av1 structure (PDB: 3U7Q) used as a model.[8] Structure refinement and modeling was performed using the CCP4-embedded programs REFMAC5 and Coot.[12-14]

Se-anomalous density maps were calculated based on the data collected at 12662 eV, while the S-anomalous maps were calculated based on the data collected at 7110 eV. Refmac-refined electron density data files (mtz files) were merged with anomalous mtz files using the CCP4-embedded program CAD. Maps were generated using fast-Fourier transform (FFT) of the merged mtz files and the Refmac-refined pdb coordinates. The CCP4 program Mapmask was used to orient the model based on the data resolution limits. Finally, the program Mapman performs map normalization and extracts the density values on an arbitrary scale at all atomic positions within a set sphere.[15] The structures were then rendered for publication in PYMOL (Figure S1).

Samples Av1Se$_{lo}$ and Av1Se$_{hi}$ were found to exhibit similar Se occupancies at each of the three bridging sites- 2B, 3A, and 5A- with roughly a 3:1 Se2B:Se3A/5A ratio (Table S1). Av1Se$_{reac}$ exhibits a smaller Se2B:3A/5A ratio of nearly 1:1, predominantly due to decreased Se occupancy at the 2B position, while Av1SeCO exhibits a ratio of nearly 1:9 Se2B:Se3A/5A. An important observation from the preparation of Av1Se$_{reac}$ is that the highest Se occupancy occurs at the 2B site. Consequently, a rearrangement occurs during reactivation of CO inhibited FeMoco such that species at the 3A/5A belt positions can migrate to the 2B position. This observation complements the finding that the 2B site migrates to the 3A/5A positions during reaction with CO, as described in the original characterization of the reactivities of Se and CO to the FeMoco.[6]

Table S1. Se quantitation via anomalous dispersion and ICP-MS experiments

	Anomalous Dispersion						ICP-MS
Sample	**2B (%)**	**3A (%)**	**5A (%)**	**χ_{Se2B}**	**$\chi_{Se3A/5A}$**	**Se:FeMoco**	**Se:FeMoco**
Av1Se$_{lo}$	103	16	20	0.74	0.26	1.39 ± 0.09	1.09 ± 0.13
Av1Se$_{hi}$	96	16	18	0.74	0.26	1.30 ± 0.09	1.37 ± 0.09
Av1Se$_{reac}$	45	18	23	0.52	0.48	0.86 ± 0.09	0.90 ± 0.22
Av1SeCO	11	40	39	0.12	0.88	0.90 ± 0.09	*0.66 ± 0.15
Av1$_{wt}$	-	-	-	-	-	-	0.09 ± 0.12

*ICP-MS results from sample Av1SeCO revealed anomalously low Se concentrations relative to both Mo and Fe, similar to the separately prepared wild-type MoFe sample, Av1$_{wt}$. The ICP-MS Se:FeMoco ratio presented in Table S1 for Av1SeCO corresponds to the Se-incorporated, CO-inhibited sample used to prepare Av1Se$_{reac}$.

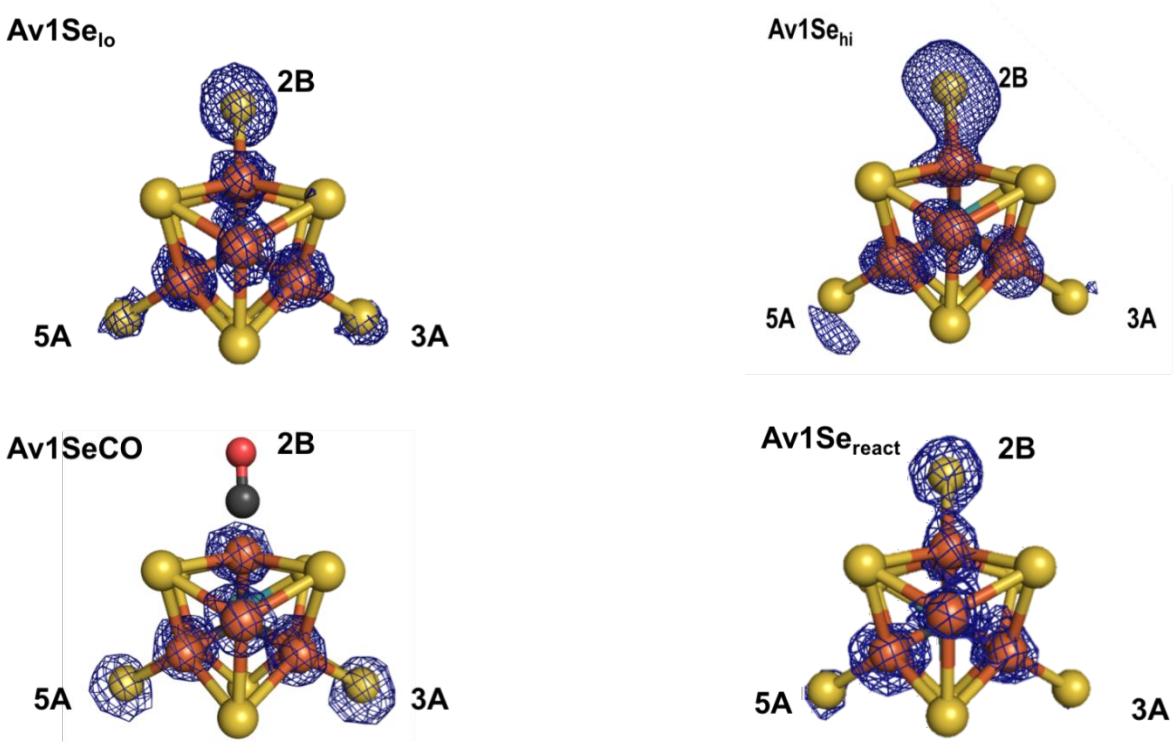

Figure S1. Anomalous Fourier difference plots calculated at 12662 eV (blue) contoured at 5.0 σ for Av1Se$_{lo}$ (top left), Av1Se$_{hi}$ (top right), Av1SeCO (bottom left), and Av1Se$_{reac}$ (bottom right). See Tables S2-S5 for individual refinement statistics.

Table S2. Diffraction data collection and processing statistics for Av1SeCO.

Av1SeCO	
Data collection statistics	**High resolution**
Wavelength (Å)	0.979
Resolution range (Å)	36.93-1.70 (1.73-1.70)
Unique reflections	213040 (10556)
Completeness (%)	98.6 (98.8)
Anomalous completeness (%)	98.3 (98.6)
Multiplicity	6.9 (6.9)
Anomalous multiplicity	3.5 (3.5)
Space group	$P2_1$
Unit cell parameters	
a, b, c	77.19, 128.00, 107.63
α, β, γ	90.00, 109.15, 90.00
R_{merge}	0.109 (0.529)
$R_{p.i.m.}$	0.067 (0.333)

I/σ(I)	11.0 (3.3)
Data processing statistics	
R_{work} / R_{free}	0.176 / 0.199
r.m.s.d. bond lengths (Å)	0.022
r.m.s.d. bond angles (°)	2.092
Average B-factor (Å^2)	15.368

Table S3. Diffraction data collection and processing statistics for Av1Se$_{lo}$.

Av1Se$_{lo}$	
Data collection statistics	**High resolution**
Wavelength (Å)	0.979
Resolution range (Å)	37.85-1.60 (1.63-1.60)
Unique reflections	269898 (13363)
Completeness (%)	98.7 (98.9)
Anomalous completeness (%)	93.9 (95.2)
Multiplicity	3.4 (3.3)
Anomalous multiplicity	1.6 (1.6)
Space group	$P2_1$
Unit cell parameters	
a, b, c	80.87, 131.02, 106.96
α, β, γ	90.00, 110.62, 90.00
R_{merge}	0.057 (0.202)
$R_{p.i.m.}$	0.044 (0.149)
I/σ(I)	14.4 (5.3)
Data processing statistics	
R_{work} / R_{free}	0.152 / 0.172
r.m.s.d. bond lengths (Å)	0.027
r.m.s.d. bond angles (°)	1.616
Average B-factor (Å^2)	13.455

Table S4. Diffraction data collection and processing statistics for Av1Se$_{hi}$.

$Av1Se_{hi}$	
Data collection statistics	**High resolution**
Wavelength (Å)	0.979
Resolution range (Å)	37.81-1.90 (1.93-1.90)
Unique reflections	160550 (7979)
Completeness (%)	98.7 (99.1)
Anomalous completeness (%)	84.8 (79.8)
Multiplicity	3.5 (3.5)
Anomalous multiplicity	1.5 (1.8)
Space group	$P2_1$
Unit cell parameters	
a, b, c	80.76, 130.38, 106.90
α, β, γ	90.00, 110.54, 90.00
R_{merge}	0.110 (0.261)
$R_{p.i.m.}$	0.105 (0.244)
I/σ(I)	6.0 (3.4)
Data processing statistics	
R_{work} / R_{free}	0.188 / 0.229
r.m.s.d. bond lengths (Å)	0.020
r.m.s.d. bond angles (°)	1.980
Average B-factor (Å^2)	15.214

Table S5. Diffraction data collection and processing statistics for $Av1Se_{reac}$.

$Av1Se_{react}$	
Data collection statistics	**High resolution**
Wavelength (Å)	0.979
Resolution range (Å)	39.41-2.30 (2.34-2.30)
Unique reflections	85985 (4564)
Completeness (%)	98.1 (98.5)
Anomalous completeness (%)	98.0 (98.5)
Multiplicity	7.0 (7.0)
Anomalous multiplicity	3.6 (3.5)
Space group	$P2_1$
Unit cell parameters	

a, b, c	76.98, 129.33, 106.75
α, β, γ	90.00, 108.84, 90.00
R_{merge}	0.104 (0.401)
$R_{p.i.m.}$	0.064 (0.250)
I/σ(I)	12.8 (4.1)
Data processing statistics	
R_{work} / R_{free}	0.202 / 0.245
r.m.s.d. bond lengths (Å)	0.020
r.m.s.d. bond angles (°)	1.935
Average B-factor (Å^2)	24.515

Se Quantitation via Inductively-Coupled Plasma Mass Spectrometric (ICP-MS) Studies

Excess sample for HERFD experiments as well as protein crystals were used for ICP-MS. Both sets of samples were not subjected to X-ray radiation. The solution samples were directly dissolved in 3 mL of 2% nitric acid (HNO_3), while the crystal samples were resuspended in 50 uL of ddH_2O before being mixed with 3 mL of 2% HNO_3. All samples were analyzed using a quadrupole-based inductively coupled plasma-mass spectrometer (Agilent 8800 ICP-QQQ) at the Environmental Analysis Center at Caltech. Samples were analyzed in helium mode to avoid any argon-argon dimers that may form in the plasma. Standards were generated by comparing ion counts from prepared selenium, molybdenum, and iron standards, all prepared in 2% HNO_3.

Absolute Se concentrations were taken relative to absolute Mo and Fe concentrations (assuming 1 Mo and 15 Fe per FeMoco/P cluster pair), and the average of the two measures is reported as Se:FeMoco in Table S1. For comparison, a separately prepared wild-type MoFe sample ($Av1_{wt}$) was also quantified by ICP-MS and revealed 0.09 equivalents of Se per FeMoco. This value is interpreted as the minimum error for the ICP-MS experiments.

EPR Spectra of Se-substituted FeMoco samples

EPR spectra were recorded at the Caltech Electron Paramagnetic Resonance (EPR) Facility with a Bruker EMX X-band CW-EPR spectrometer using an Oxford ESR 900 liquid helium/nitrogen flow-through cryostat. The temperature was 10K, microwave power 2 mW, and microwave frequency 9.46GHz. The Se-substituted FeMoco sample $Av1Se_{EPR}$ (Figure S2, red) reveals a broadened $S = 3/2$ signal centered around 1800 Gauss, qualitatively similar to the $S = 3/2$ native FeMoco signal (Figure S2, blue). The $S = 1/2$ signal in $Av1Se_{EPR}$ centered near 3400 Gauss corresponds to the reduced F-cluster (the sample was not purified via size-exclusion chromatography). The CO-inhibited, Se-substituted sample $Av1SeCO_{EPR}$ (Figure S2, green) reveals the near-complete loss of the $S = 3/2$ signal and generation of a new $S = 1/2$ signal consistent with the lo-CO species previously reported in the literature.[16]

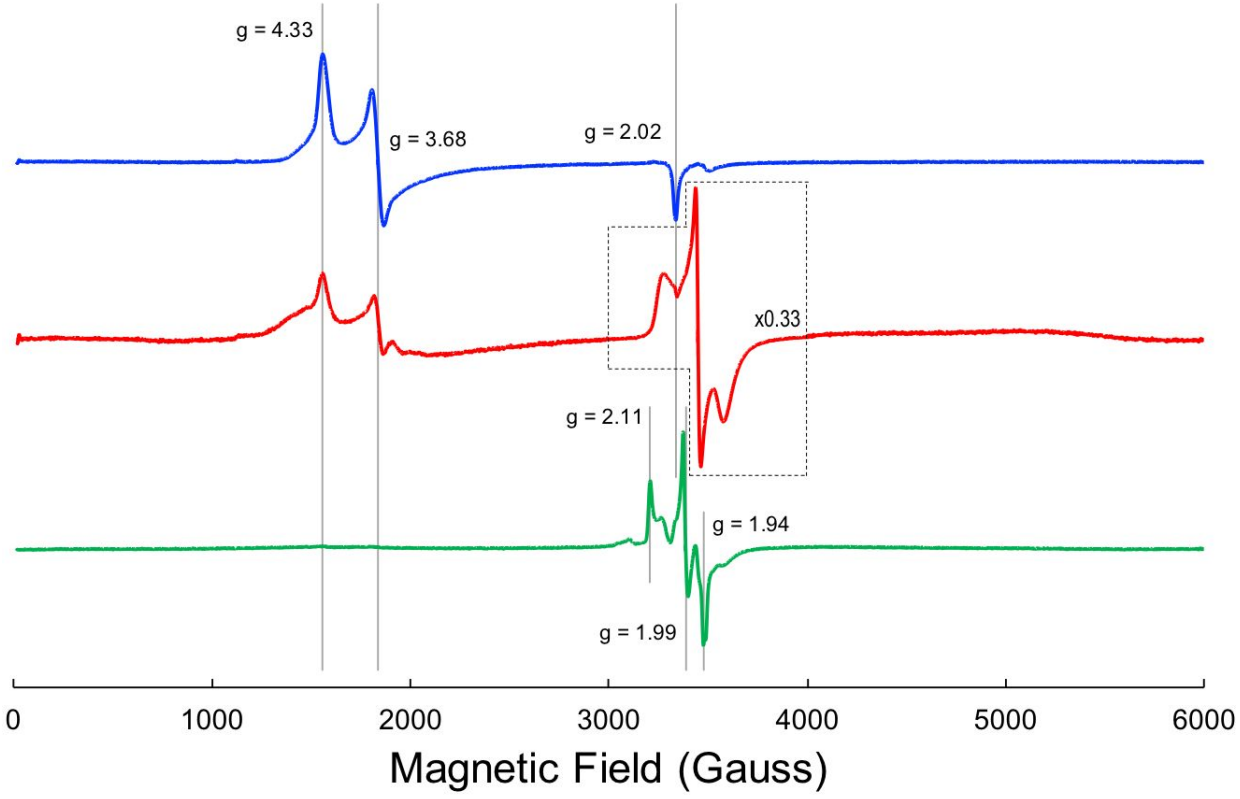

Figure S2. Continuous wave X-band EPR of native Av1 (blue), $Av1Se_{EPR}$ (red) and $Av1SeCO_{EPR}$ (green). Principal g-values for $S = 3/2$ of native Av1 and $S = 1/2$ of $Av1SeCO_{EPR}$ are emphasized with gray vertical lines. $Av1Se_{EPR}$ data between 3000 and 4000 gauss scaled to 33% for clarity.

Correlations of Pre-edge Area and δ_d with Average Formal Fe Oxidation State

Figure S3 reveals linear correlations of pre-edge area and δ_d with the average formal Fe oxidation state in a synthetic model complex series supported by chelating dianionic bis(benzimidazolato) ligands (S XAS spectra and fits, Figure S4). This series is unique in that it is the only well characterized Fe_2S_2 series spanning all three oxidation state levels (diferric, mixed-valent, and diferrous). Similar trends have been observed in other complexes for both terminal and bridging ligands at the S and Cl K-edges, as shown in Figure S5-S7. In these cases, the monomeric species exist only in two oxidation states, (Fe^{II} and Fe^{III}), while dimeric species are only stable in one oxidation state ($Fe^{III}Fe^{III}$). The experimental data (solid squares for the monomers, solid circles for the dimers) has been complemented by theoretical values determined for the hypothetical [$Fe^{II}Fe^{III}$] and [$Fe^{II}Fe^{II}$] species (open circles). The experimental data exhibits the general trend that pre-edge intensity increases and $|\delta_d|$ increases as the average formal oxidation state of Fe increases, while the dimeric complexes (including the theoretical values) reproduces the linear correlations observed in Figure S3.

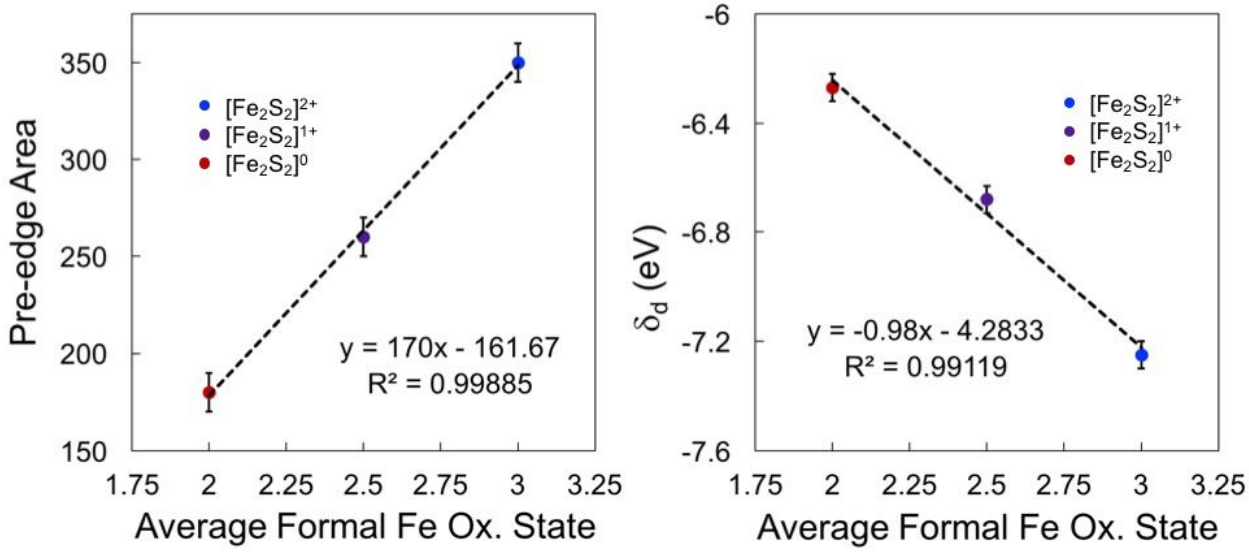

Figure S3. Linear correlations between pre-edge areas and average formal Fe oxidation states (left) and δ_d and average formal Fe oxidation states (right) of synthetic model complexes $[Fe_2S_2]^{2+}$ (blue), $[Fe_2S_2]^{1+}$ (purple), $[Fe_2S_2]^{0}$ (red) supported by chelating dianionic bis(benzimidazolato) ligands. Corresponding XAS spectra presented in Figure S4. Data from reference [17].

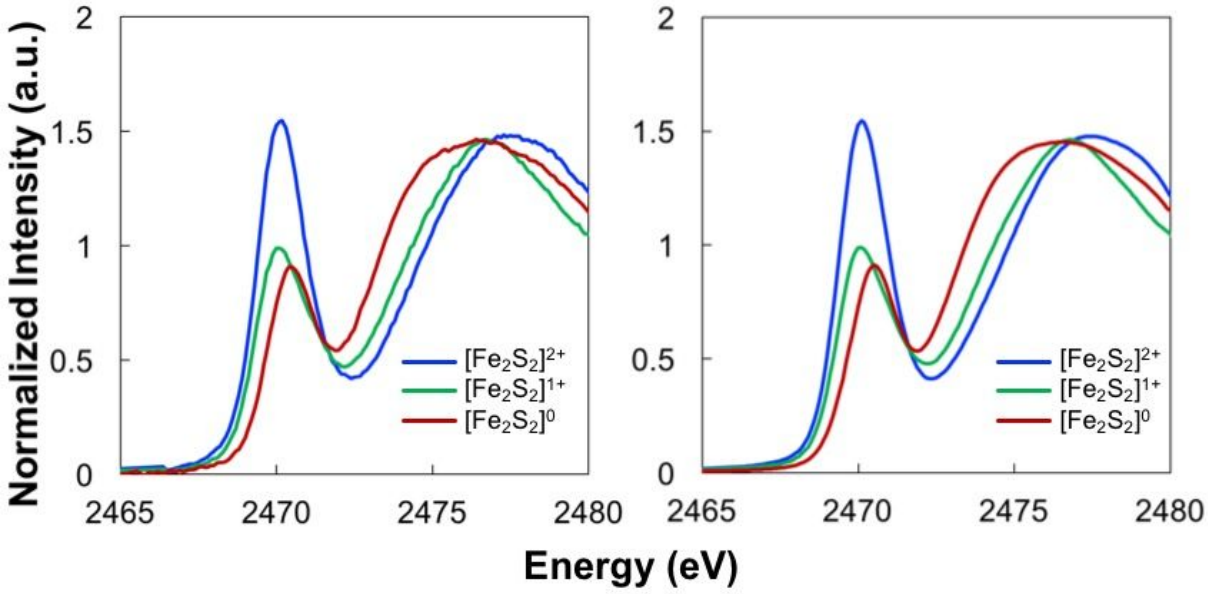

Figure S4. Experimental S K-edge spectra of synthetic model complexes $[Fe_2S_2]^{2+}$ (blue), $[Fe_2S_2]^{+}$ (green), and $[Fe_2S_2]^{0}$ (red) supported by chelating dianionic bis(benzimidazolato) ligands (left), and corresponding Gaussian fits (right). Adapted from reference 17 with permission from the American Chemical Society (2016).

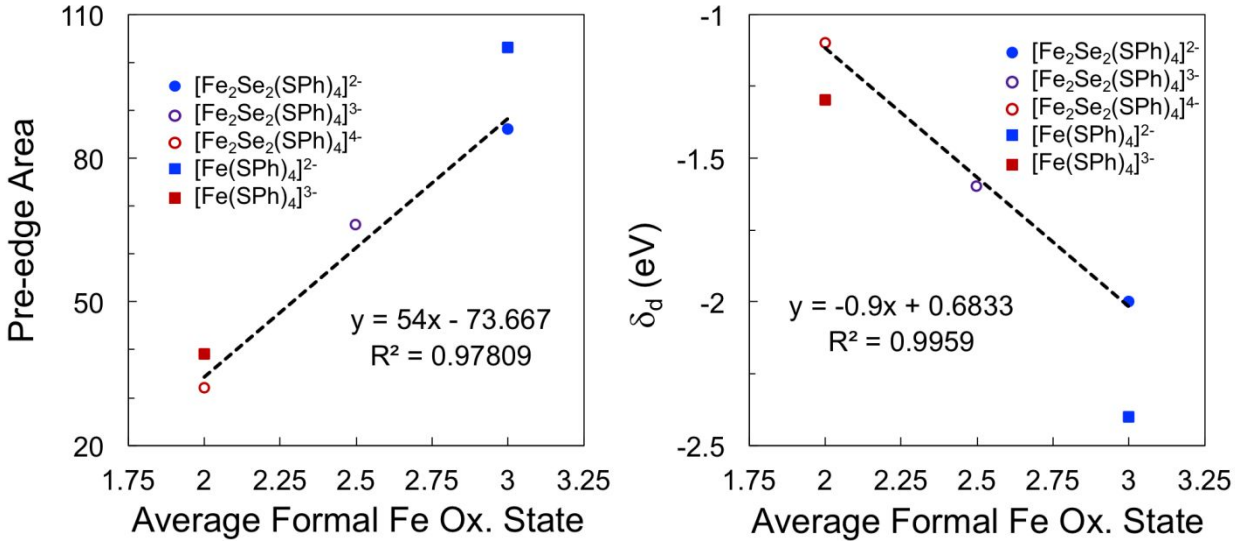

Figure S5. Plots of S K-edge XAS pre-edge areas vs. average formal Fe oxidation states (left) and δ_d vs. average formal Fe oxidation states (right) of synthetic model complexes $[Fe_2Se_2(SPh)_4]^{2-}$ (solid blue circle), $[Fe(SPh)_4]^{2-}$ (solid blue square), and $[Fe(SPh)_4]^{3-}$ (solid red square). Theoretical values are also included for $[Fe_2Se_2(SPh)_4]^{3-}$ (open purple circle) and $[Fe_2Se_2(SPh)_4]^{4-}$ (open red circle). Linear fit for circle data points only (one experimental and two theoretical values). Experimental and theoretical values from reference [18].

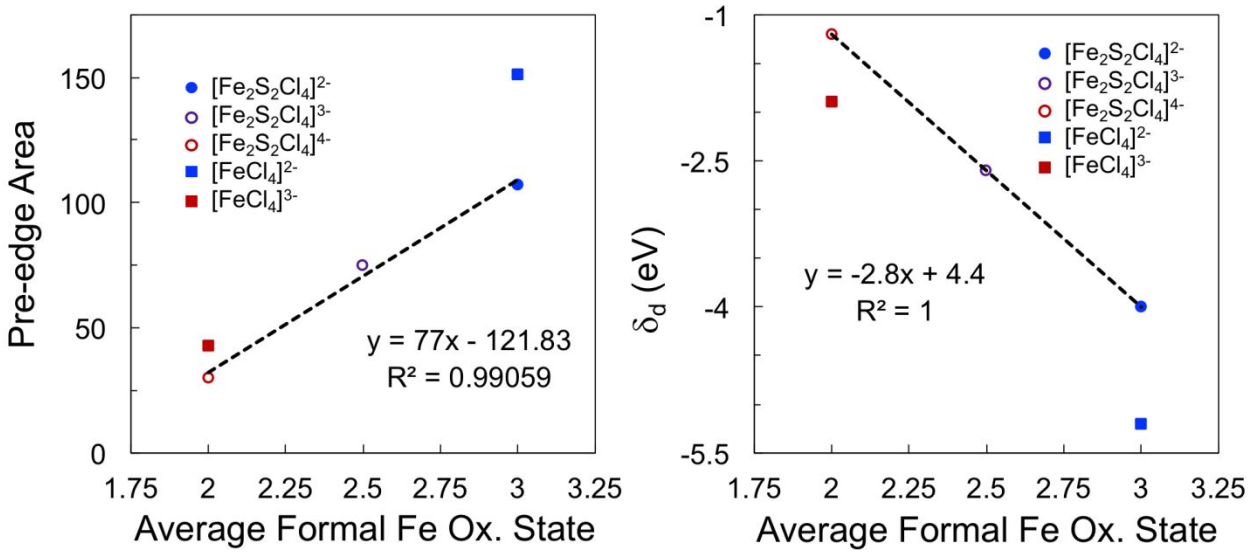

Figure S6. Plots of Cl K-edge XAS pre-edge areas vs. average formal Fe oxidation states (left) and δ_d vs. average formal Fe oxidation states (right) of synthetic model complexes $[Fe_2S_2Cl_4]^{2-}$ (solid blue circle), $[FeCl_4]^{2-}$ (solid blue square), and $[FeCl_4]^{3-}$ (solid red square). Theoretical values are also included for $[Fe_2S_2Cl_4]^{3-}$ (open purple circle) and $[Fe_2S_2Cl_4]^{4-}$ (open red circle). Linear fit for circle data points only (one experimental and two theoretical values). Experimental and theoretical values from reference [18].

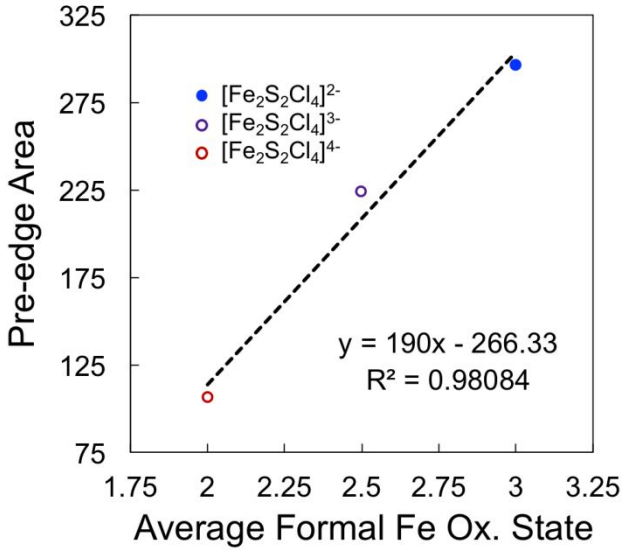

Figure S7. Plot of S K-edge XAS pre-edge areas vs. average formal Fe oxidation states of synthetic model complex $[Fe_2S_2Cl_4]^{2-}$ (solid blue circle) and theoretical values for $[Fe_2S_2Cl_4]^{3-}$ (open purple circle) and $[Fe_2S_2Cl_4]^{4-}$ (open red circle). Experimental and theoretical values from reference [18].

Fits of Experimental Se HERFD XAS and S XAS Spectra

The experimental data is shown in black. Individual edge Gaussians are shown as thin red lines and their sum is given as a thick red line. Individual pre-edge pseudo-Voigt functions are shown as thin dark blue lines and their sum is given as a thick dark blue line. The difference between the fit and the experimental data is shown as a thin light blue line.

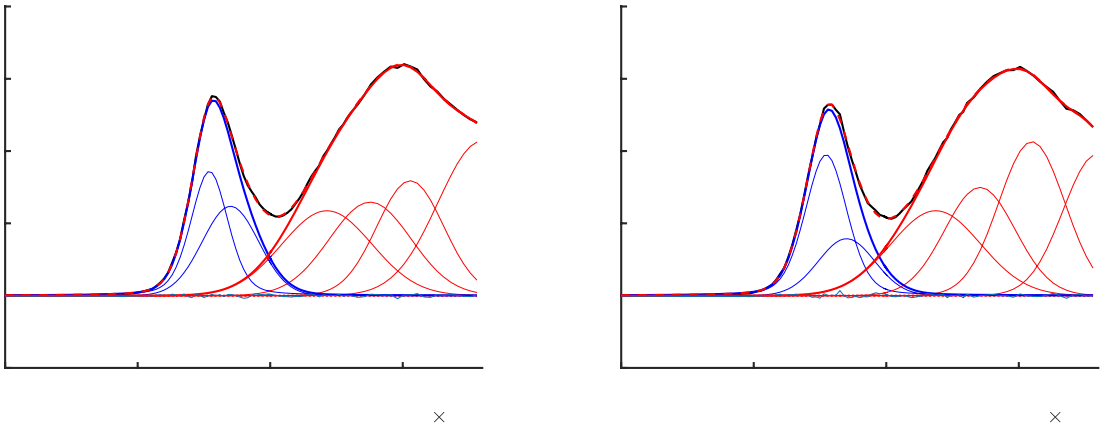

Figure S8. Fits of Se HERFD XAS for Av1Se$_{lo}$ (left) and Av1Se$_{hi}$ (right).

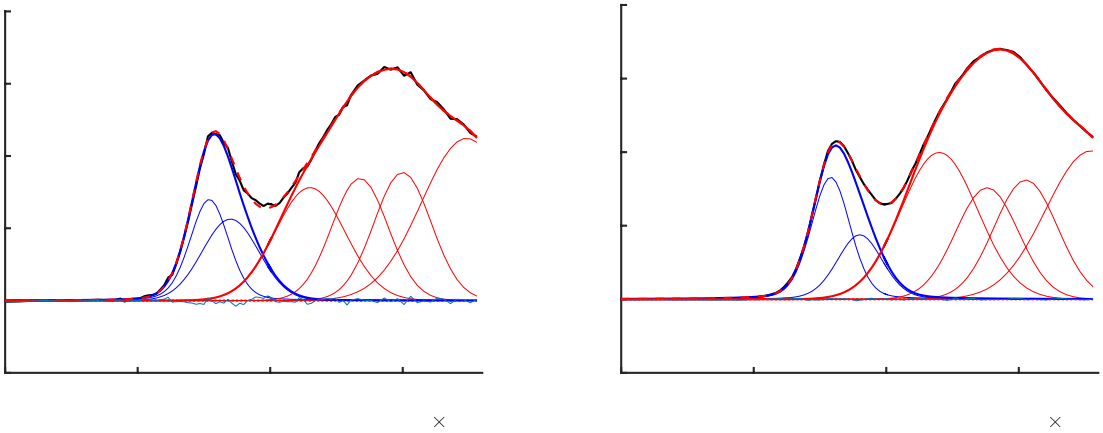

Figure S9. Fits of Se HERFD XAS for Av1Se$_{reac}$ (left) and Av1SeCO (right).

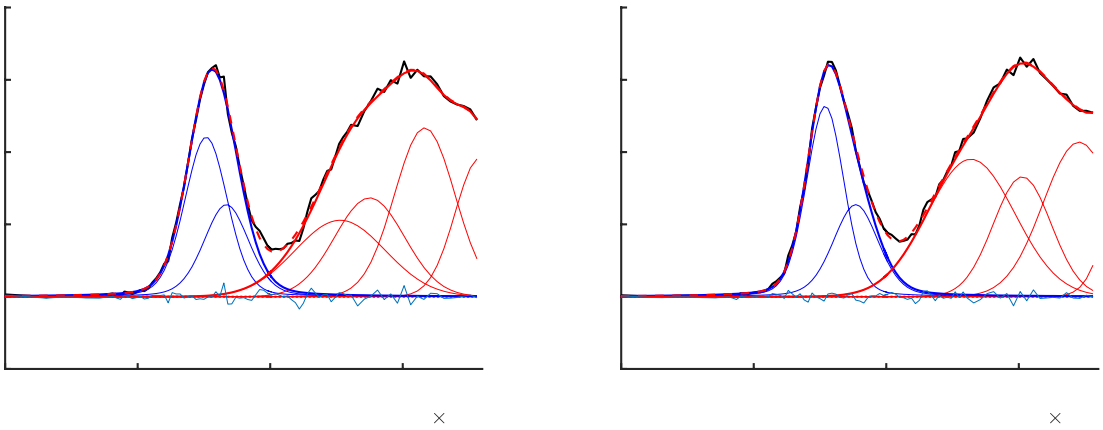

Figure S10. Fits of Se HERFD XAS for Se_{2B} deconvoluted from $Av1Se_{hi}/Av1Se_{reac}$ (left) and $Av1Se_{lo}/Av1Se_{reac}$ (right).

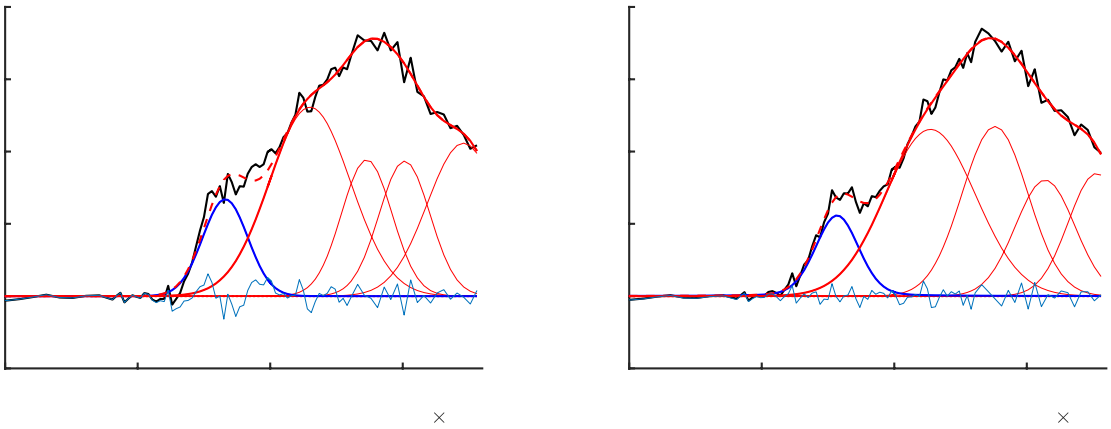

Figure S11. Fits of Se HERFD XAS for $Se_{3A/5A}$ deconvoluted from $Av1Se_{hi}/Av1Se_{reac}$ (left) and $Av1Se_{lo}/Av1Se_{reac}$ (right).

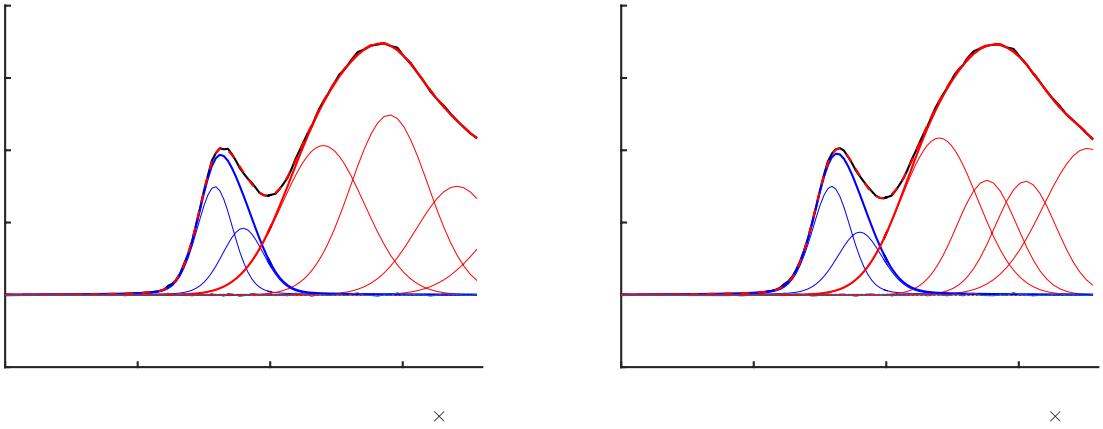

Figure S12. Fits of Se HERFD XAS for $COSe_{3A/5A}$ derived from Av1SeCO and Se_{2B} from $Av1Se_{hi}/Av1Se_{reac}$ (left) and $Av1Se_{lo}/Av1Se_{reac}$ (right).

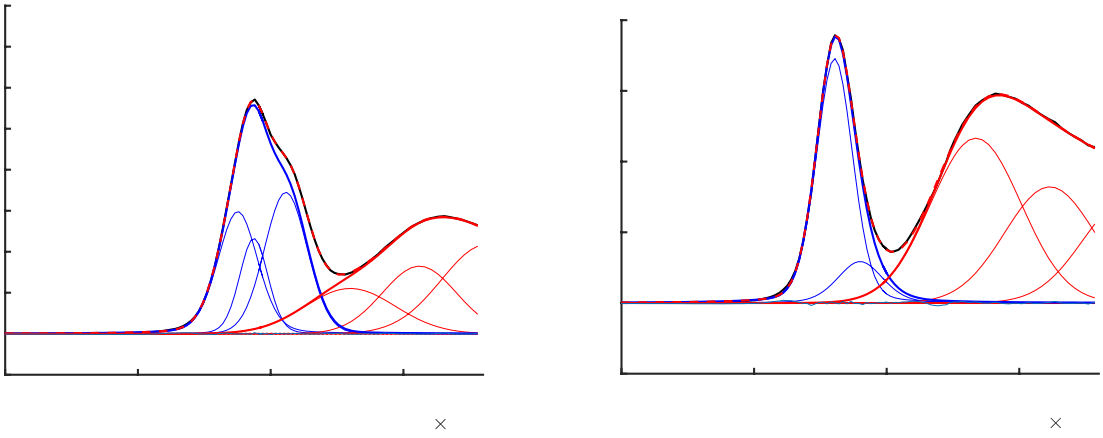

Figure S13. Fits of Se HERFD XAS for selenocystine (left) and synthetic complex $[Et_4N]_2[Fe_2Se_2(SPh)_4]$ (right).

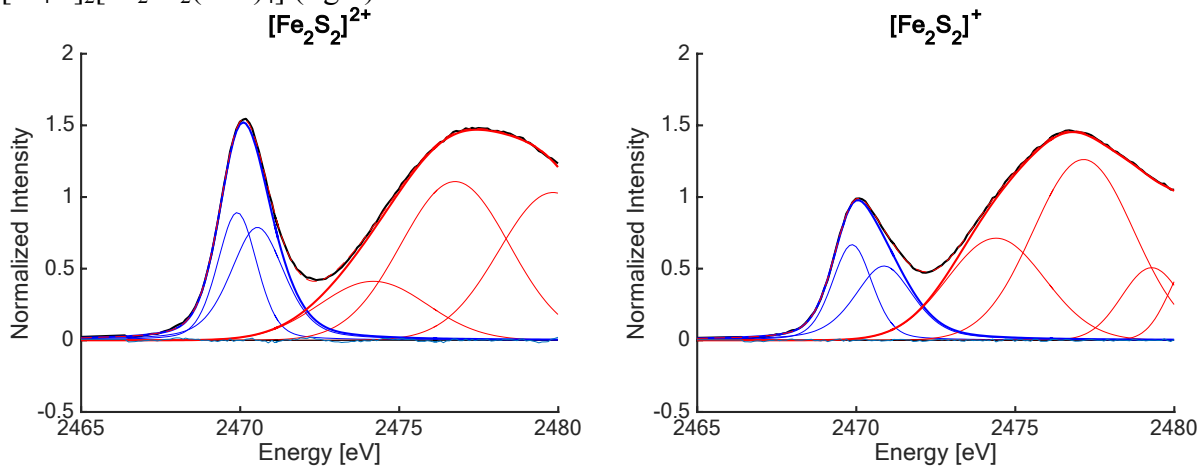

Figure S14. Fits of S XAS for synthetic complexes $[Fe_2S_2]^{2+}$ (left) and $[Fe_2S_2]^{+}$ (right).

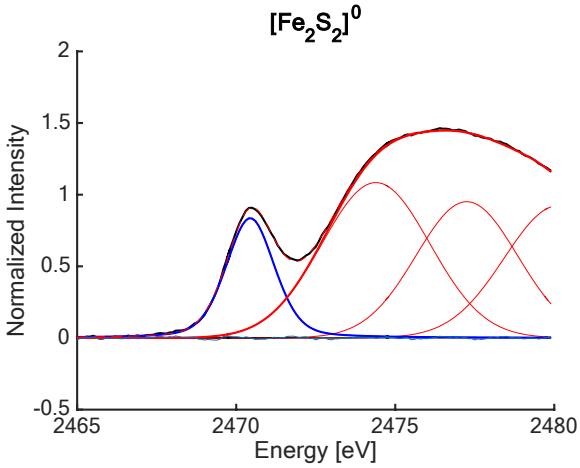

Figure S15. Fit of S XAS for synthetic complex $[Fe_2S_2]^0$.

Fits of Calculated TDDFT S and Se XAS Spectra

The TDDFT data is shown in black. Individual edge Gaussians are shown as thin red lines and their sum is given as a thick red line. Individual pre-edge pseudo-Voigt functions are shown as thin dark blue lines and their sum is given as a thick dark blue line. The difference between the fit and the TDDFT data is shown as a thin light blue line.

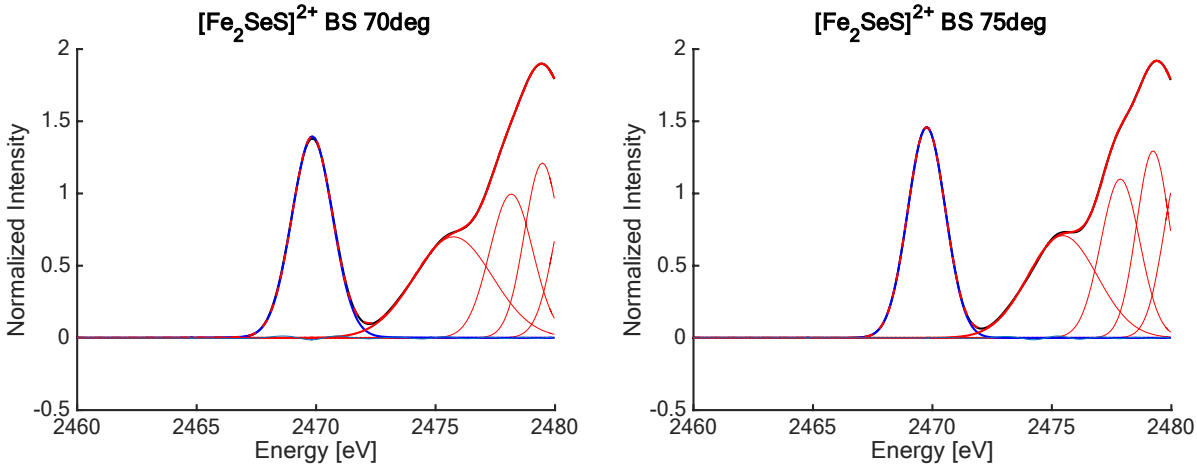

Figure S16. Fits of TDDFT S XAS for fictitious $S = 0$ complex $[Fe_2SeS]^{2+}$ with Fe–Se–Fe angles of 70° (left) and 75° (right).

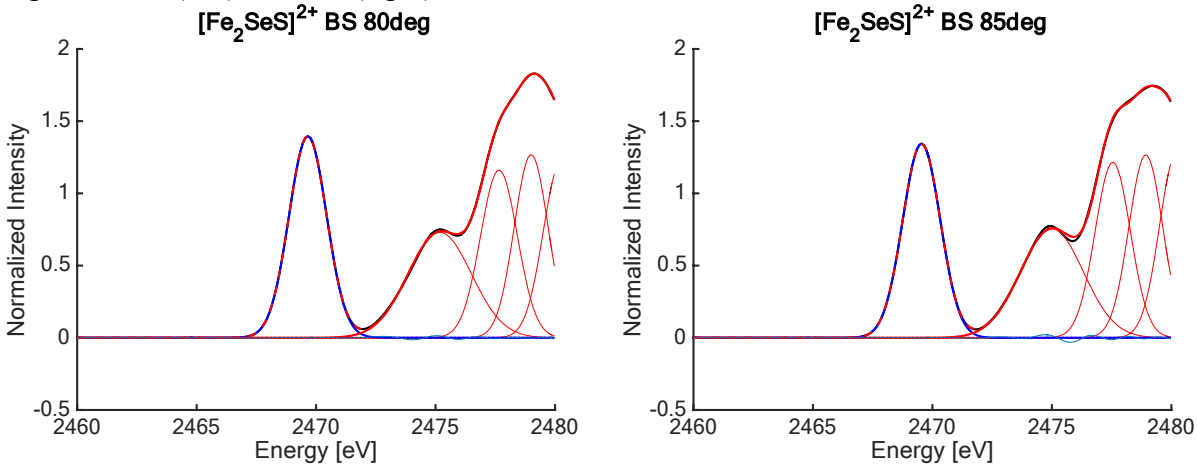

Figure S17. Fits of TDDFT S XAS for fictitious $S = 0$ complex $[Fe_2SeS]^{2+}$ with Fe–Se–Fe angles of 80° (left) and 85° (right).

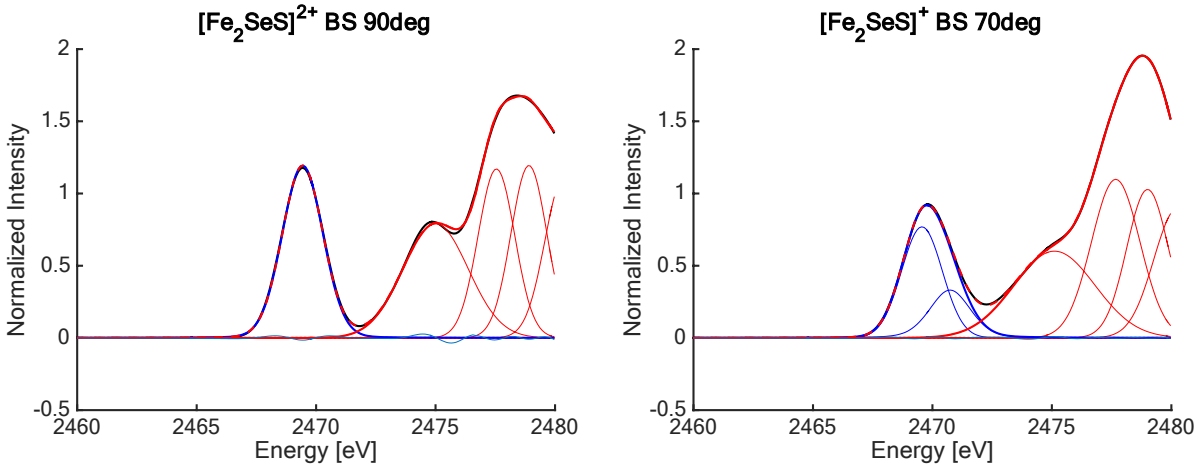

Figure S18. Fits of TDDFT S XAS for fictitious $S = 0$ complex $[Fe_2SeS]^{2+}$ with Fe–Se–Fe angle of 90° (left) and $S = ½$ complex $[Fe_2SeS]^{+}$ with Fe–Se–Fe angle of 70° (right).

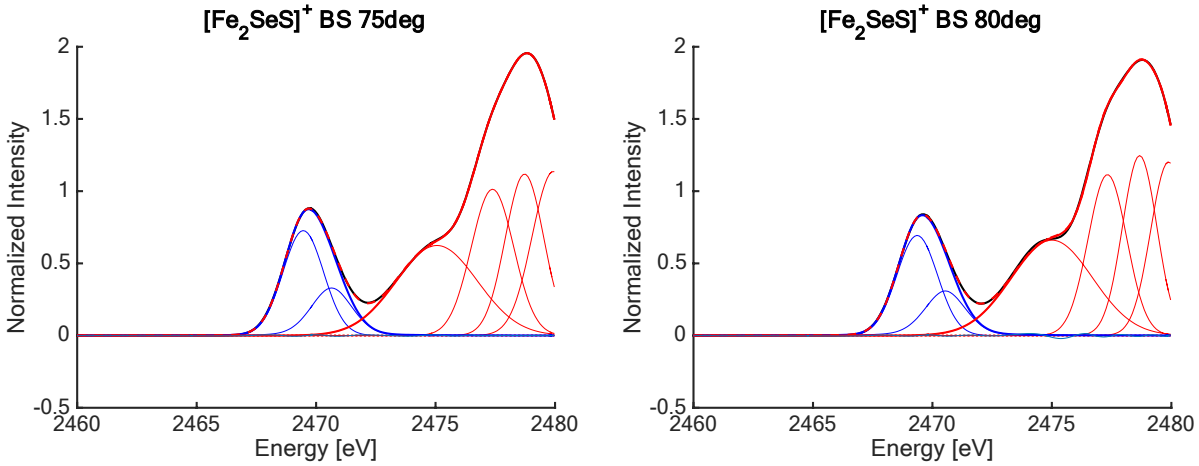

Figure S19. Fits of TDDFT S XAS for fictitious $S = ½$ complex $[Fe_2SeS]^{+}$ with Fe–Se–Fe angles of 75° (left) and 80° (right).

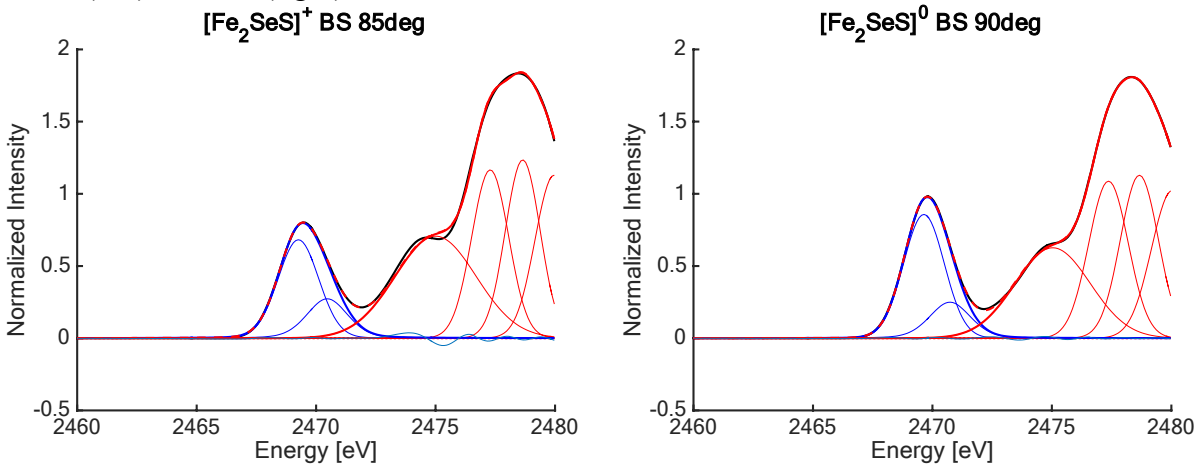

Figure S20. Fits of TDDFT S XAS for fictitious $S = ½$ complex $[Fe_2SeS]^{+}$ with Fe–Se–Fe angles of 85° (left) and 90° (right).

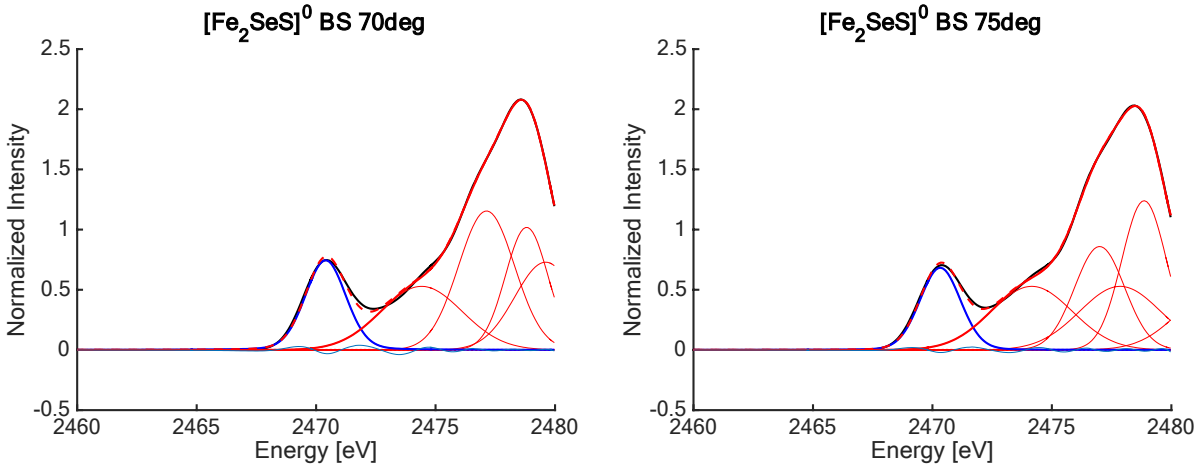

Figure S21. Fits of TDDFT S XAS for fictitious $S = 0$ complex $[Fe_2SeS]^0$ with Fe–Se–Fe angles of 70° (left) and 75° (right).

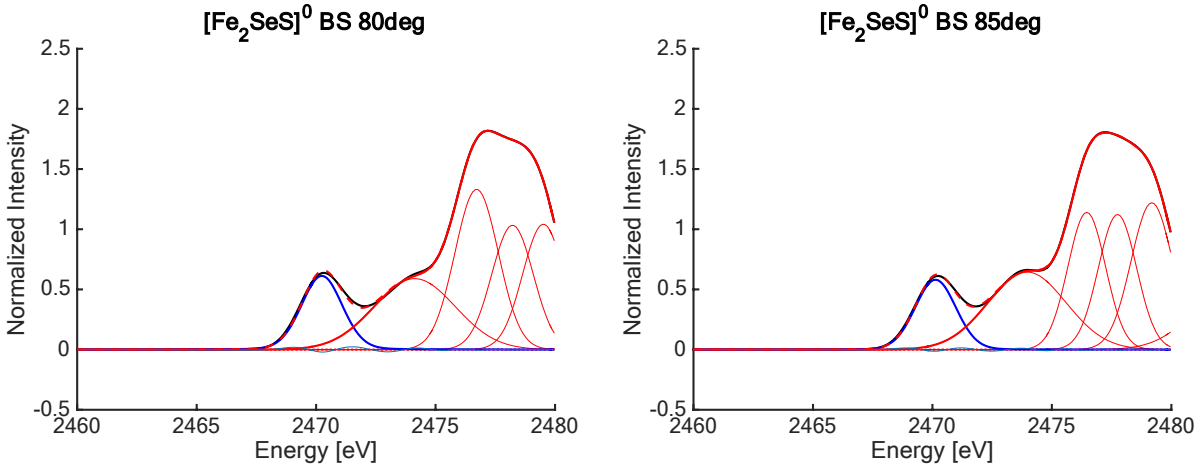

Figure S22. Fits of TDDFT S XAS for fictitious $S = 0$ complex $[Fe_2SeS]^0$ with Fe–Se–Fe angles of 80° (left) and 85° (right).

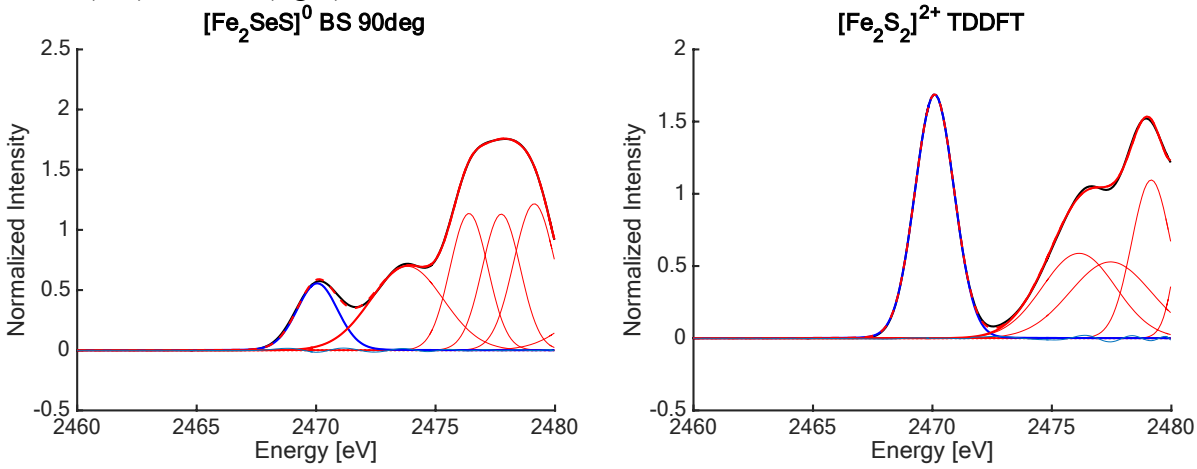

Figure S23. Fits of TDDFT S XAS for fictitious $S = 0$ complex $[Fe_2SeS]^0$ with Fe–Se–Fe angle of 90° (left) and synthetic $S = 0$ complex $[Fe_2S_2]^{2+}$ (right).

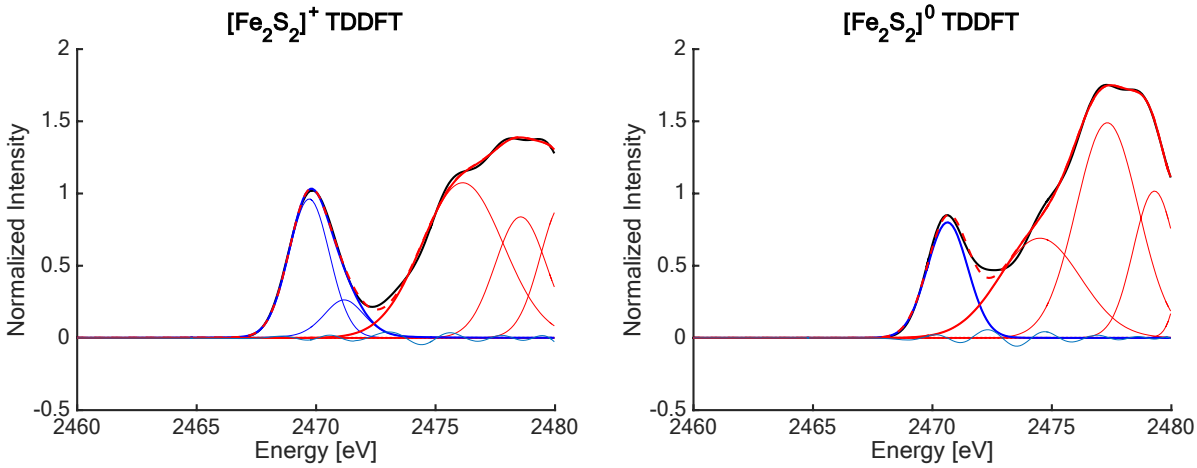

Figure S24. Fits of TDDFT S XAS for synthetic $S = ½$ complex $[Fe_2SeS]^+$ (left) synthetic $S = 0$ complex $[Fe_2S_2]^0$ (right).

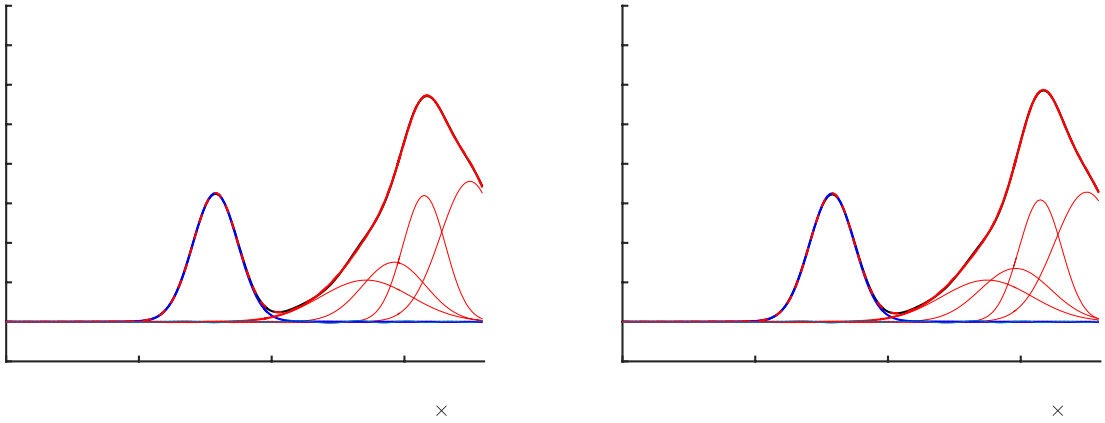

Figure S25. Fits of TDDFT Se XAS for fictitious $S = 0$ complex $[Fe_2SeS]^{2+}$ with Fe–Se–Fe angles of 70° (left) and 75° (right).

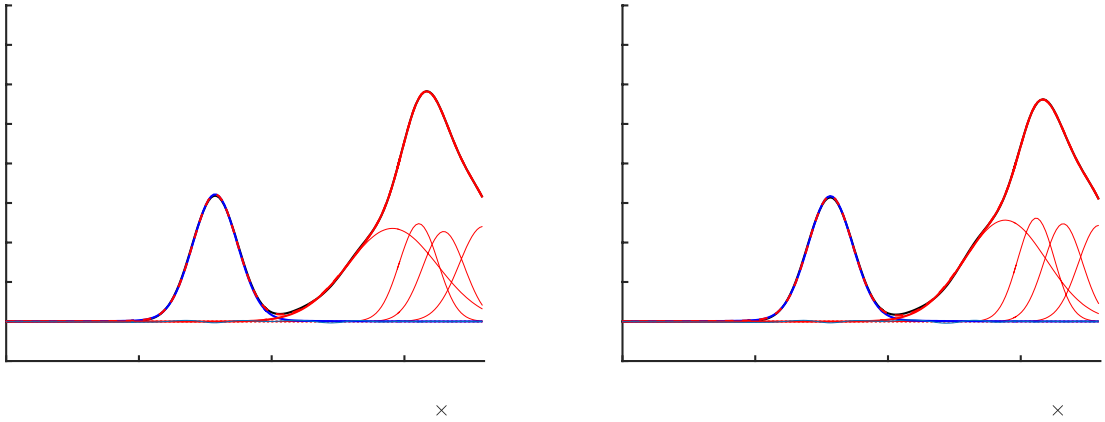

Figure S26. Fits of TDDFT Se XAS for fictitious $S = 0$ complex $[Fe_2SeS]^{2+}$ with Fe–Se–Fe angles of 80° (left) and 85° (right).

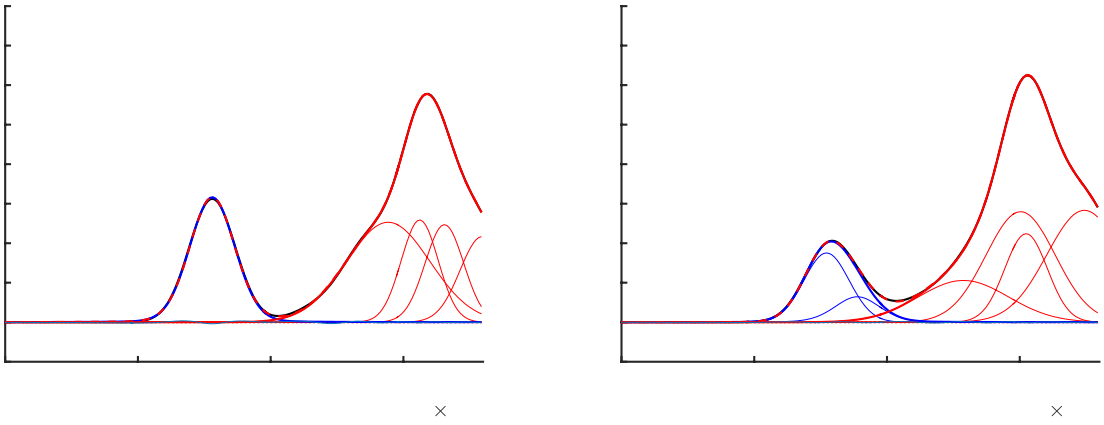

Figure S27. Fits of TDDFT Se XAS for fictitious $S = 0$ complex $[Fe_2SeS]^{2+}$ with Fe–Se–Fe angle of 90° (left) and $S = ½$ complex $[Fe_2SeS]^{+}$ with Fe–Se–Fe angle of 70° (right).

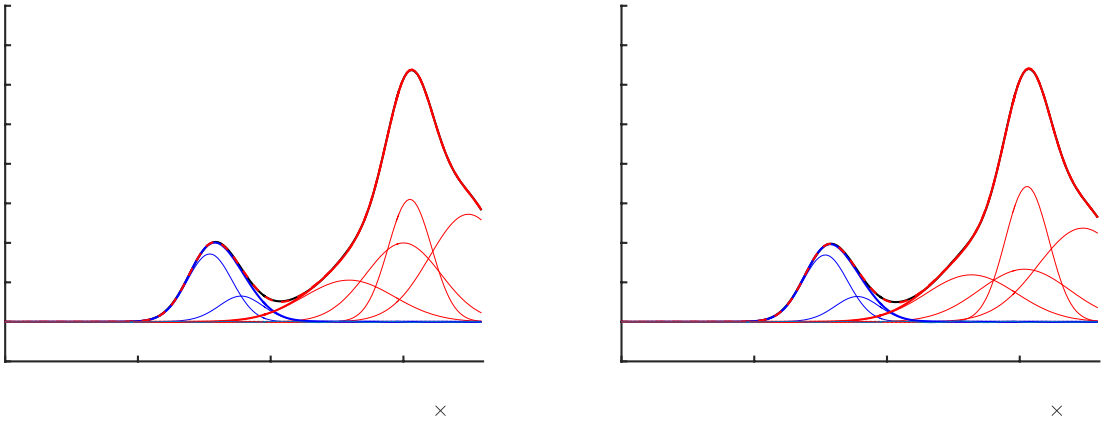

Figure S28. Fits of TDDFT Se XAS for fictitious $S = ½$ complex $[Fe_2SeS]^{+}$ with Fe–Se–Fe angles of 75° (left) and 80° (right).

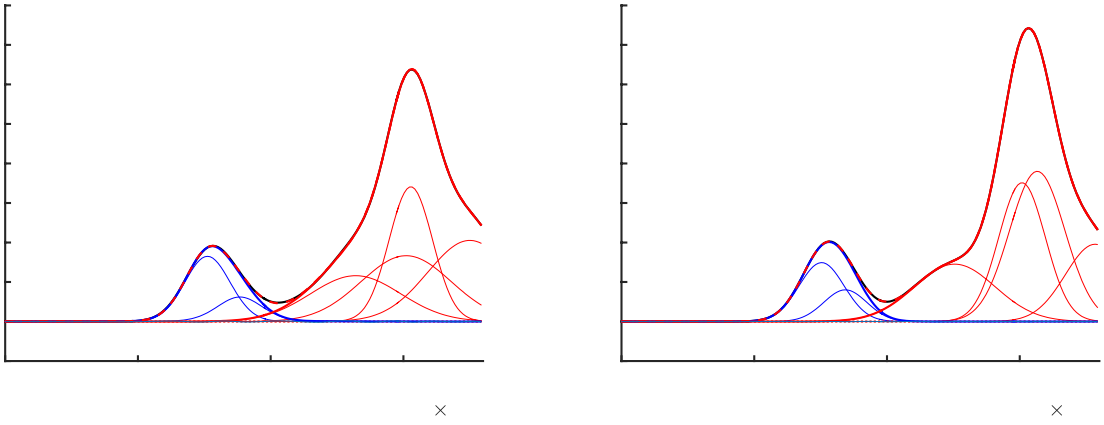

Figure S29. Fits of TDDFT Se XAS for fictitious $S = ½$ complex $[Fe_2SeS]^{+}$ with Fe–Se–Fe angles of 85° (left) and 90° (right).

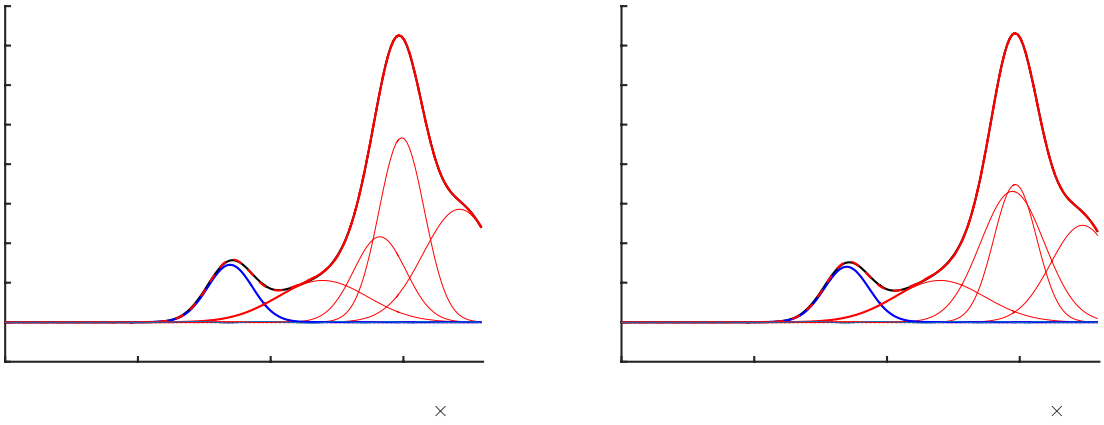

Figure S30. Fits of TDDFT Se XAS for fictitious $S = 0$ complex $[Fe_2SeS]^0$ with Fe–Se–Fe angles of 70° (left) and 75° (right).

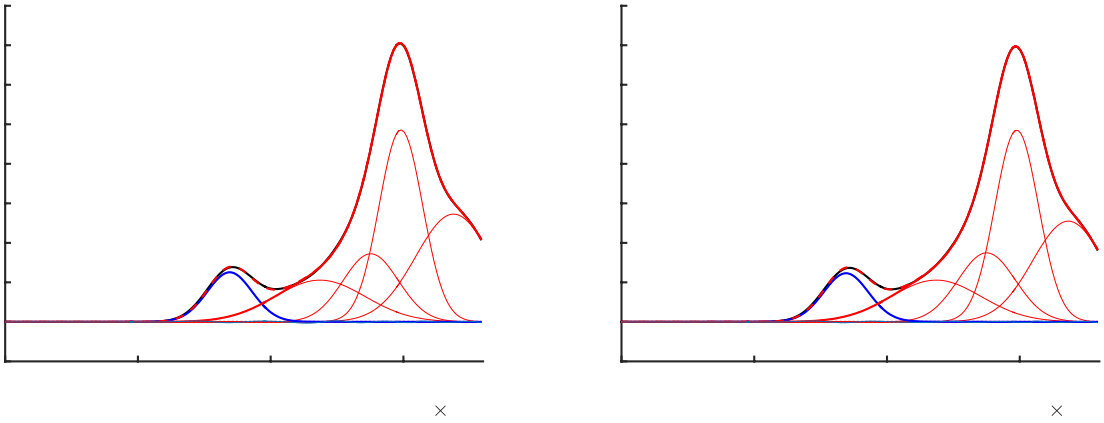

Figure S31. Fits of TDDFT Se XAS for fictitious $S = 0$ complex $[Fe_2SeS]^0$ with Fe–Se–Fe angles of 80° (left) and 85° (right).

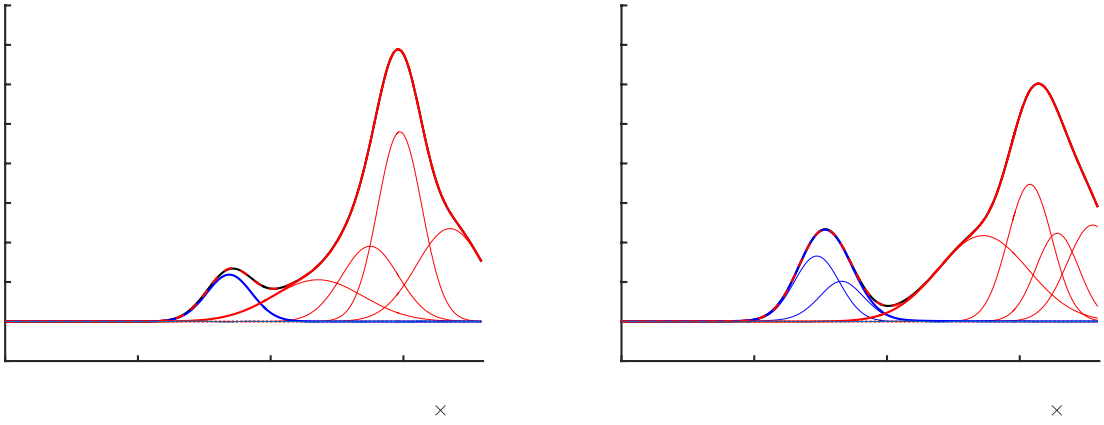

Figure S32. Fits of TDDFT Se XAS for fictitious $S = 0$ complex $[Fe_2SeS]^0$ with Fe–Se–Fe angle of 90° (left) and $S = 5$ complex $[Fe_2SeS]^{2+}$ with Fe–Se–Fe angle of 70° (right).

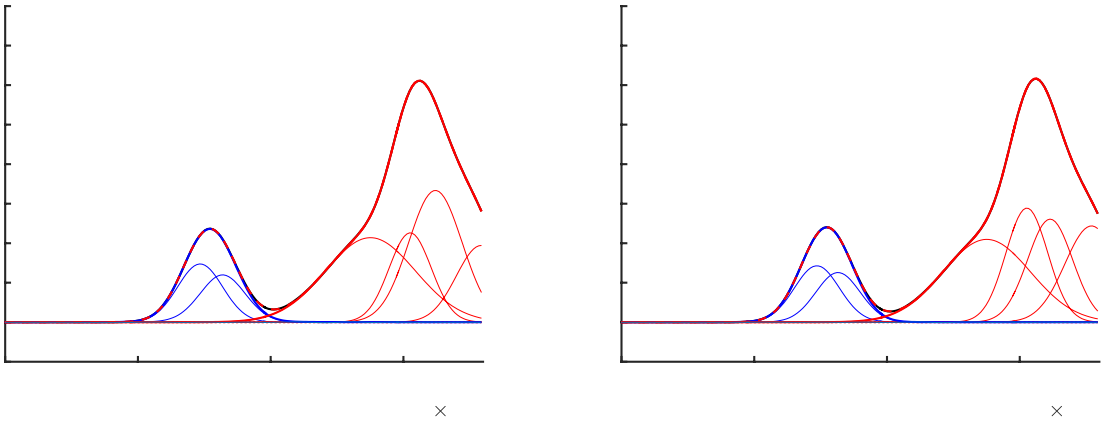

Figure S33. Fits of TDDFT Se XAS for fictitious $S = 5$ complex $[Fe_2SeS]^{2+}$ with Fe–Se–Fe angles of 75° (left) and 80° (right).

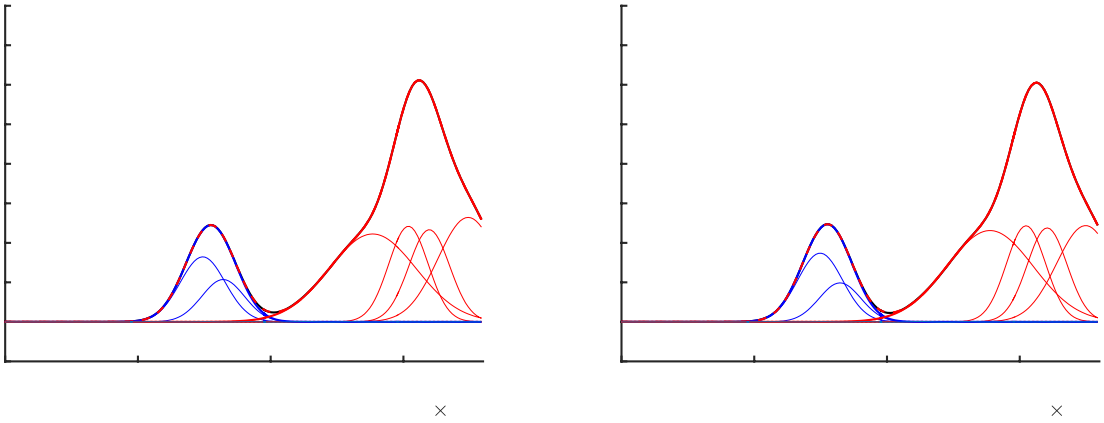

Figure S34. Fits of TDDFT Se XAS for fictitious $S = 5$ complex $[Fe_2SeS]^{2+}$ with Fe–Se–Fe angles of 85° (left) and 90° (right).

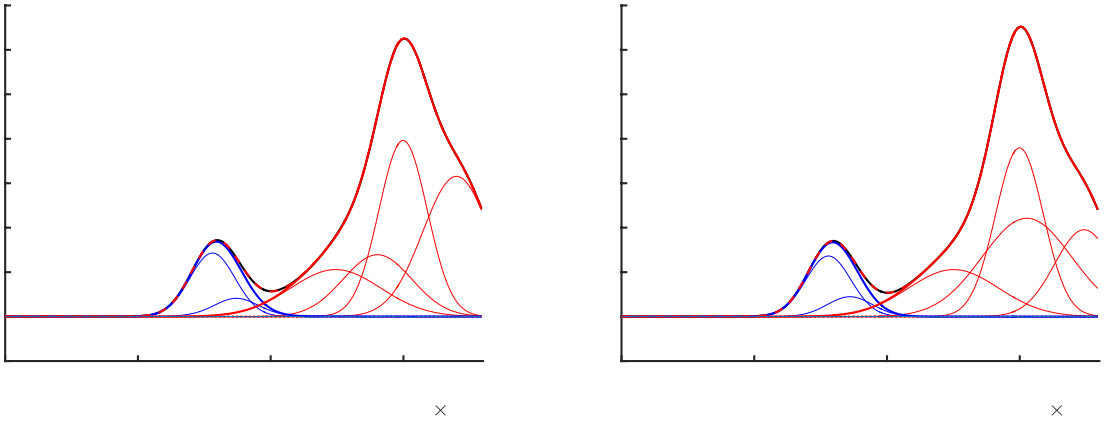

Figure S35. Fits of TDDFT Se XAS for fictitious $S = 9/2$ complex $[Fe_2SeS]^{+}$ with Fe–Se–Fe angles of 70° (left) and 75° (right).

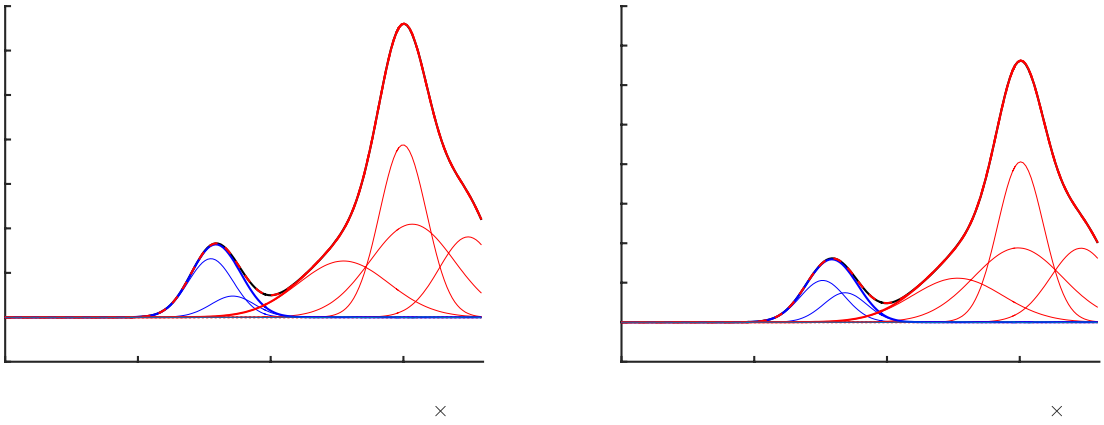

Figure S36. Fits of TDDFT Se XAS for fictitious $S = 9/2$ complex $[Fe_2SeS]^+$ with Fe–Se–Fe angles of 80° (left) and 85° (right).

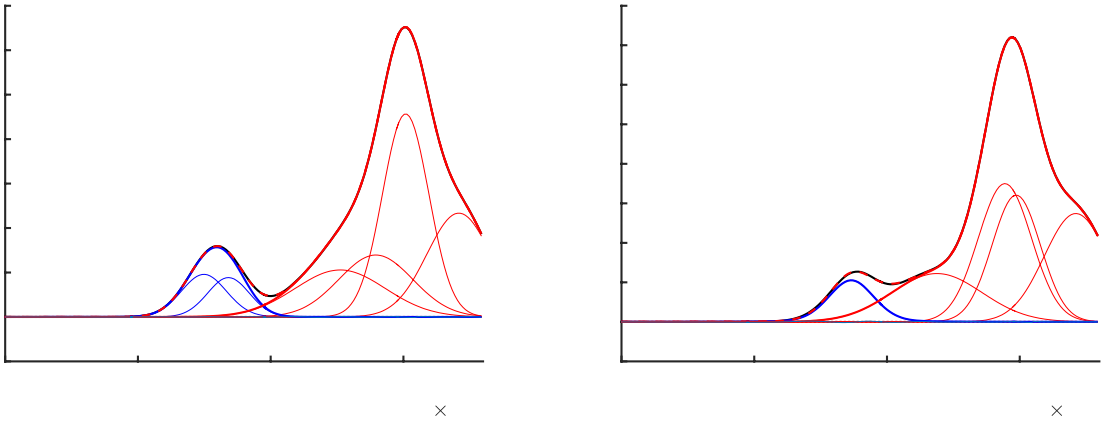

Figure S37. Fits of TDDFT Se XAS for fictitious $S = 9/2$ complex $[Fe_2SeS]^+$ with Fe–Se–Fe angle of 90° (left) and $S = 4$ complex $[Fe_2SeS]^0$ with Fe–Se–Fe angle of 70° (right).

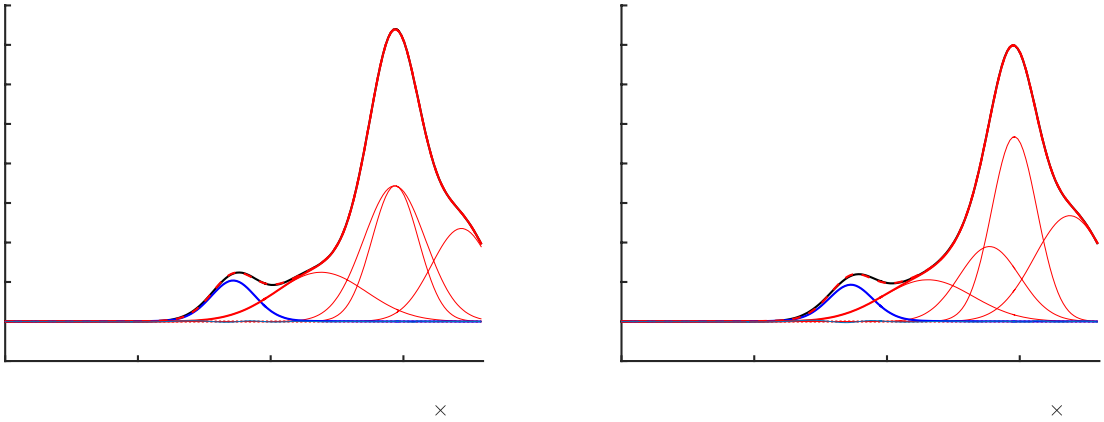

Figure S38. Fits of TDDFT Se XAS for fictitious $S = 4$ complex $[Fe_2SeS]^0$ with Fe–Se–Fe angles of 75° (left) and 80° (right).

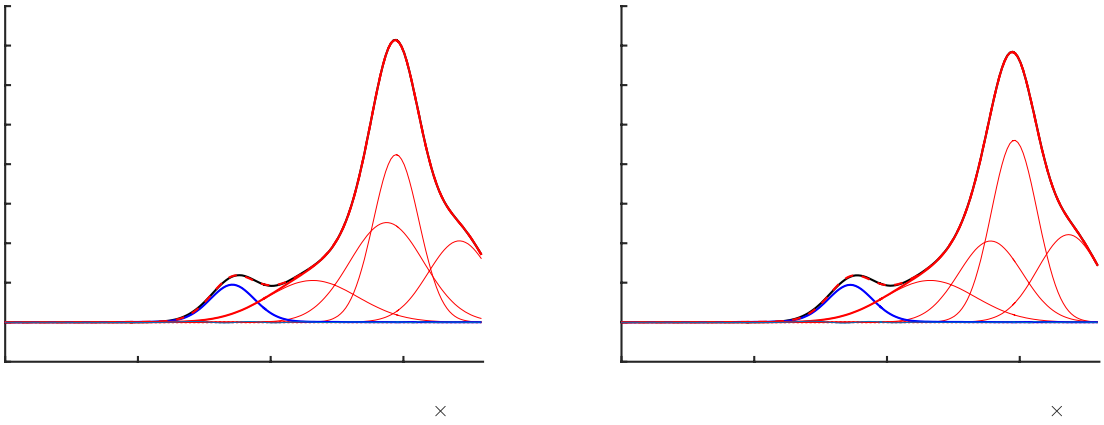

Figure S39. Fits of TDDFT Se XAS for fictitious $S = 4$ complex $[Fe_2SeS]^0$ with Fe–Se–Fe angles of 85° (left) and 90° (right).

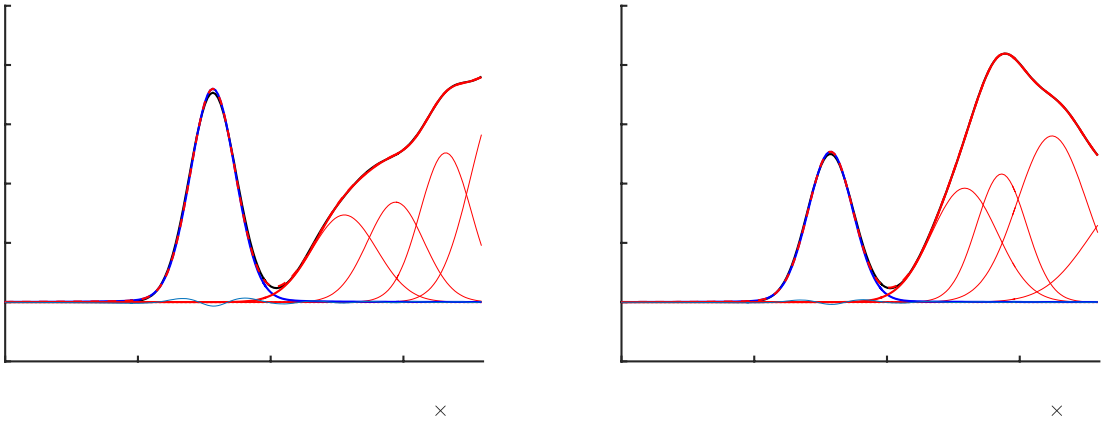

Figure S40. Fits of TDDFT Se XAS for fictitious $S = 0$ hydrogen-bonded complex $[Fe_2Se_2]^{2+}$ with one Se not interacting with H-bonds (left) and one Se interacting with 4 H-bonds (right).

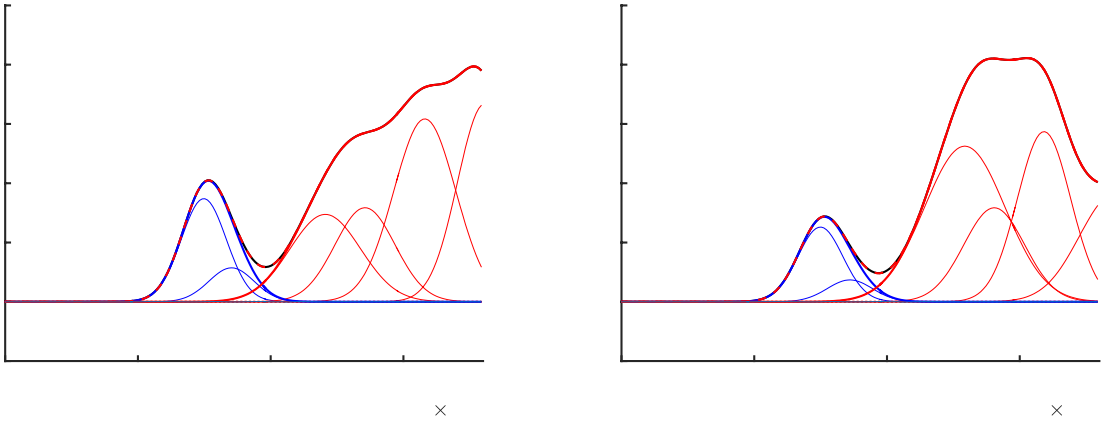

Figure S41. Fits of TDDFT Se XAS for fictitious $S = ½$ hydrogen-bonded complex $[Fe_2Se_2]^{+}$ with one Se not interacting with H-bonds (left) and one Se interacting with 4 H-bonds (right).

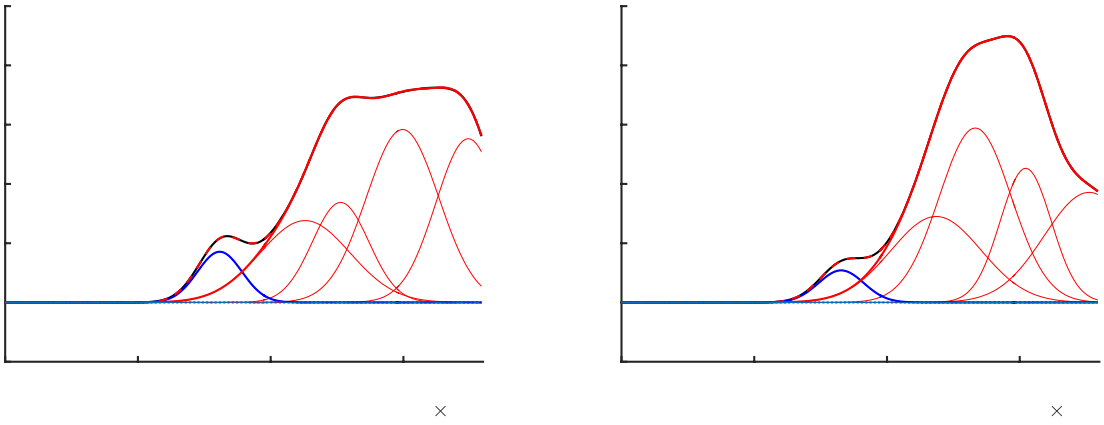

Figure S42. Fits of TDDFT Se XAS for fictitious $S = 0$ hydrogen-bonded complex $[Fe_2Se_2]^0$ with one Se not interacting with H-bonds (left) and one Se interacting with 4 H-bonds (right).

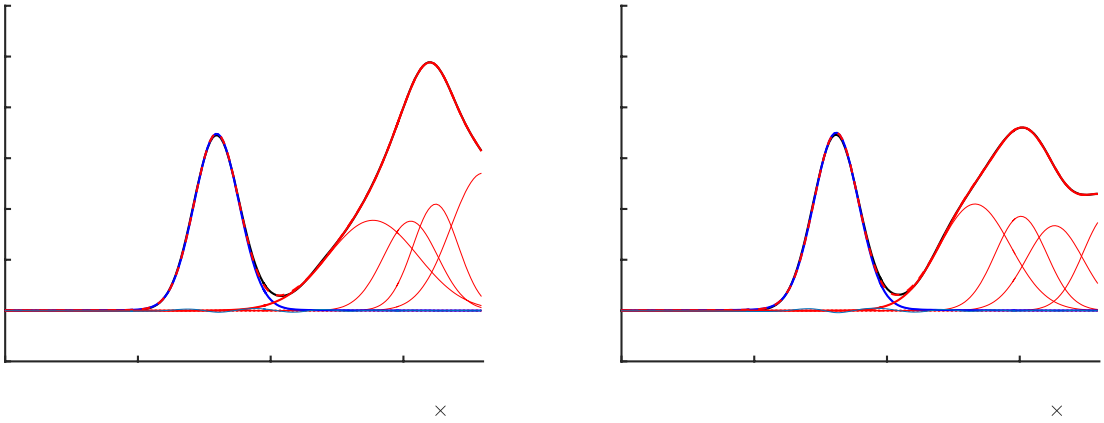

Figure S43. Fits of TDDFT Se XAS for crystallographic $S = 0$ complex $[Fe_2Se_2(SPh)_4]^{2-}$ in the absence of $[Et_4N]^+$ (left) and presence of 4 $[Et_4N]^+$ (right).

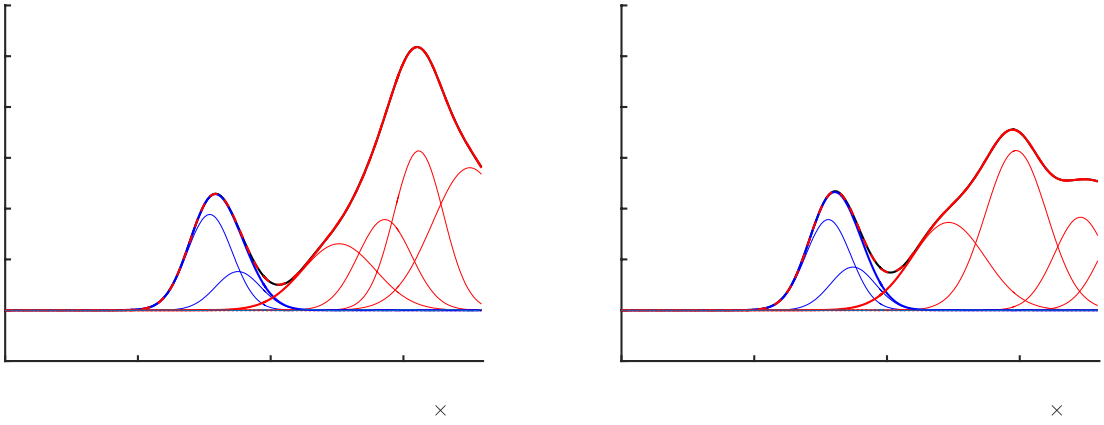

Figure S44. Fits of TDDFT Se XAS for fictitious $S = ½$ complex $[Fe_2Se_2(SPh)_4]^{3-}$ in the absence of $[Et_4N]^+$ (left) and presence of 4 $[Et_4N]^+$ (right).

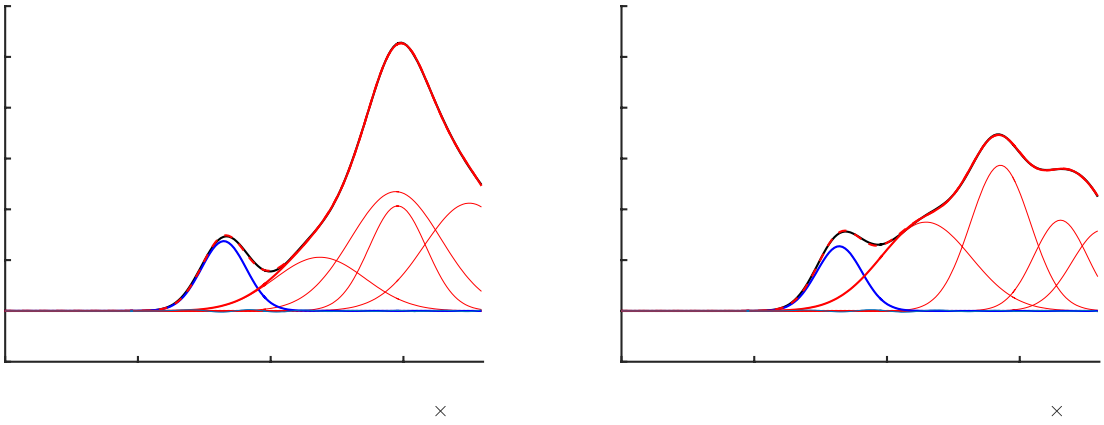

Figure S45. Fits of TDDFT Se XAS for fictitious $S = 0$ complex $[Fe_2Se_2(SPh)_4]^{4-}$ in the absence of $[Et_4N]^+$ (left) and presence of 4 $[Et_4N]^+$ (right).

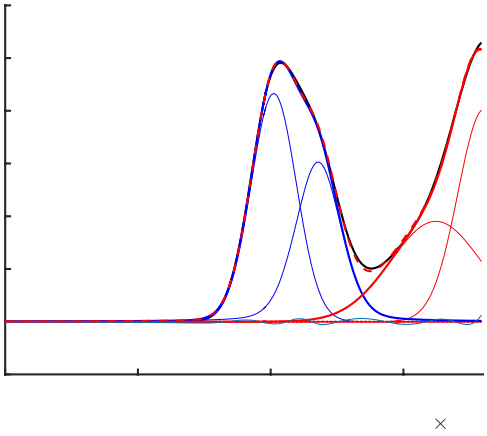

Figure S46. Fit of TDDFT Se XAS for selenocystine.

Experimental Se HERFD EXAFS Fits

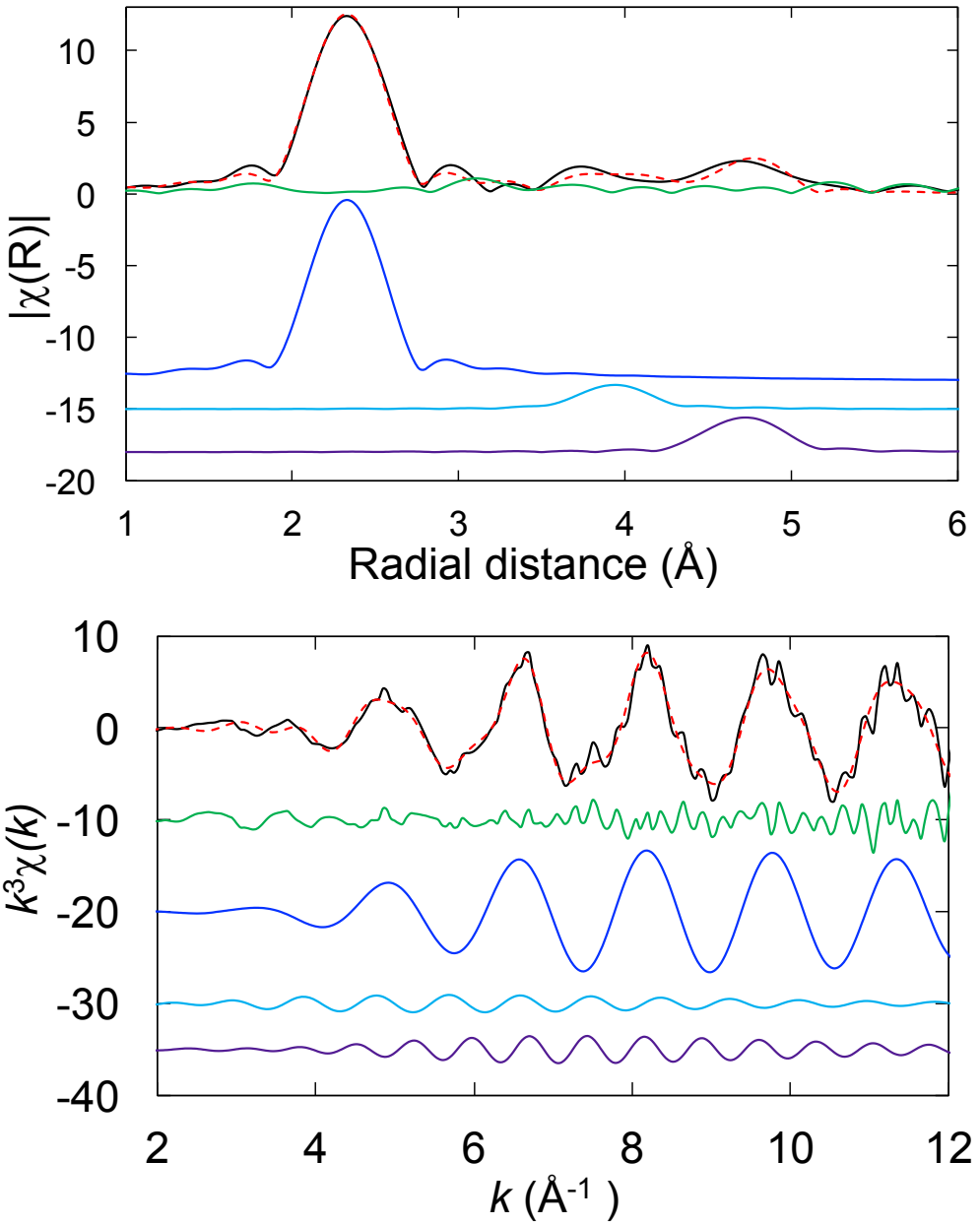

Figure S47. Multicomponent fits of Fourier transform (top) and k-space (bottom) Se HERFD EXAFS data for Av1Se$_{lo}$. Experimental data are given in black, total fit in dashed red, and residual in green. Fit components first shell Se–Fe are given in dark blue, first shell Se–S in light blue, and second shell Se–Fe' in purple. Fit components are offset for clarity.

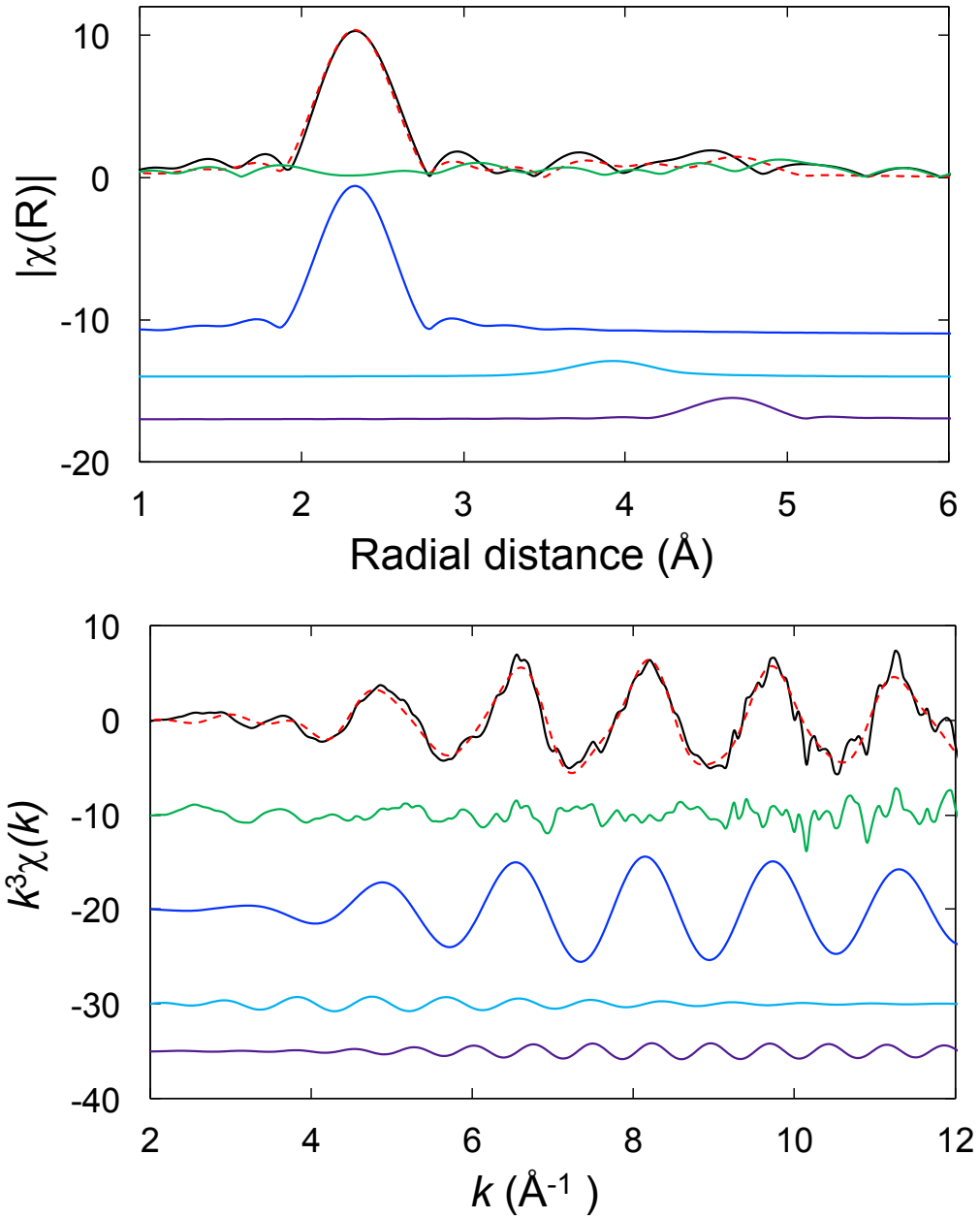

Figure S48. Multicomponent fits of Fourier transform (top) and k-space (bottom) Se HERFD EXAFS data for Av1Se$_{hi}$. Experimental data are given in black, total fit in dashed red, and residual in green. Fit components first shell Se–Fe are given in dark blue, first shell Se–S in light blue, and second shell Se–Fe' in purple. Fit components are offset for clarity.

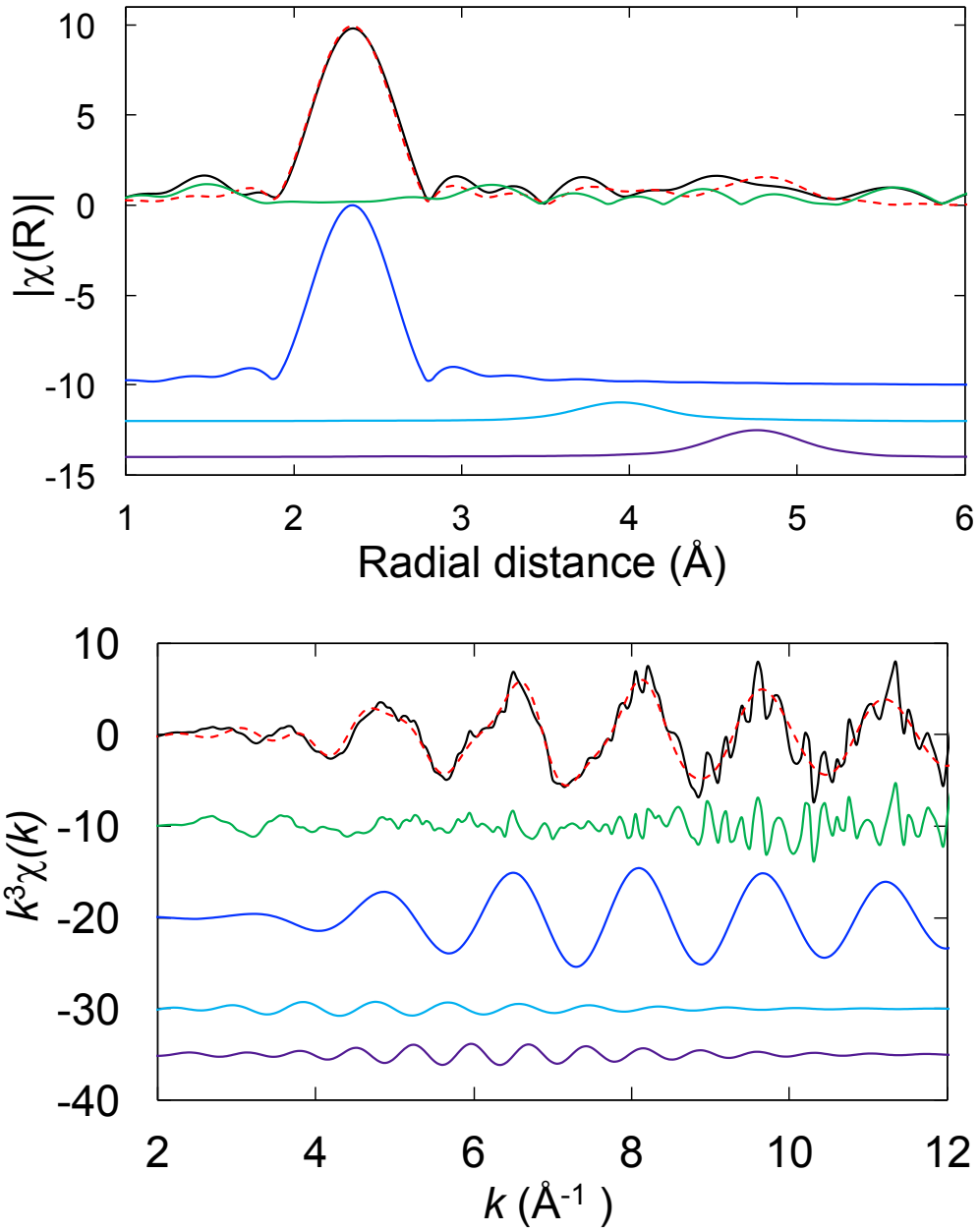

Figure S49. Multicomponent fits of Fourier transform (top) and k-space (bottom) Se HERFD EXAFS data for Av1Se$_{reac}$. Experimental data is given in black, total fit in dashed red, and residual in green. Fit components first shell Se–Fe are given in dark blue, first shell Se–S in light blue, and second shell Se–Fe' in purple. Fit components are offset for clarity.

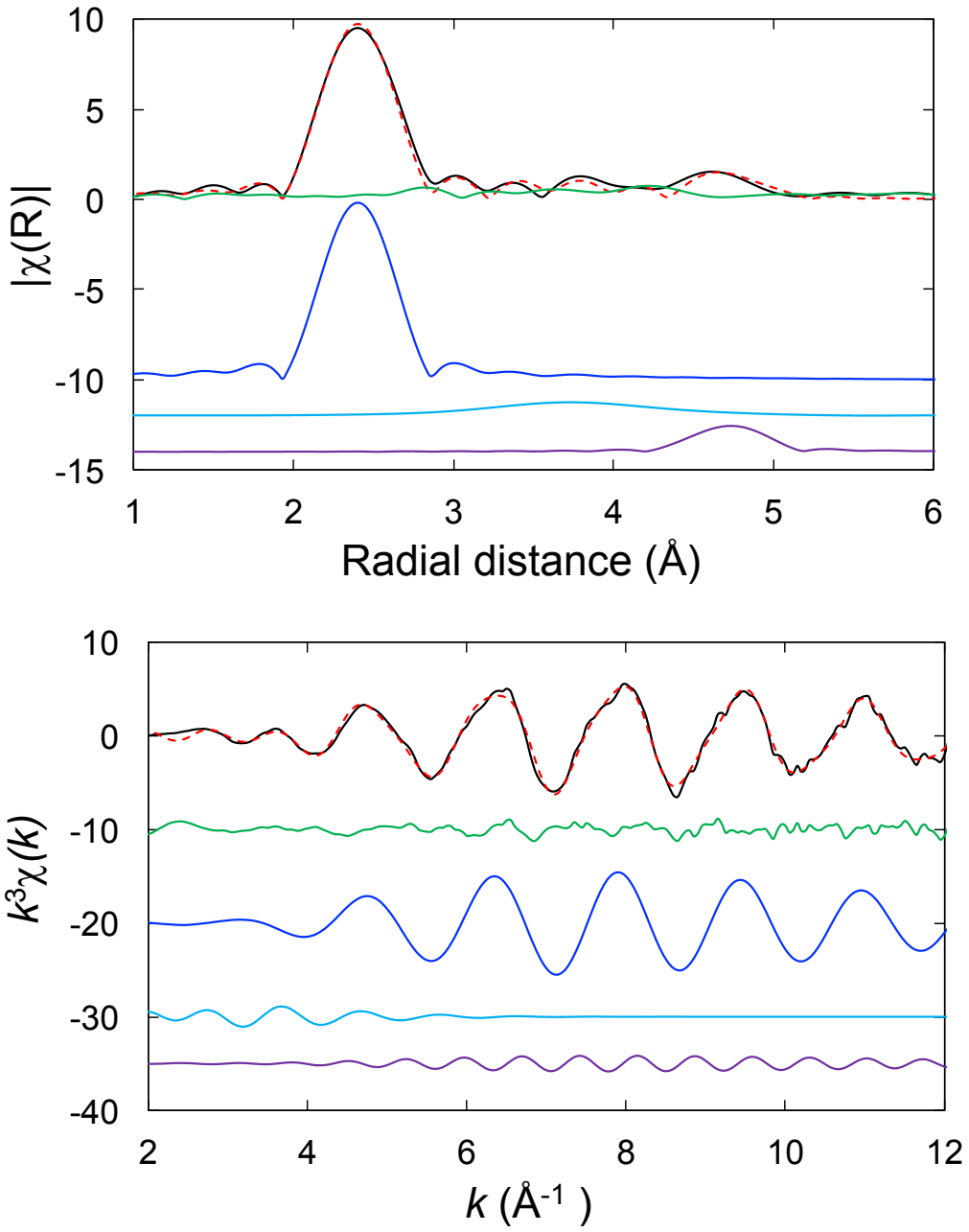

Figure S50. Multicomponent fits of Fourier transform (top) and k-space (bottom) Se HERFD EXAFS data for Av1SeCO. Experimental data is given in black, total fit in dashed red, and residual in green. Fit component first shell Se–Fe is given in dark blue, first shell Se–S in light blue, and second shell Se–Fe' in purple. Fit components are offset for clarity.

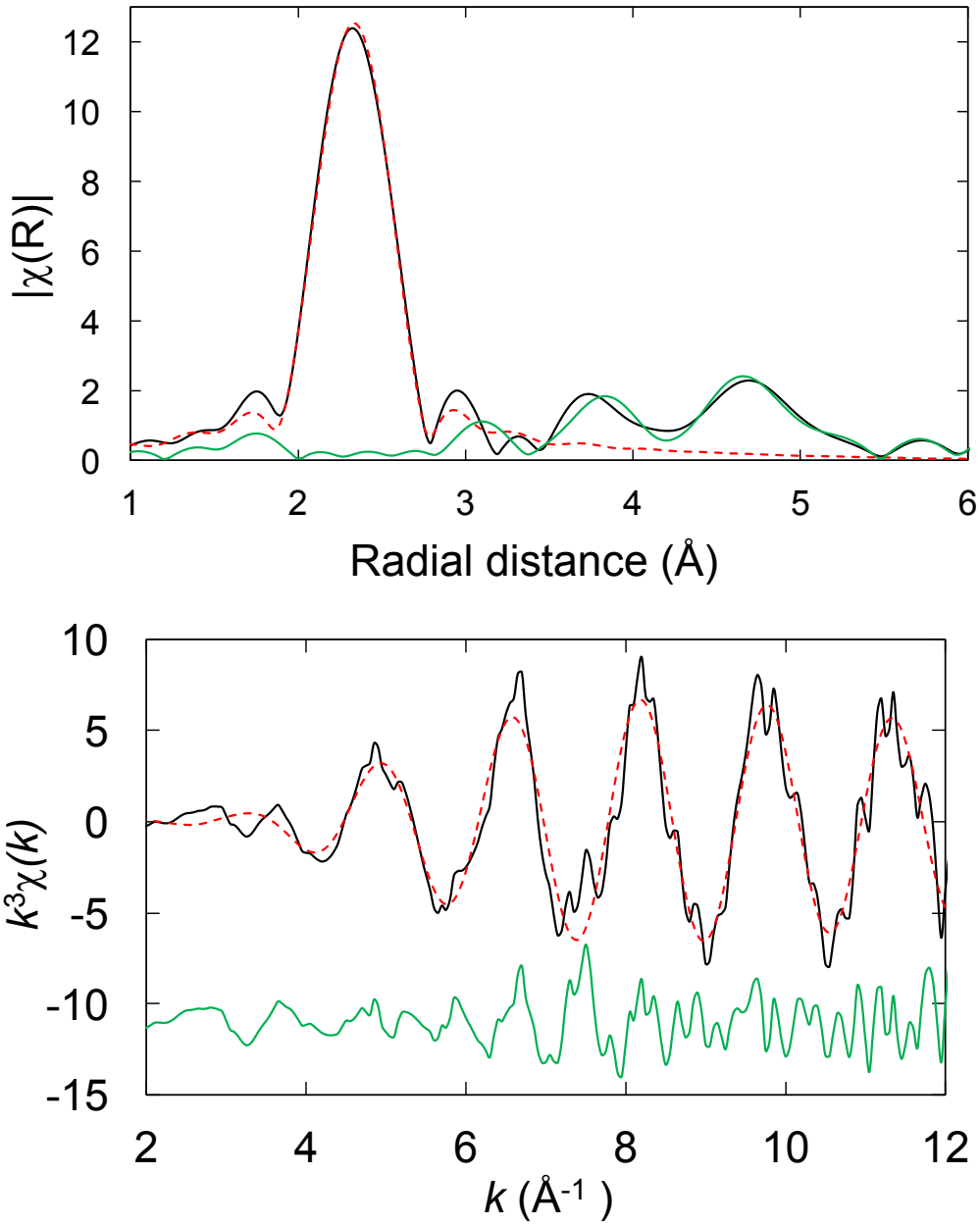

Figure S51. Single component fit of Fourier transform (top) and k-space (bottom) Se HERFD EXAFS data for Av1Se_{lo}. Experimental data is given in black, fit in dashed red, and residual in green.

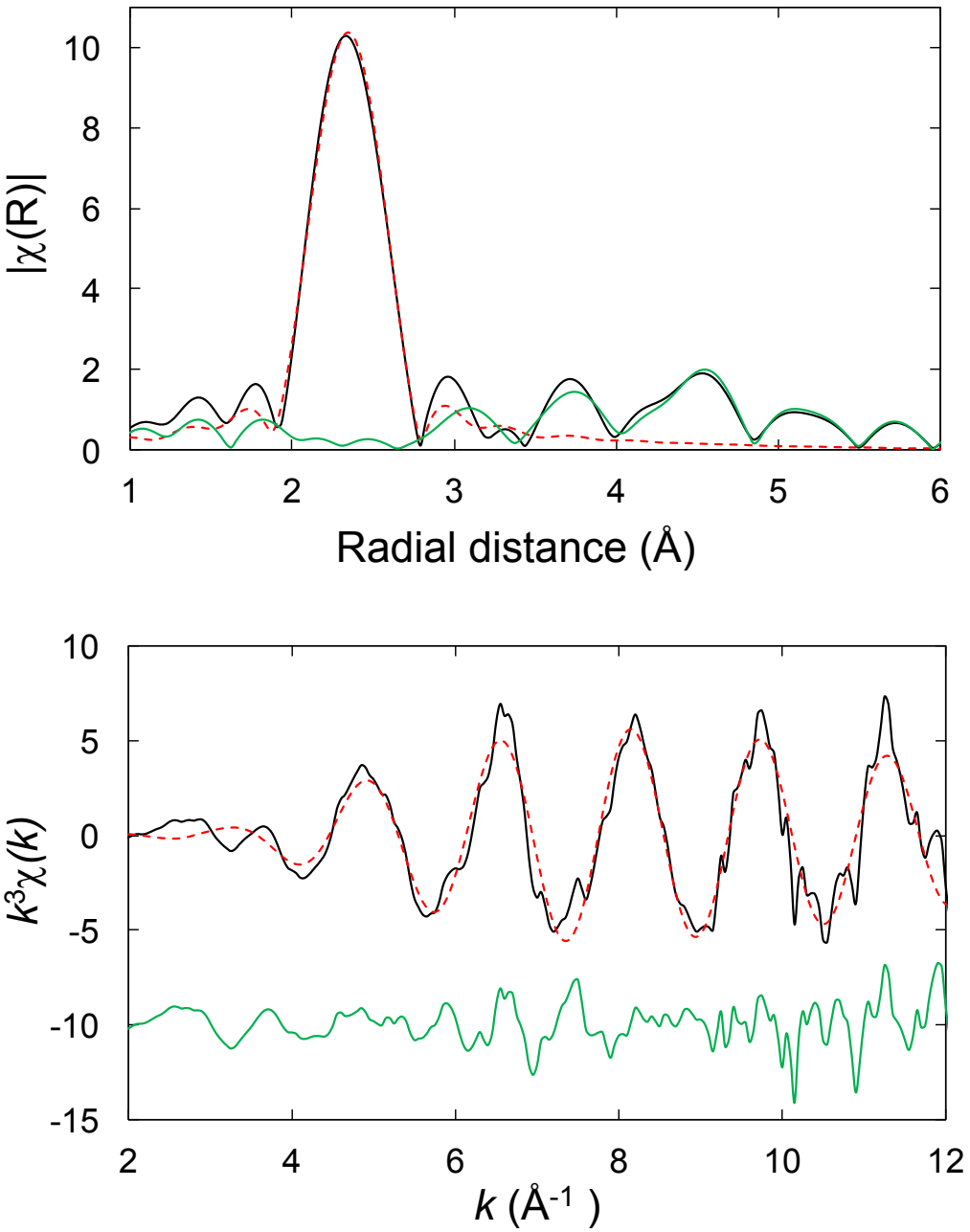

Figure S52. Single component fit of Fourier transform (top) and k-space (bottom) Se HERFD EXAFS data for Av1Se$_{hi}$. Experimental data is given in black, fit in dashed red, and residual in green.

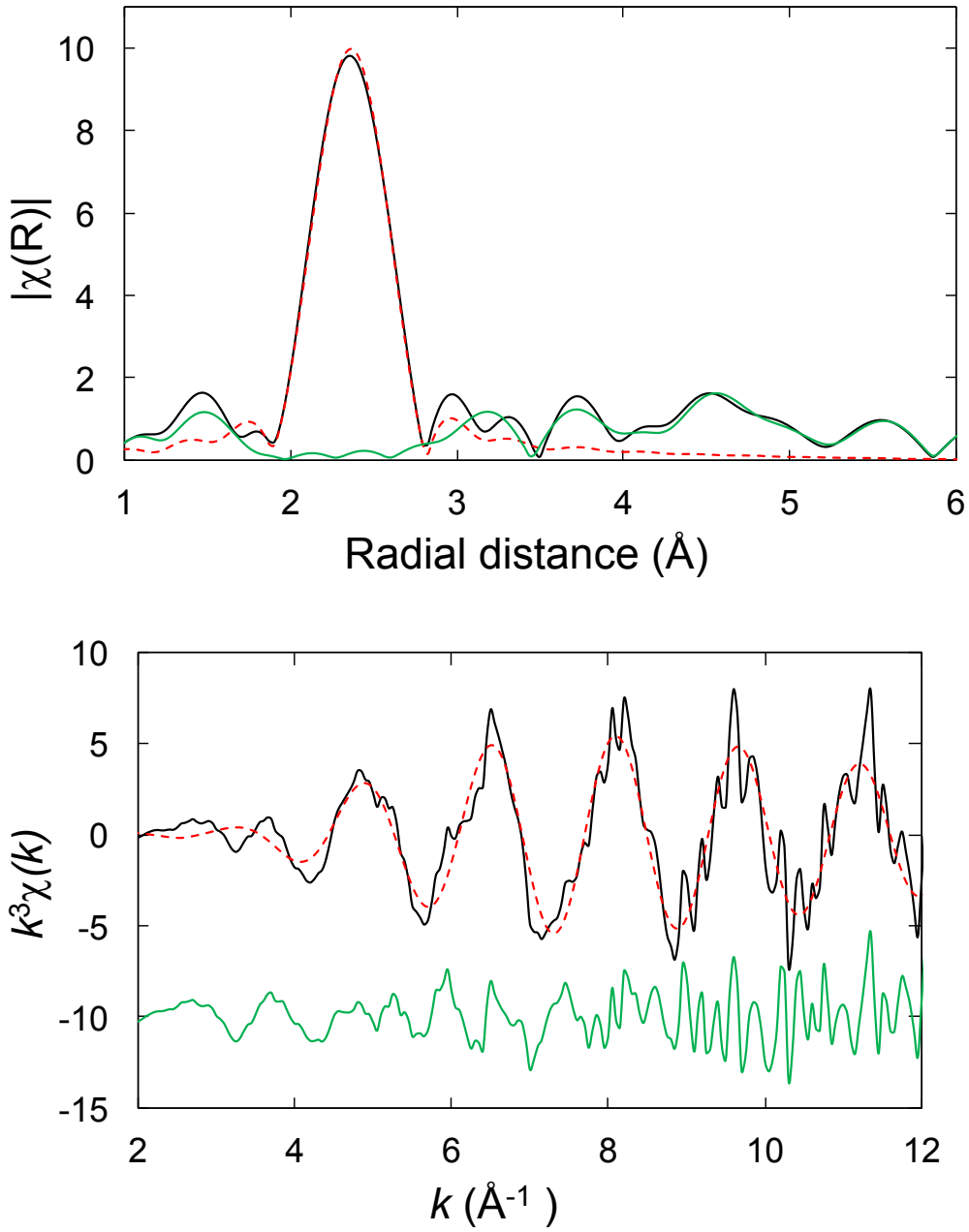

Figure S53. Single component fit of Fourier transform (top) and k-space (bottom) Se HERFD EXAFS data for Av1Se$_{reac}$. Experimental data are given in black, total fit in dashed red, and residual in green.

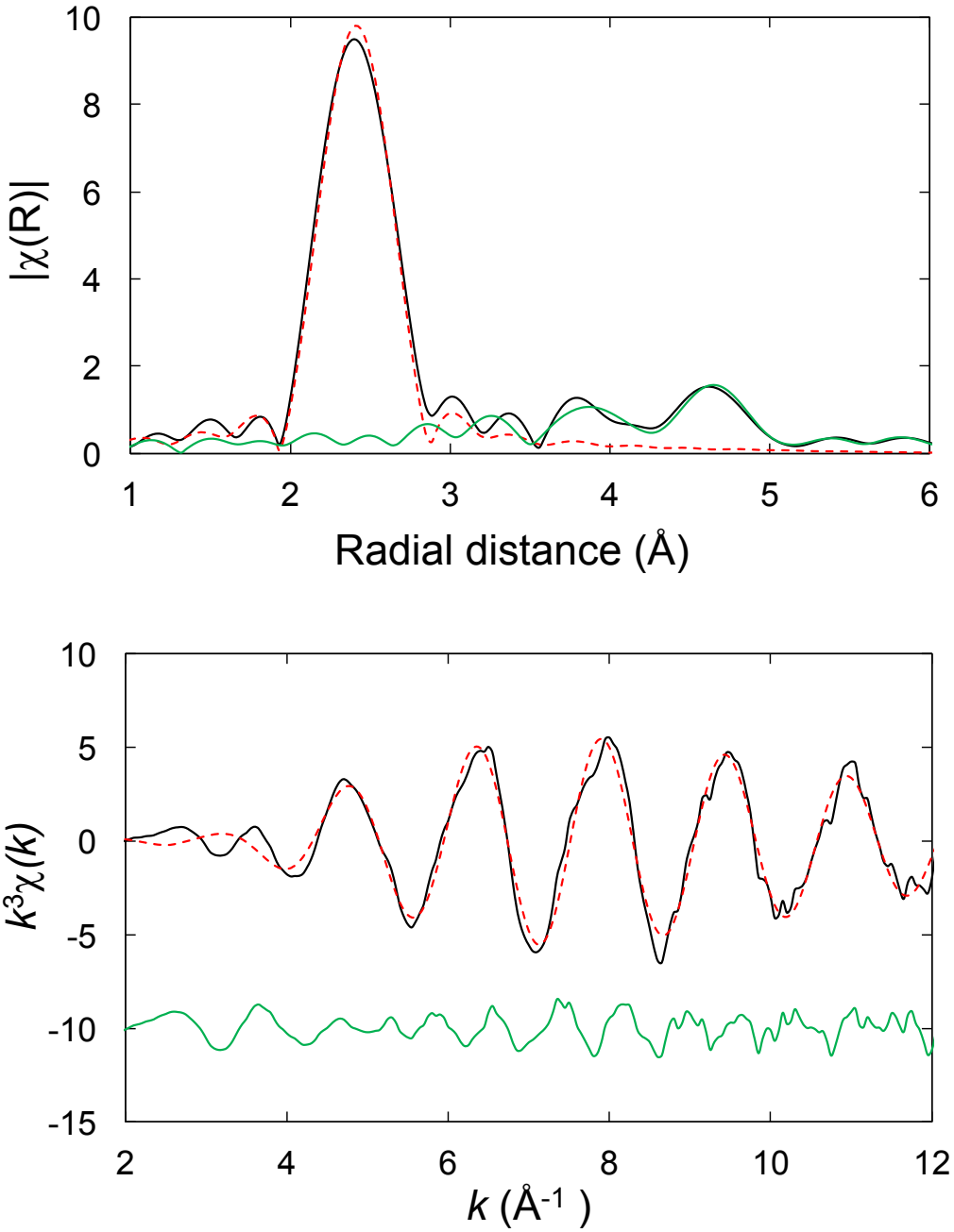

Figure S54. Single component fit of Fourier transform (top) and k-space (bottom) Se HERFD EXAFS data for Av1SeCO. Experimental data are given in black, total fit in dashed red, and residual in green.

Table S6. Parameters for single component single scattering path fits to Se HERFD EXAFS data and deconvoluted average Se–Fe distances at the 2B and 3A/5A positions

Sample	Path	ΔE_0 (eV)	N	R (Å)	σ^2 (10^{-3} Å^2)	R-factor	Reduced χ^2
$Av1Se_{lo}$	Se–Fe	4.361	2	2.318 (0.007)	2.24 (0.84)	0.06913	27.17
$Av1Se_{hi}$	Se–Fe	4.621	2	2.328 (0.007)	3.29 (0.87)	0.07139	14.49
$Av1Se_{reac}$	Se–Fe	4.838	2	2.343 (0.008)	3.90 (0.89)	0.07367	4.36
Av1SeCO	Se–Fe	5.001	2	2.394 (0.006)	5.24 (0.75)	0.04940	52.65

Position	Deconvoluted average Se–Fe distance (Å)
Se_{2B}	2.30 (0.01)
$Se_{3A/5A}$	2.39 (0.01)
$COSe_{3A/5A}$	2.41 (0.01)

[a]E_0 = 12,661.55 eV

Sample ORCA input files

ORCA input file for H-atom optimization of X-ray crystallographic structure:

```
! UKS TPSSh def2-TZVP def2/J ZORA D3BJ CPCM RIJCOSX TightSCF
! Grid5 Finalgrid6 SlowConv
! Normalprint Opt

%maxcore 4000

%method
IntaccX 4.01,4.01,4.34 #Changing the 3 radial grids
GridX 1,1,2 #Changing the 3 angular grids
end

%method SpecialGridAtoms 26
        SpecialGridIntAcc 7
end

%geom
optimizehydrogens True #Optimize only the H-atom positions
end

%basis
        newgto H "def2-SVP" end
        newgto C "def2-SVP" end
end

%scf
        MaxIter 500
end

%pal nprocs 12
end

*xyzfile +2 11 Fe2Se2SPh4Et4N4.xyz
```

ORCA input file for full geometry optimization (ferromagnetic case):

```
! UKS TPSSh ZORA-def2-TZVP def2/J ZORA D3BJ CPCM RIJCOSX TightSCF
! Grid5 Finalgrid6 SlowConv
! Normalprint Opt

%maxcore 4000

%method
IntaccX 4.01,4.01,4.34 #Changing the 3 radial grids
GridX 1,1,2 #Changing the 3 angular grids
end

%method SpecialGridAtoms 26
```

```
        SpecialGridIntAcc 7
end

%basis
        newgto H "def2-SVP" end
        newgto C "def2-SVP" end
end

%scf
        MaxIter 500
end

%pal nprocs 12
end

*xyzfile -2 11 Fe2SeS_S4C4H8_diferric.xyz
```

ORCA input file for full geometry optimization (ferromagnetic case) with bond angle constraint:

```
! UKS TPSSh ZORA-def2-TZVP def2/J ZORA D3BJ CPCM RIJCOSX TightSCF
! Grid5 Finalgrid6 SlowConv
! Normalprint Opt
! MORead
%moinp "Fe2SeS_S4C4H8_diferric_HS_opt.gbw"

%maxcore 4000

%method
IntaccX 4.01,4.01,4.34 #Changing the 3 radial grids
GridX 1,1,2 #Changing the 3 angular grids
end

%method SpecialGridAtoms 26
        SpecialGridIntAcc 7
end

%scf
        MaxIter 500
end

%geom
Constraints
{A 0 2 1 70 C} #Constrain the Fe-Se-Fe angle to 70 degrees, let all other parameters relax
end
end

%basis
        newgto H "def2-SVP" end
        newgto C "def2-SVP" end
end
```

```
%pal nprocs 12
end

*xyzfile -2 11 Fe2SeS_S4C4H8_diferric_HS_opt.xyz
```

ORCA input file for full geometry optimization (broken symmetry antiferromagnetic case):

```
! UKS TPSSh ZORA-def2-TZVP def2/J ZORA D3BJ CPCM RIJCOSX TightSCF
! Grid5 Finalgrid6 SlowConv
! Normalprint Opt

%maxcore 4000

%method
IntaccX 4.01,4.01,4.34 #Changing the 3 radial grids
GridX 1,1,2 #Changing the 3 angular grids
end

%method SpecialGridAtoms 26
        SpecialGridIntAcc 7
end

%basis
        newgto H "def2-SVP" end
        newgto C "def2-SVP" end
end

%scf
        MaxIter 500
        FlipSpin 1
        FinalMs 0
end

%pal nprocs 12
end

*xyzfile -2 11 Fe2SeS_S4C4H8_diferric.xyz
```

ORCA TDDFT input file for Se (or S) X-ray Absorption Spectroscopy (XAS) calculation on broken symmetry solution:

```
! UKS TPSSh ZORA-def2-TZVP def2/J ZORA D3BJ CPCM RIJCOSX TightSCF
! Grid5 Finalgrid6 SlowConv
! Normalprint
! MORead
%moinp "Fe2SeS_S4C4H8_diferric_BS_opt.gbw"

%method
IntaccX 4.01,4.01,4.34 #Changing the 3 radial grids
GridX 1,1,2 #Changing the 3 angular grids
end
```

```
%method SpecialGridAtoms 26
        SpecialGridIntAcc 7
end

%basis
        newgto H "def2-SVP" end
        newgto C "def2-SVP" end
end

%tddft  NRoots 100
        MaxDim          1000
        OrbWin[0]=0,0,-1,-1 #For S XAS, change donor orbital range accordingly, i.e. 5,5,-1,-1
        OrbWin[1]=0,0,-1,-1 #For S XAS, change donor orbital range accordingly, i.e. 5,5,-1,-1
#       XASLoc[0]=0,0
#       XASLoc[1]=0,0
        DoQuad          True
        TDA     True
end

%pal nprocs 12
end

*xyzfile -2 1 Fe2SeS_S4C4H8_diferric_BS_opt.xyz
```

Structures for TDDFT Calculations

Structure of BS-optimized antiferromagnetic $[Fe_2SeS(S_2C_2H_4)_2]^{2-}$ unconstrained.

Fe	4.61512201275408	10.28819646158858	0.64981928840600
Fe	6.82062356634465	11.71299201736145	-0.07999115798790
Se	5.92995150584276	9.88645886583187	-1.26340427753225
S	5.63679458402972	11.89654563706646	1.78179925840267
S	2.41518165204493	10.79194058721359	0.20358200264937
S	4.15580619085377	8.35541417475491	1.80451129964968
S	9.11208981184330	11.60304599737620	0.08509688831946
S	6.80093999831043	13.70900662175078	-1.22233487751811
C	2.32141488134819	8.49292180923434	1.78396316190142
C	1.79506696372972	9.08378042123902	0.48144255981980
C	8.56147720715498	13.65063321727703	-1.74132522487144
C	9.48333307933412	13.27151603317854	-0.58931211498751
H	1.91521509409570	7.47929579700381	1.93036621527176
H	2.00503109383499	9.11504031715642	2.63456261795408
H	2.08720268681454	8.45341762951562	-0.37180463229081
H	0.69471492529099	9.13736692990631	0.50681028320222
H	8.82542747449104	14.65089203172785	-2.12046053897073
H	8.67041815309332	12.93302370096858	-2.56843703480277
H	10.52960371992537	13.25507321031096	-0.93491551593686
H	9.40093539886338	14.00877853953769	0.22335179932191

Structure of BS-optimized antiferromagnetic $[Fe_2SeS(S_2C_2H_4)_2]^{2-}$ with constraint ∠Fe–Se–Fe = 70°.

Fe	4.59923632457864	10.38027443762605	0.78566556528800
Fe	6.76621853238719	11.78589919738180	-0.01317707381202

Se	5.84229072655980	9.96254916946678	-1.17777835731308
S	5.62859728034898	12.00116816974663	1.87203020830902
S	2.39764514300394	10.87610916396184	0.36241578787013
S	4.15637867744582	8.44976326378672	1.95730914569000
S	9.05332655600791	11.60492279602170	0.13411577490991
S	6.79438042781671	13.76912119291545	-1.16265387139813
C	2.32899433261835	8.44789412990810	1.73736168697069
C	1.88704850359764	9.11150906712989	0.43729680195043
C	8.52242475544846	13.60076281291625	-1.75790021462802
C	9.47781594556542	13.21876468780416	-0.63346330656960
H	1.99707329303103	7.39740610209094	1.75638042476558
H	1.87439109235030	8.96498105826042	2.59578917478100
H	2.31163908398933	8.58072035860010	-0.42826568525129
H	0.78875553573806	9.08009955815816	0.35311929417647
H	8.81801803149957	14.57124876528390	-2.18737345398817
H	8.55582543631516	12.84713516284235	-2.55912015165700
H	10.50347829873655	13.13206502118407	-1.02692213472978
H	9.47281202296114	13.99294588491460	0.14849038463578

Structure of BS-optimized antiferromagnetic $[Fe_2SeS(S_2C_2H_4)_2]^{2-}$ with constraint ∠Fe–Se–Fe = 75°.

Fe	4.52514434538146	10.36706323334815	0.80390084399568
Fe	6.79952964812207	11.81297501818913	-0.08917382257470
Se	5.78202561551524	9.99905841662820	-1.13199336197650
S	5.62256081597056	12.02692786040042	1.80658550985287
S	2.32237999159934	10.84337986092119	0.38646501652199
S	4.12113872470565	8.44072518958620	1.99087534274284
S	9.07865708437306	11.57538897253046	0.03998160211670
S	6.84547028062620	13.78467793555970	-1.25620550269073
C	2.29344093444048	8.41274902984713	1.76680880091048
C	1.84097592061688	9.06953820895473	0.46659803218949
C	8.60153713230106	13.65271524200551	-1.77926031945473
C	9.51404219769132	13.22902551834207	-0.63390677656729
H	1.97728225883573	7.35743119041649	1.78488870554591
H	1.83072928597276	8.92257610905723	2.62512332768580
H	2.27247262612562	8.54491640353816	-0.39933694541072
H	0.74328420039797	9.02119841749423	0.38321738553573
H	8.90434467996656	14.64362314653616	-2.15353921112840
H	8.67677264435017	12.93549350053080	-2.61036506906451
H	10.55563254708585	13.16896793329053	-0.98841290776111
H	9.46892906592206	13.96690881282355	0.18106934953112

Structure of BS-optimized antiferromagnetic $[Fe_2SeS(S_2C_2H_4)_2]^{2-}$ with constraint ∠Fe–Se–Fe = 80°.

Fe	4.46236902811179	10.35094009590410	0.85794171359969
Fe	6.86004504615785	11.85702276197271	-0.07640023834487
Se	5.77552402568532	10.05435257343621	-1.03814690265521
S	5.63098738058943	12.02034028301926	1.82551250200408
S	2.27072944847145	10.81867447444219	0.40029781688700
S	4.06716072437012	8.41834388869269	2.03179821996389

S	9.13647631888539	11.60866702534448	0.03682332466721
S	6.88589653069159	13.82331484363392	-1.24826250168730
C	2.24377781624793	8.37618122464624	1.76847905445224
C	1.80866114851366	9.03771890400211	0.46462009951575
C	8.63330394664159	13.67278078781481	-1.79979616149434
C	9.56525935021291	13.25328153611113	-0.66864252797372
H	1.93714486760843	7.31800765257762	1.77286227349625
H	1.76097056307780	8.87531738017316	2.62187140337425
H	2.25996861335522	8.52327562713469	-0.39739026545694
H	0.71321004473768	8.97823072259881	0.36217396924835
H	8.93758301598943	14.65746741524415	-2.18893869299380
H	8.68637777148194	12.94802193807579	-2.62610242249888
H	10.59859747240534	13.18392183752717	-1.04495024607171
H	9.54230688676510	13.99947902764865	0.13956958196799

Structure of BS-optimized antiferromagnetic $[Fe_2SeS(S_2C_2H_4)_2]^{2-}$ with constraint ∠Fe–Se–Fe = 85°.

Fe	4.47522941399693	10.26636959240089	0.94640329879466
Fe	7.00254214934906	11.89273826281241	0.09787095586774
Se	5.93821178153572	10.07368062037256	-0.83879901344668
S	5.69347822727200	11.90732791942734	1.98249704731255
S	2.32821702279632	10.81452870895633	0.38225676660590
S	3.97674686088018	8.31946846312709	2.04093869814481
S	9.28728444417155	11.76936743870716	0.17063322019743
S	6.88308188447507	13.84290080370447	-1.08690034089186
C	2.16139676428375	8.36161496654654	1.72115899946970
C	1.79713008961189	9.05178619375106	0.41054692678440
C	8.55985980411914	13.62998855756463	-1.81303624616264
C	9.61579043364535	13.32701975576745	-0.75582607107546
H	1.80921249146040	7.31802673569191	1.70664761207212
H	1.67386474713790	8.87581751908983	2.56280025826265
H	2.25658963057726	8.52861400762897	-0.44176643479389
H	0.70437200580743	9.03639820740412	0.26995849567125
H	8.81267695936399	14.56696920565348	-2.33414991282658
H	8.52372255241504	12.82309653557840	-2.56085006584401
H	10.60176744785078	13.21593802601904	-1.23471453709285
H	9.67517528925025	14.15368847979644	-0.03234965704928

Structure of BS-optimized antiferromagnetic $[Fe_2SeS(S_2C_2H_4)_2]^{2-}$ with constraint ∠Fe–Se–Fe = 90°.

Fe	4.32560771354719	10.29676848755944	0.84075960762247
Fe	6.96617710705785	11.88921057857008	-0.22533821535408
Se	5.70544283347259	10.13688263172285	-1.01273378136313
S	5.63299186628490	11.99549912544881	1.69905920210511
S	2.13084796887579	10.73143488612909	0.39353382966316
S	4.00256045322556	8.36188637419546	2.01970723185673
S	9.22667308747093	11.59536499086219	-0.10711082555864
S	6.99277075789298	13.84772938697298	-1.39792503739449
C	2.16913369012888	8.32402322427273	1.83423551462370

C	1.68436342942493	8.94789632342906	0.52920874272322
C	8.78038809079024	13.77234779860784	-1.82698511214669
C	9.64536757563164	13.30102105921524	-0.66316552941705
H	1.85885597585558	7.26815014226389	1.88321050941777
H	1.72440501917246	8.85110768226500	2.69142652602625
H	2.10813659439238	8.41120426312357	-0.33311613521131
H	0.58655535286362	8.88063048928094	0.46650032635635
H	9.08366751994798	14.78656212983820	-2.13140718295799
H	8.90829128752661	13.10342160004994	-2.69106026133478
H	10.70396616324111	13.28957223649051	-0.96781150054289
H	9.54014751319680	13.98462658970218	0.19233209088623

Structure of optimized ferromagnetic $[Fe_2SeS(S_2C_2H_4)_2]^{2-}$ unconstrained.

Fe	4.60402265280352	10.16408807729650	0.83523906589228
Fe	6.99371705935602	11.71510207697997	-0.02091650555971
Se	6.09245993030773	9.71129280941233	-1.02575508376618
S	5.78287751375461	11.78736020135783	1.91198364725122
S	2.47132650279483	10.78143340688577	0.27953862234264
S	3.98011317043204	8.24693216658467	1.92268109640299
S	9.28350783056786	11.69548373016736	0.01900027826838
S	6.82166879265718	13.66088589068573	-1.21077712712976
C	2.15723684322785	8.43806858616303	1.76769150510149
C	1.74693194329388	9.10190735684693	0.45909313372358
C	8.56494137070508	13.70796251634805	-1.79143360167159
C	9.55536826901822	13.37236182184498	-0.68352741706048
H	1.71609092045169	7.43101930487077	1.83554530111565
H	1.79559305239787	9.02867422127027	2.62251403349382
H	2.06064544532783	8.48772477108439	-0.39825885317491
H	0.65156810989700	9.21234088791422	0.41790045640681
H	8.75598417695024	14.72433552307260	-2.17038237409171
H	8.67743674769025	13.00355017020861	-2.62903391511880
H	10.58307936185732	13.39741927589735	-1.07950576345654
H	9.48178030650896	14.10739720510864	0.13172350103078

Structure of optimized ferromagnetic $[Fe_2SeS(S_2C_2H_4)_2]^{2-}$ with constraint ∠Fe–Se–Fe = 70°.

Fe	4.67695985292544	10.18445245570018	0.80455885009761
Fe	6.93640577434559	11.64315524359061	-0.03164509067678
Se	6.11303722576720	9.60588614329741	-1.11022508734303
S	5.81917786643705	11.76848345620723	1.93949847858814
S	2.55071407767870	10.81936575388372	0.24557010440819
S	4.02966743989377	8.28835503054083	1.91721339674190
S	9.22744571386999	11.64566827907864	0.00602545137244
S	6.75215404013176	13.59005167626259	-1.22088458601856
C	2.20999777911880	8.50023263874098	1.76118402983915
C	1.81028469275573	9.14883077237937	0.44227012669505
C	8.50432983077101	13.68091600266039	-1.76936454689390
C	9.47927684063721	13.34395136335152	-0.64899630760667

H	1.75569043917326	7.50017432281757	1.84488906480038
H	1.85725155241762	9.10844174290492	2.60735570344762
H	2.12285472072440	8.52089353744100	-0.40540858112954
H	0.71609704198556	9.26802816592716	0.39528211884336
H	8.68232443958906	14.70754300880544	-2.12653785413265
H	8.64542253305978	12.99350555456073	-2.61658240210722
H	10.51425294119059	13.39998225037755	-1.02254653815284
H	9.37300519752744	14.05742260147208	0.18166366922730

Structure of optimized ferromagnetic $[Fe_2SeS(S_2C_2H_4)_2]^{2-}$ with constraint ∠Fe–Se–Fe = 75°.

Fe	4.61338901541604	10.17057570381169	0.84139568288823
Fe	6.98710810800260	11.70915708531261	-0.01518767226402
Se	6.09515154646925	9.69754422447751	-1.02867968840799
S	5.78906377442387	11.78919945178657	1.92277543375167
S	2.48255595348613	10.79212521218874	0.28623423075465
S	3.98415410125031	8.25654796002860	1.93015167634521
S	9.27600895879218	11.69270966570269	0.02169672525733
S	6.81202052691434	13.65305379304267	-1.20650274473725
C	2.16178457280725	8.44245112347593	1.76277441192916
C	1.75877390819226	9.11111073852140	0.45474000344662
C	8.55437933470970	13.70182155444497	-1.79036706372278
C	9.54638823163759	13.36833145570732	-0.68391706725542
H	1.72311742307713	7.43372579855393	1.82184303156630
H	1.79335610202912	9.02620444997704	2.61936664957916
H	2.07864246996594	8.50153997368746	-0.40358252020309
H	0.66341178204751	9.21924191265991	0.40776638727169
H	8.74433823252986	14.71801380570828	-2.17025288963013
H	8.66505612563247	12.99653921365260	-2.62738445357512
H	10.57337314430582	13.39313383072123	-1.08187390522685
H	9.47427668831063	14.10231304653878	0.13232377223258

Structure of optimized ferromagnetic $[Fe_2SeS(S_2C_2H_4)_2]^{2-}$ with constraint ∠Fe–Se–Fe = 80°.

Fe	4.56337903463866	10.13385102396511	0.86634995931473
Fe	7.04526278151956	11.75876446254970	0.00460910158582
Se	6.10040374108381	9.76975112772077	-0.94884690009937
S	5.77459585784372	11.77301805587632	1.91796287349437
S	2.43600102936556	10.76189085778334	0.30683626078538
S	3.93552298982047	8.21089640839318	1.93595738035996
S	9.33333550285275	11.74551927377744	0.03973150932841
S	6.86100050879239	13.70204015179266	-1.18483227272469
C	2.11293701737957	8.40015471534203	1.76509184977003
C	1.71132763473475	9.08027576541022	0.46207456865800
C	8.59071535803091	13.72098737110992	-1.80704785701498
C	9.60498457072277	13.39975935778635	-0.71668699215290
H	1.67356955393059	7.39133667244616	1.81490662878051
H	1.74279010193311	8.97752222869341	2.62528609755980
H	2.03165599019915	8.47725674744604	-0.40069951552620

H	0.61616042044840	9.18999856252450	0.41495641058823
H	8.78225971882042	14.72721426593170	-2.21183797266567
H	8.67630728657329	12.99830546567187	-2.63221463148572
H	10.62197813745701	13.40158358937366	-1.14011853371496
H	9.56216276385305	14.15521389640564	0.08184203515922

Structure of optimized ferromagnetic $[Fe_2SeS(S_2C_2H_4)_2]^{2-}$ with constraint ∠Fe–Se–Fe = 85°.

Fe	4.49028285201774	10.10861213461786	0.83371949959869
Fe	7.08243064504022	11.83401874995391	0.00030299386263
Se	6.08536341020808	9.87879994382338	-0.92863258521998
S	5.70081428457535	11.79562826183951	1.86148373345818
S	2.35398483016408	10.69736212930069	0.27394043118635
S	3.91466933423206	8.16529513745254	1.88960783630399
S	9.36814438767280	11.78941569279610	0.06378072399941
S	6.93253860356233	13.78101497962342	-1.18420089333071
C	2.08684805114405	8.35833214949906	1.78530123263960
C	1.63511056432166	9.01924449573235	0.48896809936380
C	8.65893078996758	13.75032577610339	-1.81643813924522
C	9.67322507480761	13.42166614886257	-0.72833047479211
H	1.64794773374011	7.35150221183321	1.86688667402924
H	1.75242574729731	8.94934156874728	2.65066299311180
H	1.91792063901204	8.40179443079055	-0.37656861192033
H	0.53925504403915	9.13169288878671	0.48536993415104
H	8.87163337523588	14.74578363784750	-2.23689329149020
H	8.72120975562592	13.01428091423813	-2.63179057530928
H	10.68601169301409	13.38911727198301	-1.16046899414853
H	9.65760318432188	14.19211147616889	0.05661941375159

Structure of optimized ferromagnetic $[Fe_2SeS(S_2C_2H_4)_2]^{2-}$ with constraint ∠Fe–Se–Fe = 90°.

Fe	4.39178034712863	10.06881693384809	0.68999906484879
Fe	7.08205976277493	11.90260270800042	-0.10835652940986
Se	6.02816283119229	9.99028610605048	-1.02589624558957
S	5.56519224231317	11.84670914509127	1.67516838160630
S	2.22557862589441	10.57876015232559	0.17592745214411
S	3.92057288697781	8.12163048749381	1.78329577605677
S	9.35831242246910	11.79477314593003	0.05191078839825
S	7.03254288052034	13.86016969377443	-1.27861348454459
C	2.09270275666803	8.32980955529096	1.84544602866070
C	1.51865804745151	8.92609611416535	0.56616072969545
C	8.79029730845079	13.81244013265758	-1.81674670439916
C	9.73768016292160	13.43751417521454	-0.68428703980523
H	1.65872273173313	7.33298143745098	2.02139902630032
H	1.84662203478105	8.96723575861681	2.70742708457554
H	1.70415076241448	8.25677686393093	-0.28684562956790
H	0.42964451804443	9.05559335089542	0.66991920734403
H	9.04284939762804	14.81395390653126	-2.19894043474752
H	8.88352815784358	13.09629493363567	-2.64663417740921

H	10.77093900268643	13.39247537500807	-1.06351628744510
H	9.69635312010625	14.19042002408829	0.11650299328782

Structure of BS-optimized antiferromagnetic $[Fe_2SeS(S_2C_2H_4)_2]^{3-}$ unconstrained.

Fe	4.55963664490296	10.33926649317461	0.78459538652835
Fe	6.75474584740586	11.71212399448470	-0.13670518491617
Se	5.71380961069945	9.82009313085995	-1.21472493879406
S	5.64044634670266	11.95365307446378	1.83171806469673
S	2.31296819448588	10.83063549257877	0.44044106969558
S	4.06277778825238	8.42097184064580	2.03086211764062
S	9.07245915762896	11.62514305281148	-0.00324224777409
S	6.88904784408089	13.66914654159759	-1.40577254908815
C	2.23863313611431	8.39853013588101	1.80076711129367
C	1.80003732706900	9.06759521063648	0.50310351034917
C	8.68126216470881	13.72887602586276	-1.80379492834213
C	9.54800404370507	13.28468572853113	-0.63368658756684
H	1.91311094049213	7.34525541110801	1.81115451695243
H	1.77054363260441	8.90552584144096	2.65877849911318
H	2.23191873763815	8.53993188077896	-0.36138355219967
H	0.70182309531972	9.03116209339800	0.41324096162809
H	8.94060975313955	14.76204558615826	-2.09041334744400
H	8.87447426335553	13.08063937098921	-2.67454038439068
H	10.60528427073086	13.24657381006417	-0.94657913878203
H	9.46475720096339	14.01348528453435	0.18950162139999

Structure of BS-optimized antiferromagnetic $[Fe_2SeS(S_2C_2H_4)_2]^{3-}$ with constraint ∠Fe–Se–Fe = 70°.

Fe	4.56440468876316	10.33742735984467	0.78520494837194
Fe	6.75711485852569	11.70730464557520	-0.13260347629393
Se	5.71874505425133	9.81381185432439	-1.21429151151477
S	5.64522404786607	11.94785900582293	1.83690211028676
S	2.31916861584311	10.83354978568998	0.43998115961981
S	4.06381568400020	8.41871764980986	2.02882512351209
S	9.07498879657040	11.62663417057270	-0.00109717997337
S	6.88529470035820	13.66498217890709	-1.40250288852798
C	2.23954546086996	8.40149809712522	1.79930128406859
C	1.80221780188098	9.07186602196824	0.50180323793216
C	8.67590502119623	13.72594566519899	-1.80411620371233
C	9.54502942638405	13.28589844640652	-0.63409849004478
H	1.91120396134952	7.34909364375530	1.80953874699633
H	1.77293354017771	8.90953316130339	2.65749688870035
H	2.23253029487825	8.54343208394988	-0.36298957628895
H	0.70388937324094	9.03785253860190	0.41240322347877
H	8.93459499780067	14.75827074185143	-2.09429320925298
H	8.86788958764322	13.07511944936524	-2.67318890490147
H	10.60224431860910	13.25168859003032	-0.94767492203407
H	9.45960976979122	14.01485490989671	0.18871963957777

Structure of BS-optimized antiferromagnetic $[Fe_2SeS(S_2C_2H_4)_2]^{3-}$ with constraint ∠Fe–Se–Fe = 75°.

Fe	4.44321088478813	10.37333144704405	0.76300407053230
Fe	6.74070326522936	11.82868871341039	-0.20792580782981

Se	5.61028835678533	9.98593751578433	-1.23796121758213
S	5.52791095867659	12.04886839464353	1.74186841583156
S	2.17228284723886	10.77960784427004	0.49219514930103
S	4.06849189993427	8.41643656005615	1.99221391302251
S	9.04792883681168	11.65092335045838	0.01136624374926
S	6.98776839675817	13.76076326294303	-1.48706662067237
C	2.23880647730860	8.33142061281841	1.82487775798981
C	1.73089308390975	8.99671269414048	0.55077391185968
C	8.79482861428108	13.74708237275567	-1.82438467893541
C	9.60594661771402	13.28445967300770	-0.62180030529127
H	1.95169690123192	7.26706018601246	1.83452975594434
H	1.78306975166271	8.81295639780780	2.70388325032782
H	2.15313160276517	8.49594049266359	-0.33423922432631
H	0.63260296619899	8.91889809322790	0.49667033350802
H	9.10222936314144	14.76597453355522	-2.11423653364487
H	8.98981902615571	13.08119204623801	-2.68121782270661
H	10.67048293532320	13.20360754286761	-0.89981472337025
H	9.52425721408507	14.02547826629529	0.19058413229267

Structure of BS-optimized antiferromagnetic $[Fe_2SeS(S_2C_2H_4)_2]^{3-}$ with constraint ∠Fe–Se–Fe = 80°.

Fe	4.35631620148958	10.36586597197087	0.74490204188230
Fe	6.77119427000941	11.89963167222635	-0.25569064323414
Se	5.57972907884754	10.07684422930968	-1.22030423724248
S	5.46668888848369	12.07276734122164	1.68497246011935
S	2.07868207401803	10.71919216946988	0.47910961504374
S	4.04472278959046	8.39671522675845	1.96742937134122
S	9.06759796799867	11.68793625980800	0.01520424715200
S	7.06340442116211	13.82380135829473	-1.52727524416389
C	2.21227402447067	8.29367747009408	1.85094188651529
C	1.66435353938389	8.93175533599564	0.57945249968682
C	8.87438849609033	13.77705517536048	-1.83922504491767
C	9.66267347322609	13.30571587424190	-0.62446889077509
H	1.93653443150053	7.22688627569764	1.88553214670703
H	1.77541224910724	8.78558675998093	2.73364841667255
H	2.06946688639850	8.42059581557601	-0.30756636275007
H	0.56612274206902	8.84079090760567	0.55477526118554
H	9.20237393508507	14.78962932513255	-2.12820094355281
H	9.06868816634860	13.10546804898291	-2.69166946260213
H	10.72820422544517	13.20196929794918	-0.89053988772804
H	9.58752213927546	14.05345548432359	0.18229277066048

Structure of BS-optimized antiferromagnetic $[Fe_2SeS(S_2C_2H_4)_2]^{3-}$ with constraint ∠Fe–Se–Fe = 85°.

Fe	4.27575692134883	10.35074265423059	0.73404583924080
Fe	6.82366664108677	11.94427516982729	-0.30060174717266
Se	5.56226800456956	10.13848416734098	-1.19368777576013
S	5.42799007406530	12.07153983369946	1.64105879713839
S	1.99656100817961	10.66283333380942	0.45436158689437
S	4.01143950425017	8.37456512992700	1.94964646777841
S	9.10746060128686	11.72485533479059	0.01047333492809
S	7.12979429997538	13.85634154010618	-1.56995922179700
C	2.17759192836349	8.26779602735432	1.87855737824935

C	1.60055088944799	8.87431417715888	0.60476385113731
C	8.94457745030270	13.80444458168263	-1.85740533817216
C	9.71520152029887	13.33794283131768	-0.62918429660197
H	1.90553389446694	7.20164129185790	1.94524425419825
H	1.76183359959494	8.78108076491494	2.75909381767052
H	1.99259221056221	8.34679364364539	-0.27851603641838
H	0.50284105047359	8.77522919787479	0.60346469225376
H	9.27720681500469	14.81533369164692	-2.14711406790208
H	9.14881754043150	13.12853615739181	-2.70400157655356
H	10.78396261764940	13.22882980674382	-0.87956968718124
H	9.63070342864117	14.08976066467936	0.17264972806993

Structure of BS-optimized antiferromagnetic $[Fe_2SeS(S_2C_2H_4)_2]^{3-}$ with constraint ∠Fe–Se–Fe = 90°.

Fe	5.20677940709374	9.67115090253934	0.73415716326670
Fe	7.18526761396323	11.05857364442584	0.24461297257752
Se	6.94889708598863	8.71916961579879	-0.64171762619794
S	6.22060135430543	10.91940786135484	2.26931396766299
S	3.38129314174572	10.68789894739259	-0.31043509841813
S	3.86371885953710	8.02289252321266	1.68281216615532
S	9.26347460443777	11.98981034414980	0.30129829539828
S	6.47410527785900	12.63673882829106	-1.28696605300974
C	2.30432948130901	8.99079932076963	1.64043319338453
C	2.03876626574098	9.56572722611694	0.25500579161246
C	8.06681223701373	13.42552036476894	-1.75830326158748
C	8.99367689737441	13.58889478599187	-0.56497367988263
H	1.48548952831940	8.31446155511615	1.93639310976829
H	2.36348845887892	9.80123398262782	2.38351643405754
H	1.93192348814309	8.74478717858858	-0.47161384691945
H	1.09871395304905	10.14178431627380	0.25628732822931
H	7.85006509796081	14.40829791913900	-2.21042307087022
H	8.55887317478646	12.80349691162201	-2.52456051205932
H	9.97487605593387	13.97373056076625	-0.89091211077292
H	8.56519801655964	14.31096321105404	0.14939483760488

Structure of optimized ferromagnetic $[Fe_2SeS(S_2C_2H_4)_2]^{3-}$ unconstrained.

Fe	4.79212776205826	10.22908208258341	0.93337791062495
Fe	6.88140059417166	11.52341474382005	0.02146692788330
Se	6.05879225507475	9.46316983470475	-0.97806231321721
S	6.07467110362234	11.65362286903359	2.16693513254073
S	2.65995964523927	10.97952999210556	0.38296223371461
S	3.96727797597789	8.38903324186500	2.18145238343595
S	9.23948708240506	11.55715040789048	-0.11002668374081
S	6.62571114005528	13.49489257675000	-1.19827381561390
C	2.19831325499359	8.55614065938172	1.70457939205758
C	2.00041014054320	9.26365167341891	0.36800753346302
C	8.36590121165346	13.63666883524042	-1.77460798738332
C	9.37755422595524	13.29763947632145	-0.68560994339703
H	1.76389547367875	7.54400018932053	1.65480536333515
H	1.66867459566598	9.10952384834282	2.49616809428449

H	2.50352197274656	8.70117420422759	-0.43440280082627
H	0.92601074682252	9.31561557219004	0.12561801461536
H	8.51615189756669	14.67395819936249	-2.11713182355641
H	8.51289139147720	12.97038015461413	-2.63883984300151
H	10.39905160829882	13.44014028058673	-1.07647996918113
H	9.24454592199343	13.97655115824032	0.17138219396241

Structure of optimized ferromagnetic $[Fe_2SeS(S_2C_2H_4)_2]^{3-}$ with constraint ∠Fe–Se–Fe = 70°.

Fe	4.54346773258003	10.36283209673609	0.68380861865993
Fe	6.75695492206254	11.76732185896493	-0.18159507368019
Se	5.79918982478910	9.87426386546997	-1.31278151893703
S	5.60445253675869	12.07131149902190	1.77777203878552
S	2.27478253447703	10.79314379100359	0.31745369167504
S	4.11783171006793	8.42637153008726	1.96051191779223
S	9.09003530223533	11.54169925613559	-0.04403142331276
S	6.88199959011247	13.76937931285907	-1.38957002612747
C	2.28309255091428	8.43493065641576	1.82534170091421
C	1.78443789135274	9.03198048554408	0.51344205925924
C	8.67627351061885	13.70191555837986	-1.77648114462333
C	9.51358822395541	13.24522358229370	-0.58723434394432
H	1.93728394720636	7.39172219724310	1.91564967331172
H	1.86591251781252	9.00097708488896	2.67297479219882
H	2.17989147087946	8.45432978208086	-0.33657902201872
H	0.68352249567652	8.98311837686194	0.47406852226020
H	8.98695030119007	14.71352840022831	-2.08593061638934
H	8.83789370059172	13.02308949374241	-2.62820674636807
H	10.58145314163197	13.24953477637473	-0.86247577158042
H	9.37733609508686	13.93866639566769	0.25718267212466

Structure of optimized ferromagnetic $[Fe_2SeS(S_2C_2H_4)_2]^{3-}$ with constraint ∠Fe–Se–Fe = 75°.

Fe	4.45164838416079	10.34555516666268	0.64526543357542
Fe	6.78354119763628	11.84592834410706	-0.25606836671049
Se	5.75159485189930	9.98213094608819	-1.33886809265330
S	5.53182022338728	12.10676513777071	1.66637970610661
S	2.16540820619136	10.71981327209573	0.32246947079225
S	4.09718112512943	8.38933099366843	1.89958511570245
S	9.10101526036308	11.56986527754813	-0.05898144515877
S	6.98198655472464	13.83939179957830	-1.47007584003799
C	2.25840083544795	8.38237430456411	1.85962538971780
C	1.68907000161418	8.96130960620899	0.56905704400007
C	8.78790718982506	13.74796357663984	-1.79135128033085
C	9.57549555577067	13.26759044672639	-0.57777486860518
H	1.92753497403235	7.33712954695472	1.97689261178889
H	1.88091134912494	8.95341664049788	2.72219812551159
H	2.03656478126402	8.37144946396015	-0.29334658028542
H	0.58774427093533	8.91328163871197	0.59086337588775
H	9.12410750688079	14.75773657670541	-2.07892792182322

H	8.96835572971706	13.07486620383081	-2.64372608799090
H	10.65188970057251	13.25194906896742	-0.81664808580185
H	9.42417230132290	13.95749198871306	0.26675229631506

Structure of optimized ferromagnetic $[Fe_2SeS(S_2C_2H_4)_2]^{3-}$ with constraint ∠Fe–Se–Fe = 80°.

Fe	4.54675377889564	10.13081199321208	0.76290785002258
Fe	7.00748750770285	11.74061690639831	-0.09941959100653
Se	6.03674333077351	9.79944377691132	-1.07384457530791
S	5.73825481223508	11.80904684891671	1.84462867168025
S	2.34399822950982	10.70516234685382	0.25643582055671
S	3.93500495679063	8.17696734208994	1.90794524186974
S	9.34925383803857	11.71484808375505	-0.02060727218828
S	6.91793424822089	13.74093501350493	-1.28727430268114
C	2.10974720498952	8.39461153097515	1.82077528588976
C	1.64633851034876	9.02429983271193	0.51200695198260
C	8.67889572232517	13.76954670459622	-1.81070867843619
C	9.63231671805812	13.40883205616405	-0.67729241932449
H	1.65157718018567	7.39859125178270	1.93715530406098
H	1.78419400488746	9.01641802459252	2.66910932414071
H	1.93221890900193	8.38457626230038	-0.33716862532010
H	0.54751473726851	9.11669811233074	0.51087234456905
H	8.90148524795509	14.78614073457461	-2.17453495872328
H	8.81531562844622	13.07180762586986	-2.65133290895795
H	10.67197048905406	13.45296290797677	-1.04197402943813
H	9.52934494531227	14.13302264448291	0.14564056661159

Structure of optimized ferromagnetic $[Fe_2SeS(S_2C_2H_4)_2]^{3-}$ with constraint ∠Fe–Se–Fe = 85°.

Fe	4.50844773880632	10.04568705203014	0.73789917914947
Fe	7.08843066500976	11.76028514765487	-0.10807108817275
Se	6.06292240520161	9.84217037357602	-1.05437149573346
S	5.74859524212982	11.72551486064137	1.81703337711143
S	2.31632070558565	10.63083318598972	0.20194701923265
S	3.87893862269206	8.09881655980759	1.86599792823234
S	9.42339710361693	11.77804914382465	-0.00962619399197
S	6.96715133429506	13.75833354759672	-1.29694250397272
C	2.05914815882408	8.37514445626345	1.84275614733198
C	1.56700727405141	8.98616962040285	0.53630920979239
C	8.72718772839215	13.80630812767582	-1.82350651275723
C	9.68747763807281	13.46704655388701	-0.68993996080568
H	1.57484530043430	7.39782157623801	2.00233556632635
H	1.78811087551154	9.02823091462563	2.68661725217737
H	1.79350463037185	8.31229272023159	-0.30433508448542
H	0.47351681285003	9.12170682440171	0.57670182111718
H	8.93633482239403	14.82243875323321	-2.19629081539853
H	8.86976531063923	13.10353637382394	-2.65889735069931
H	10.72544461415164	13.51665698594057	-1.05827964082451
H	9.57980301696969	14.19829722215515	0.12598314637038

Structure of optimized ferromagnetic $[Fe_2SeS(S_2C_2H_4)_2]^{3-}$ with constraint ∠Fe–Se–Fe = 90°.

Fe	4.38909722255804	10.01534747957875	0.57182279414569
Fe	7.06755777342981	11.87477781084411	-0.19335530775647
Se	6.01473706881930	9.98840226452658	-1.15503312688244
S	5.56110000386261	11.81363479280414	1.62866376992822
S	2.16588554524351	10.46372150415010	0.04426599716601
S	3.89672094699931	8.06384937505286	1.74303649380581
S	9.38304516884918	11.82933018003378	0.06243214976205
S	7.08081866606445	13.86719803619327	-1.38758480600053
C	2.08526959770720	8.35330283024753	1.89970236837919
C	1.44841878686460	8.86811251884972	0.61400276510790
C	8.86497526320002	13.84320017330961	-1.82712053023907
C	9.75396667489324	13.48843526673702	-0.64177295014445
H	1.62149601819116	7.39427143888434	2.18331282128583
H	1.90920865651525	9.06761311923023	2.71865834001037
H	1.56459375307515	8.12232909158791	-0.18759415580511
H	0.36945225929354	9.02800145936772	0.77501427338857
H	9.12866908083435	14.84527080688066	-2.20292556655385
H	9.02170951047756	13.12286875415105	-2.64473785639340
H	10.80926688199692	13.48412968889917	-0.96052344981051
H	9.64036112112477	14.24154340867159	0.15305597660612

Structure of BS-optimized antiferromagnetic $[Fe_2SeS(S_2C_2H_4)_2]^{4-}$ unconstrained.

Fe	4.42875844516041	10.36896943229035	0.38875514127700
Fe	6.68501693109120	11.85977508201897	-0.37894054528493
Se	5.69655219455018	10.04177674985002	-1.66958073987752
S	5.39133994844231	12.12622339413368	1.48234199106118
S	2.08566756949745	10.48855764558711	0.09716139585938
S	4.11098037087959	8.41024715508669	1.68419754539766
S	9.00701750186402	11.67642345653891	0.05255328803877
S	7.11795034297744	13.82555481585621	-1.61780701327614
C	2.28966054731175	8.38263459046695	1.92751146910629
C	1.53341371086533	8.83817342437611	0.68703567324276
C	8.94916510594143	13.80099112415127	-1.76619639428331
C	9.62854762352292	13.31795436151623	-0.49190908442678
H	1.98552954241764	7.35570647122861	2.19399767015264
H	2.03218239885111	9.03701172166533	2.77742261254325
H	1.68044283124152	8.10557921936195	-0.12448764621221
H	0.45244505132276	8.88364379170403	0.90593148722486
H	9.29691996699899	14.81912176937913	-2.01222542991950
H	9.22914600454641	13.14163890996567	-2.60517352301583
H	10.71806991690124	13.24696050037611	-0.65408997024054
H	9.45754399561631	14.04839638444669	0.31682207263296

Structure of BS-optimized antiferromagnetic $[Fe_2SeS(S_2C_2H_4)_2]^{4-}$ with constraint ∠Fe–Se–Fe = 70°.

Fe	4.42712154950634	10.37356477399995	0.37387221448770
Fe	6.67270190954026	11.86028815938648	-0.39449320040834
Se	5.68226944855571	10.04611056150640	-1.69410961145753

S	5.38161038228894	12.13427797317172	1.46517001906534
S	2.08096541121485	10.48998615912511	0.09950865596803
S	4.12192306065849	8.40884801061177	1.66273280094944
S	8.99362640676309	11.66535727671306	0.04503338808301
S	7.12103445418212	13.82472334633283	-1.62897473338668
C	2.30408690145498	8.38567453987639	1.92880989003217
C	1.53502382689686	8.83947467827651	0.69547870651044
C	8.95328772073163	13.80011417230571	-1.76115232681430
C	9.61982858576432	13.31039548618714	-0.48265269044573
H	2.00025397997506	7.36014017508184	2.20123761986092
H	2.05664140416856	9.04300795510393	2.77943896892352
H	1.67476044989704	8.10638757957512	-0.11690438128101
H	0.45616622695780	8.88496895996645	0.92459329081891
H	9.30367988614545	14.81936791210010	-1.99875464821640
H	9.24141935404537	13.14474435154355	-2.60059238111311
H	10.71120545943776	13.24183301465711	-0.63310463546280
H	9.43874358181547	14.03607491447883	0.32818305388639

Structure of BS-optimized antiferromagnetic $[Fe_2SeS(S_2C_2H_4)_2]^{4-}$ with constraint ∠Fe–Se–Fe = 75°.

Fe	4.40252364693728	10.32286676181092	0.46851912183680
Fe	6.75943412807673	11.88265591969965	-0.35321073499612
Se	5.71338953444463	10.05720969409154	-1.54474372238875
S	5.45111378107735	12.07735159977947	1.53498380245619
S	2.06411401207374	10.50295257399194	0.16940187233918
S	4.04609306488604	8.34407594014633	1.71094548814493
S	9.08358005732885	11.71764691646255	0.02938613903713
S	7.14489859982585	13.84627685888583	-1.60973001033349
C	2.21934818365130	8.32364723962850	1.91932964056463
C	1.48693381664130	8.83696769184813	0.68699486977558
C	8.97345471640422	13.83516514519215	-1.79765616549381
C	9.68524396652960	13.35873904011730	-0.53858337336187
H	1.90279349137046	7.28902539011680	2.13644917344010
H	1.95168057773740	8.94354473235359	2.79166335869323
H	1.63788986199478	8.13620973193907	-0.15132861037402
H	0.40350455450418	8.88636101487789	0.89195312977233
H	9.30720501980936	14.85584224780698	-2.05179615232115
H	9.23954522054673	13.17751711274200	-2.64240255613827
H	10.77031806180676	13.28969002050522	-0.72860296833367
H	9.53328570435340	14.09159436800403	0.27174769768101

Structure of BS-optimized antiferromagnetic $[Fe_2SeS(S_2C_2H_4)_2]^{4-}$ with constraint ∠Fe–Se–Fe = 80°.

Fe	4.68721719707669	9.87450339069030	0.70886997607012
Fe	7.14979460308476	11.55357546885135	-0.08772351447100
Se	6.25393583813109	9.55894791088398	-1.07969485446542
S	5.96870812955290	11.40954537559999	1.92663443493449
S	2.50702326612333	10.52767514181303	0.07100510750241
S	3.77486639184511	8.02683428866013	1.82693262955016
S	9.46728891761515	11.88961153160499	0.00059747966793
S	6.94537719927690	13.53857224121243	-1.36154103601248
C	1.98108706060611	8.43881719206854	1.84819133762119
C	1.51729998847100	9.05111031552761	0.53398601016042

C	8.69330178767193	13.85775957354185	-1.83085731722043
C	9.65515252976483	13.58915626861540	-0.68213782640003
H	1.41392058294153	7.51562105705746	2.05660226651078
H	1.78613477481744	9.14463574596590	2.67321211881250
H	1.59859650110588	8.29946456448323	-0.26980510979598
H	0.45669167074387	9.34671767451879	0.61034012446630
H	8.78875393094037	14.90615193262090	-2.16224139312513
H	8.95568486268478	13.21311236321942	-2.68681248916742
H	10.69581662439546	13.71397758504771	-1.02806013561166
H	9.47969814315095	14.31955037801709	0.12582219097325

Structure of BS-optimized antiferromagnetic $[Fe_2SeS(S_2C_2H_4)_2]^{4-}$ with constraint ∠Fe–Se–Fe = 85°.

Fe	4.51605437252561	9.96417014911159	0.61795922720120
Fe	7.09717069220428	11.72508675160984	-0.17553163561143
Se	6.09396509326002	9.80165673448381	-1.16584075442344
S	5.74545936222188	11.63595470647709	1.76780431692102
S	2.27633756744293	10.41490387957987	0.02708483222015
S	3.80243767581936	8.08692087549344	1.81980365316661
S	9.42598235199197	11.88252605463186	0.01130174472577
S	7.08306450962654	13.71018681981576	-1.44470461061463
C	1.98517857171842	8.36642709417785	1.90788296993157
C	1.41711079595957	8.89179937068268	0.59670333387185
C	8.86589447183781	13.89989879277324	-1.84616099712626
C	9.75974540470147	13.56456456869854	-0.66064924198396
H	1.49718568522546	7.41327127551945	2.17436117914225
H	1.77379000827611	9.08654682797395	2.71632302327296
H	1.51001963757412	8.11591880140161	-0.18205657852124
H	0.34381968731397	9.11905304995595	0.71717725950871
H	9.04781809342306	14.93856940535971	-2.17134514981585
H	9.11232770621256	13.23699839745428	-2.69267043057911
H	10.81915598455785	13.61499979636708	-0.96523813664962
H	9.60383232810700	14.30588664843250	0.14111599536343

Structure of BS-optimized antiferromagnetic $[Fe_2SeS(S_2C_2H_4)_2]^{4-}$ with constraint ∠Fe–Se–Fe = 90°.

Fe	4.26487503769974	10.12965144028500	0.45868524971672
Fe	6.95151611033854	11.97328528617693	-0.38032757976917
Se	5.81200681637029	10.12904828568058	-1.35288611471109
S	5.41648834621132	11.97820412265555	1.47289209863121
S	1.96006460647422	10.30558984588358	0.05483727985196
S	3.88080511323742	8.19038326788762	1.72591718895502
S	9.25666048073385	11.86116821890369	0.03344363046304
S	7.28111779709514	13.93730336631303	-1.62531173479215
C	2.05854421982793	8.25608682961031	1.96968881017848
C	1.31348366195794	8.71775082354938	0.72359463368120
C	9.10690354621068	13.94104548995200	-1.84394594552728
C	9.84982801864845	13.48639090416583	-0.59427173360937
H	1.70802156903087	7.25110417410613	2.26040603884661
H	1.83928674251935	8.93975230236072	2.80681554732140
H	1.38964916633728	7.94722714146920	-0.06176358430714

H	0.24386570115930	8.84986291532442	0.96087603329782
H	9.42478019623271	14.96243922505913	-2.11427329670870
H	9.36144993535821	13.27881681944695	-2.68836271715935
H	10.92746829828854	13.40180171532844	-0.81595891846033
H	9.72953463626820	14.23842782584160	0.20326511410111

Structure of optimized ferromagnetic $[Fe_2SeS(S_2C_2H_4)_2]^{4-}$ unconstrained.

Fe	4.38000302835308	10.31371945592654	0.46415809528859
Fe	6.77187054733413	11.90026471339111	-0.36572247395490
Se	5.72766904283991	10.00966374808191	-1.61405859518843
S	5.41524753640192	12.11937318380989	1.52614130688261
S	2.04766901704434	10.47789730841230	0.13934436167316
S	4.04225817989312	8.34889177793652	1.72731850583034
S	9.09013883735108	11.71665282916750	0.02938110049861
S	7.15740014120714	13.85707268649059	-1.62772651911089
C	2.21543334357265	8.33855458623482	1.93599300700325
C	1.48552337691201	8.81612411442769	0.68773782418671
C	8.98778136654058	13.83516576125088	-1.79681288702432
C	9.68480021601311	13.36476961450364	-0.52711339726493
H	1.89842720969349	7.31081152750088	2.18280950455887
H	1.94776523980156	8.98361922038281	2.78962852813167
H	1.64912257788907	8.09892200408676	-0.13395064481561
H	0.40035834233148	8.85920497459388	0.88430229798189
H	9.32735671866904	14.85313795754615	-2.05381903388866
H	9.25989971261932	13.17151729127364	-2.63464445009981
H	10.77301696697824	13.30421992094555	-0.70061135986397
H	9.51460859855473	14.09575732403697	0.28096482917581

Structure of optimized ferromagnetic $[Fe_2SeS(S_2C_2H_4)_2]^{4-}$ with constraint ∠Fe–Se–Fe = 70°.

Fe	4.39872620536003	10.34223602520086	0.36392023993921
Fe	6.70523243811888	11.87262594574969	-0.42137479281517
Se	5.69406544787973	10.00734117772126	-1.75816777981478
S	5.36687472594281	12.15419396129905	1.46485439235842
S	2.05667734675487	10.47449786564808	0.08338203199473
S	4.11656279847643	8.37499893494528	1.63851120599809
S	9.01517842001905	11.65235937216479	0.02152444550918
S	7.13380760134320	13.84391570322480	-1.64899158825390
C	2.30362423047540	8.39254267550665	1.93853093383716
C	1.52062512295048	8.83076117285060	0.70803811148450
C	8.96828476266045	13.81081037955399	-1.75731989838260
C	9.61871883191094	13.31700625145588	-0.47190968459103
H	1.98938036021364	7.37840934916255	2.23954510748925
H	2.08318811023900	9.07306753908900	2.77797942679136
H	1.64870174686127	8.08599222551183	-0.09551582392083
H	0.44486560525777	8.88118108159584	0.95014089204318
H	9.32319509449965	14.83001889732454	-1.98774448148991
H	9.26563723204020	13.15720633758003	-2.59468468238385

H	10.71357259696475	13.26799494493814	-0.60196544747443
H	9.40943132203147	14.02818015947714	0.34456739168137

Structure of optimized ferromagnetic $[Fe_2SeS(S_2C_2H_4)_2]^{4-}$ with constraint ∠Fe–Se–Fe = 75°.

Fe	4.36495232957963	10.30278204847003	0.47559377285800
Fe	6.79523930312211	11.90572933290260	-0.36071714549986
Se	5.74101664482505	10.01199135180569	-1.57866098777077
S	5.42436808822792	12.10449619025671	1.52971830103400
S	2.03543761821565	10.46693119180816	0.14200062365937
S	4.01972161793145	8.33901156777589	1.73904657449817
S	9.11402134414686	11.73686360901728	0.03122654689929
S	7.17047962311586	13.86146202954583	-1.62541997010321
C	2.19188704484655	8.32452745944324	1.93807557021771
C	1.46627206644889	8.80681135491902	0.68906223682624
C	8.99994016417875	13.84695396028942	-1.80525571260647
C	9.70690927098483	13.38103655476484	-0.53933211535176
H	1.87543206766498	7.29510672996900	2.17842137395821
H	1.91982756504807	8.96477604246476	2.79390536623764
H	1.62788209292497	8.08995392241991	-0.13327242266308
H	0.38107754911829	8.85425050878572	0.88420956274629
H	9.33381894200594	14.86592055836698	-2.06567996240583
H	9.26903939215751	13.18338367092382	-2.64408726031548
H	10.79335847517744	13.31725281215820	-0.72237828853329
H	9.54566880027929	14.11609910391289	0.26686393631484

Structure of optimized ferromagnetic $[Fe_2SeS(S_2C_2H_4)_2]^{4-}$ with constraint ∠Fe–Se–Fe = 80°.

Fe	4.30512886368774	10.26088271785628	0.48119800844602
Fe	6.84855578234455	11.95618126783475	-0.36161692599052
Se	5.75153334596105	10.07392527676906	-1.51142534575970
S	5.40374285198569	12.07792667787296	1.50087453084242
S	1.98117729414695	10.40940224538124	0.13476364165244
S	3.96331597516870	8.29988748725592	1.74347492191563
S	9.16005186551645	11.80287914167210	0.05348864092007
S	7.22757813118296	13.91081910910593	-1.62126988797322
C	2.13618410209102	8.28163728494193	1.95139758157142
C	1.40146695121269	8.76062146590673	0.70624616236188
C	9.05491448306928	13.88107448158854	-1.82467393032371
C	9.77738307502579	13.42183827235224	-0.56473821603005
H	1.82267476292494	7.25226186217024	2.19529332434807
H	1.86954872055484	8.92288001805153	2.80811436300961
H	1.54500674896095	8.03487064712578	-0.11162768849848
H	0.31944714796026	8.82176494960035	0.91429586497877
H	9.39373726487375	14.89453053982642	-2.09961642838460
H	9.30554103817892	13.20763283505502	-2.66127935128399
H	10.85764733833309	13.32869103085861	-0.77004766512373
H	9.65171425682040	14.17563268877437	0.23046839932166

Structure of optimized ferromagnetic $[Fe_2SeS(S_2C_2H_4)_2]^{4-}$ with constraint ∠Fe–Se–Fe = 85°.

Fe	4.27442656903355	10.17488856995235	0.46541181258535
Fe	6.92190491468569	11.96204870032125	-0.37615606756804
Se	5.80170430313751	10.07588619975101	-1.44603275160713
S	5.42231704273008	11.99444900875616	1.47666951984055
S	1.96177758230059	10.34395350877096	0.09006059140535
S	3.90299947144689	8.22323323480202	1.72769504264256
S	9.23205145016854	11.84558668217980	0.03673164536464
S	7.26631112493520	13.92552930541411	-1.62598970998771
C	2.07974864224691	8.26244632886401	1.96759720574255
C	1.33474225621687	8.73499454182220	0.72541502891503
C	9.09346284288055	13.92803120926257	-1.83680328159479
C	9.82910570820506	13.47237783019495	-0.58294538385821
H	1.74053410845493	7.24892620090952	2.24135510886209
H	1.84893977648639	8.93059894868172	2.81404519577992
H	1.42940848138257	7.98100760738097	-0.07385375869791
H	0.26139260869909	8.84482861715961	0.95684114013371
H	9.41434136795553	14.94861572689447	-2.10660873746158
H	9.35124133411624	13.26471136854570	-2.67936716454728
H	10.90873538150973	13.39057815989446	-0.79585104174906
H	9.70120503340810	14.22264825044210	0.21510560579995

Structure of optimized ferromagnetic $[Fe_2SeS(S_2C_2H_4)_2]^{4-}$ with constraint ∠Fe–Se–Fe = 90°.

Fe	4.23079676834521	10.11413506899653	0.44207077720369
Fe	6.96954932639053	11.98925017688698	-0.41310983734217
Se	5.80151529799676	10.11904856647171	-1.40913321749295
S	5.41509429739123	11.95818696175758	1.43539467394558
S	1.92304747401301	10.28702712182640	0.06933513147986
S	3.86087795914814	8.17543631291657	1.71542892159152
S	9.26944356770396	11.88023085897741	0.02864072321968
S	7.31492108599563	13.95306018181128	-1.65302902504315
C	2.04202637661002	8.23837498828176	1.98469389805925
C	1.28001217401827	8.70250032011747	0.74982440735137
C	9.14391693985691	13.96235640587506	-1.84730493747361
C	9.87163598135219	13.50618437590778	-0.58917515835728
H	1.69602308030079	7.23264662098716	2.27777472705346
H	1.83498911614754	8.92018185691121	2.82631214304363
H	1.34179134134701	7.93222785352191	-0.03692973079791
H	0.21470299911970	8.83909351199427	1.00303206098343
H	9.46285796529635	14.98497144721923	-2.11144662561777
H	9.40983309007306	13.30232992584893	-2.68983829733680
H	10.95185518157718	13.42167120200454	-0.79760239244791
H	9.74145997731655	14.25642624168625	0.20838175797806

Structure of BS-optimized antiferromagnetic *o*-$C_6H_4(NHC(O)NHEt)_2$•$[L_2Fe_2Se_2]^{2-}$ (L = $[CH_2(CH_2NC(O)O^tBu)_2]^{2-}$).

Fe	7.16564914906626	10.02860681689138	6.11915042782883

Fe	5.55285531763866	12.39749047109127	6.97358704389519
Se	7.01602852760821	12.15394660291112	5.02084138674098
Se	6.09176196669812	10.46298516652756	8.17006304726033
N	8.98061725455171	9.23978396983705	6.36854905512340
N	6.33373953184736	8.43482350159486	5.20670346572352
C	5.25386739774783	8.41390846294187	4.38778696546770
C	10.04346532478543	9.82951782763008	6.96345628300450
N	3.58533467373098	12.78211356212178	6.69677024942064
N	5.85230408430531	14.26412004365311	7.66180469774106
C	6.13267778782410	14.65252756979646	8.91838734838952
C	2.50072421863775	12.20819491384217	7.26393069853338
O	9.72799225308805	11.10050986358608	7.35354202184508
O	11.15591174176636	9.33015824067122	7.16117093597075
O	4.74651548637366	7.39805617291822	3.89883502074697
O	4.77155728252353	9.66630404399922	4.14244816359246
C	3.56175354474978	9.85616632286417	3.35655149269726
O	1.37688362231590	12.71665099056529	7.35253144077969
O	2.76374961101746	10.94711903111989	7.74168579889921
C	1.83017674898631	10.29090133380697	8.63473517016446
O	6.16021611543345	15.81084495921534	9.35066220290386
O	6.39859405364465	13.56614803733223	9.72341515769553
C	3.37467987062229	11.37447702763855	3.35972158198426
C	2.37009670557003	9.17268919661216	4.04292218163813
C	3.76040616751555	9.34522674820393	1.92188236871355
C	0.52109628941053	9.94678782391226	7.90597406488611
C	2.56581086155194	9.00865569700180	9.03821117709643
C	1.56666484805073	11.16427447252050	9.87191827974441
C	3.25738559605982	14.11166832480235	6.15724565632059
C	5.40548886541548	15.35846094909058	6.79041222570938
C	4.48971188540119	14.86642204092103	5.66774330172854
H	6.26846673064766	15.88433367748034	6.34311464577429
H	4.87362656627647	16.10323238209378	7.40679220747821
H	5.05336915739359	14.23354624826020	4.96092131123759
H	4.15383396894727	15.74969227377751	5.09670213247615
H	2.73481582128216	14.70659990687066	6.92899861461416
H	2.53627080857633	14.00086867413535	5.32548272783318
C	6.78294648143703	7.07059679682772	5.50382579654603
C	9.16962669151228	7.81918693462253	6.07818918416144
C	7.94020303189799	7.00852124728644	6.49261620547817
H	10.06222604944255	7.47528643535835	6.62327294868566
H	9.37212693441439	7.65808265710569	4.99976012249199
H	7.61311453268626	7.35683242763035	7.48819223695192
H	8.22574785148818	5.94599313018199	6.59934924087240
H	7.08497043304047	6.57120120953789	4.56222248108931
H	5.93321602050205	6.47819025067313	5.89017429160029
H	0.94888189777274	10.61012649509207	10.59894775560023
H	1.04744120768831	12.08773752444735	9.58339013162352
H	2.52035885874295	11.42728312025663	10.35587577790359
H	0.73180753167241	9.31061716044104	7.03243679170550
H	0.02584984043674	10.86592961702024	7.56796004765293
H	-0.14917022590828	9.38993136298748	8.58352775799694

H	2.79631517290047	8.40347375415754	8.14925949512952
H	1.94155246116175	8.41330531849050	9.72547890630097
H	3.51822664651424	9.25268014467096	9.53040147226373
H	2.46465398751680	11.64352363189299	2.79860301202772
H	4.24008669404742	11.86630915955524	2.89237461809481
H	3.29023990245276	11.74531691038750	4.39113200214201
H	2.87287563995326	9.59380196257729	1.31560907229469
H	3.91289957749208	8.25843790237569	1.91842626166610
H	4.63505919657732	9.83392408105362	1.46575822403900
H	1.43709792296705	9.43509332079748	3.51605946025922
H	2.29417176419368	9.52480863793175	5.08261112923302
H	2.49736908821420	8.08212751544855	4.03861340043113
C	6.33670614527068	13.67557642178661	11.16487301861609
C	10.64474045192699	11.88636731628336	8.15699007848285
C	10.98949535076943	11.15187626970808	9.46231690817622
C	9.83559387779787	13.14743322408755	8.46284482402905
C	11.90169223205670	12.22514106103220	7.34302189020451
C	4.96469675934899	14.21642029936365	11.59494040696230
C	7.48589162154471	14.54604404407820	11.69419471433259
C	6.49655883744612	12.22582565658906	11.63379275908735
H	7.38363156381195	15.57103464091797	11.31510226004515
H	8.45107807585328	14.13653707011311	11.35722702630418
H	7.47889437826480	14.55391831614004	12.79795063763273
H	5.70781223592327	11.59677750100113	11.19727049515321
H	6.43717416662474	12.17154247903284	12.73381854734411
H	7.46407264430316	11.81881330298745	11.30449571794906
H	4.83805892205077	15.25468371183622	11.25984577298840
H	4.86884628533397	14.17170006705816	12.69307173956656
H	4.16758249863047	13.59971235082003	11.15105946627517
H	10.06319872397685	10.89140049320246	9.99821069265929
H	11.59252783929199	11.81048723848139	10.10997169147234
H	11.55080670693453	10.23275530374398	9.25071852799120
H	8.90107012857595	12.89045681970113	8.97975816960536
H	9.57021796078618	13.65855478396302	7.52791958370843
H	10.42192338860736	13.83721839713714	9.09153337032148
H	12.44768388519996	11.30698604276816	7.08886296903864
H	12.55907510554424	12.89427824631229	7.92370327697265
H	11.61602052657030	12.74208083749697	6.41368474245378
C	8.39070831495633	15.14718093149837	1.91314619520049
C	8.40926631405233	13.96110800658382	1.12143885785655
C	8.37556286563066	16.39734382756118	1.27166459650541
C	8.39108387596745	16.49368972638133	-0.12125439828621
C	8.40504177147802	15.33200786851720	-0.89621076315238
C	8.40861198608871	14.07930788055426	-0.28040187584388
H	8.43942433663617	13.16240343852374	-0.86470279724892
H	8.37838671620232	17.28642665957701	1.89836905204617
H	8.38506794169664	17.48042966818869	-0.59322364948463
H	8.41035728203508	15.39105705188301	-1.98863152565181
N	8.38544267875495	15.04733949836260	3.31745053047001
N	8.42288272270879	12.71025104762332	1.75441183764594
C	8.71642496566446	11.47131319757610	1.18726119680167

N	8.57303015438033	10.44019530009821	2.07585471020507
C	8.86516789126376	9.07379200140025	1.67576195717828
C	7.66623736143950	8.32365789790651	1.09033030765382
H	9.25534930374344	8.54196387269512	2.55779241241284
H	9.66895823193406	9.13078959502672	0.92744339108809
H	6.86930413912237	8.18542348169461	1.83567839823083
H	7.97893198083428	7.32524302442805	0.73801440401759
H	7.25640732507623	8.87773758998980	0.23191401596344
O	9.09437219348097	11.30562719500441	0.02856315907652
C	8.83625322213495	16.00559871072450	4.22151673769007
O	9.26497664771566	17.11551484685320	3.90986976313714
N	8.76888239109429	15.58895652214574	5.52438454207330
C	9.01045191682475	16.54034061941269	6.60283151983905
C	10.49697201651542	16.76660299612877	6.88550721379414
H	8.49140998320216	16.16316070904890	7.49575204552648
H	8.54387128673871	17.49989321958622	6.32614124255125
H	10.98978896022061	15.83127422561648	7.19135750210129
H	10.62633516875998	17.50542630602517	7.69485720523670
H	10.99262268446902	17.14923006496440	5.98133980944734
H	8.13518224676475	10.60790610613351	2.97820926039179
H	8.15565838068026	12.66953619401983	2.73482278557126
H	7.96906413441157	14.22158780182414	3.74559863139225
H	8.34180526699674	14.69374896375338	5.74323406528923

Structure of BS-optimized antiferromagnetic *o*-$C_6H_4(NHC(O)NHEt)_2$•$[L_2Fe_2Se_2]^{3-}$ (L = $[CH_2(CH_2NC(O)O^tBu)_2]^{2-}$).

Fe	7.27602065934043	9.98394104213557	6.00079491208917
Fe	5.51296569715786	12.36028134323499	7.02500633147768
Se	7.23959579547460	12.18397300594521	5.02786843999976
Se	6.01239931674700	10.14158101377615	7.96100218431548
N	9.12104354161310	9.11491685047375	6.31133537172667
N	6.55273503928536	8.39253989637111	4.87191882227237
C	5.48675197085959	8.41261495591607	4.05464464694052
C	10.16945486086916	9.67438453265396	6.93433000742495
N	3.45976966790455	12.86434126881168	6.87153109037481
N	5.77835769188396	14.34401911453491	7.62224091014310
C	6.02331252187312	14.73780559739650	8.86666846535773
C	2.40670073193773	12.42578434984542	7.55681293677536
O	9.87638251925907	10.95982527881679	7.31915196884714
O	11.27389648243174	9.15580825882064	7.17533471071429
O	4.98220672808385	7.43455926222604	3.47394451433085
O	4.98525608759156	9.67946744754678	3.90509245214665
C	3.74504103692755	9.91933695694500	3.20312998692555
O	1.21741771997637	12.78138593086052	7.44969290364171
O	2.77777517745081	11.48257129158385	8.51420587843479
C	1.79080425076054	10.73192857509105	9.23458268937991
O	5.85538515451087	15.85981729581945	9.37913547107577
O	6.55514533614521	13.68482554543534	9.62148468900332
C	3.54398781542240	11.42818243768301	3.35660009093400
C	2.58853524149667	9.16174366573420	3.87472462070406
C	3.87647618634056	9.54061170975706	1.71901381562498

C	0.89966388105180	9.93235976831377	8.26921317063768
C	2.63047353900451	9.77618342526326	10.09166526937231
C	0.94424968340876	11.65028406287807	10.13704605948966
C	3.13689930121496	14.03090335933948	6.04706836151947
C	5.19963263239824	15.38312807393820	6.76886854189539
C	4.39667962153359	14.77969642820096	5.61302320024185
H	5.99385465369014	16.03093437874030	6.34681275884092
H	4.55461495672163	16.04702316739878	7.37520770355751
H	5.04955847857695	14.10195788861427	5.03276482421010
H	4.10032061943951	15.59552994425177	4.92747033370342
H	2.47341566516494	14.71481883638192	6.61194976446153
H	2.55865676552635	13.73459855990817	5.14753614086941
C	7.01250549235805	7.02299101248337	5.09729656538936
C	9.31384511443814	7.70049177204613	6.01295092214400
C	8.02649710883249	6.90519250898571	6.22841456351964
H	10.11652162846257	7.31299733562472	6.66262918123280
H	9.66392009101403	7.55126044647756	4.96776094832379
H	7.56746303441972	7.23170748630169	7.17824927038008
H	8.28225371314883	5.83306012859900	6.33652879208864
H	7.46226420365586	6.60932308681156	4.16880581070435
H	6.14306369677713	6.37364439659749	5.31257865630822
H	0.24810506825302	11.04841326083016	10.75024834704619
H	0.38502096760705	12.36028981565624	9.51364337755711
H	1.60285776800750	12.21649395761788	10.81565246154171
H	1.52837766431735	9.28983256190106	7.63302988481417
H	0.33298982061554	10.62365128895692	7.63059901957984
H	0.20017249469842	9.29159088348465	8.83631551042688
H	3.28866837730032	9.17376115719929	9.44813548120167
H	1.97594853601648	9.11348564620659	10.68611126499927
H	3.27437042821397	10.34960200801361	10.77617460285629
H	2.60920246384238	11.74235710583312	2.86172009431228
H	4.38959655353156	11.97191867373168	2.91134643493128
H	3.49839050683523	11.69427523197300	4.42211531291286
H	2.97390519159163	9.86270083659517	1.16991377559623
H	4.00743611610170	8.45562690932738	1.61373150183378
H	4.74787243623054	10.05066843494581	1.27985299826921
H	1.63376415917720	9.43356525965060	3.39117938124694
H	2.53060351337488	9.44167102756245	4.93774016506974
H	2.74665636481654	8.07771576404447	3.79380398039983
C	6.27506145783362	13.60112519508636	11.02961439074799
C	10.77343003653365	11.71337271695965	8.15801072126491
C	11.02656120702897	10.97294193292828	9.48251755679680
C	10.00464392919100	13.01178901044189	8.41429728458172
C	12.08786872830974	12.00140974363672	7.41326652378587
C	4.76505157104528	13.73779115162779	11.28287334918569
C	7.07179122982095	14.66673874460133	11.80245712561012
C	6.73890050801034	12.18977022842990	11.40819564193110
H	6.76000826445811	15.66349680695091	11.46267766806106
H	8.14896473576932	14.54521741452948	11.60016164094863
H	6.90747826650912	14.56357669632615	12.89122310747212
H	6.23288928984392	11.44605657799969	10.77448961438427

H	6.52171377381567	11.98604453600307	12.47202829480595
H	7.82222384920880	12.08385915223590	11.24134602344001
H	4.42782868041926	14.75309986741208	11.02958687183099
H	4.53414581715652	13.52994548165296	12.34309225622532
H	4.22051682703915	13.01838318669292	10.65312299504895
H	10.06441400868070	10.75940817094441	9.97376056247064
H	11.63286262831096	11.60314534344977	10.15704229419391
H	11.54902616204172	10.02609494074851	9.29067954059355
H	9.02615521396156	12.80614513481548	8.87030242036224
H	9.82216587419880	13.52803987187336	7.46197083818108
H	10.58380796697717	13.67594373419912	9.07882426345916
H	12.60418841095272	11.05833939253111	7.18907098311038
H	12.74016954734863	12.64797079451459	8.02693518761993
H	11.86951755001066	12.52493440911818	6.46920181204809
C	8.40316366081624	15.12467854842748	1.90012493104718
C	8.28054321516527	13.94965559674189	1.09352677817870
C	8.49529858337393	16.37767702799217	1.26401797663163
C	8.49202711303070	16.48381924283987	-0.12936847347538
C	8.39126208812663	15.33503138676494	-0.91742082439319
C	8.28028052317569	14.08303439049811	-0.30660922560285
H	8.21552400953173	13.16987639434727	-0.89495738549359
H	8.59513208038484	17.25328850187126	1.90193105837958
H	8.57031579082858	17.47346570153761	-0.59173932048462
H	8.39027739157512	15.40401531194572	-2.01026944937862
N	8.42985424938275	14.99649084689623	3.29200579812784
N	8.16467189679207	12.69808588362916	1.70786578400688
C	8.52048086585169	11.46469290357608	1.16424617401868
N	8.33185853428183	10.43823109323801	2.04038888895636
C	8.77556584644451	9.09587412426808	1.71179337528290
C	7.73328874792317	8.26403096918337	0.96010545682983
H	9.04533065641725	8.60045737263654	2.65636348709142
H	9.68518166686121	9.18868687819121	1.09682235819502
H	6.84780467470142	8.06894117701211	1.58262674471444
H	8.16558840730039	7.29038424142220	0.66557194548196
H	7.42165076644356	8.79314597368415	0.04576739877149
O	8.97177522077812	11.30582540851505	0.02612371590077
C	8.75408732817016	15.96884858655683	4.23522807842374
O	9.06801611680937	17.13289154515210	3.96864846464216
N	8.70525916750328	15.49358229528726	5.51483752256000
C	8.85014794436526	16.41029899876271	6.63538857071476
C	10.31083982228010	16.75088082239569	6.94768970878949
H	8.36125777210777	15.94415458479592	7.50186613115600
H	8.30441595482181	17.33985195444836	6.40283506999849
H	10.87664299954841	15.84825786392441	7.22469046365609
H	10.37027051314722	17.46567018787829	7.78752263154075
H	10.78322101840184	17.20929990202357	6.06563025865663
H	7.96445336533770	10.63414419955918	2.97509945999278
H	7.81833010598268	12.64496158256768	2.67529353200950
H	8.18571189006973	14.08951685183785	3.70265263635892
H	8.30971493507847	14.56447889578026	5.68353896640771

Structure of BS-optimized antiferromagnetic *o*-$C_6H_4(NHC(O)NHEt)_2$•$[L_2Fe_2Se_2]^{4-}$ (L = $[CH_2(CH_2NC(O)O^tBu)_2]^{2-}$).

Fe	7.21687886983182	10.01565369961463	6.14340800161670
Fe	5.50520770024438	12.48240844379236	7.13069076888840
Se	7.18469820178559	12.35570924554888	5.09718153139702
Se	5.88454001191670	10.29099881836304	8.15807163683164
N	9.10174410224110	9.01543564644381	6.36984596694541
N	6.43427916627563	8.35709891745273	4.96967893825953
C	5.44574343230977	8.36076243837603	4.07813919904338
C	10.21291635933762	9.52297077240200	6.89592170664264
N	3.38619771974558	13.03431791466872	6.94652076817122
N	5.69918889044531	14.52193411423686	7.81018147476291
C	6.04104826417623	14.91071417520359	9.02831938041293
C	2.30145470387607	12.58409031850115	7.55573123684578
O	10.04022888002640	10.86401636118308	7.19818800827095
O	11.30478732087993	8.95402483732506	7.13062571339604
O	4.94065694375817	7.37149170164461	3.49459219379827
O	4.99352085011912	9.63959564171443	3.80639700368984
C	3.81317640046407	9.86346589873642	3.02397402811130
O	1.10228050837858	12.88469692321420	7.34957272041602
O	2.62468572466431	11.69242632629594	8.58333471025855
C	1.64121815129947	10.82563032793429	9.14608360602047
O	5.79121398868444	15.98992407824432	9.60820115184916
O	6.82352321978492	13.94127027058754	9.67966153686570
C	3.63397209735175	11.38375590466735	3.08651494647852
C	2.59246980460197	9.16302088616583	3.64878198624431
C	4.02189817526005	9.40590942826834	1.56733230308970
C	0.95596003972452	9.98540059891378	8.05466889402195
C	2.45836590135605	9.91513503968166	10.07260453101786
C	0.60534073012942	11.63164526432955	9.95664993941275
C	3.10020611880810	14.14562648074078	6.04555460552993
C	4.98194260110558	15.55361402975813	7.05958883754920
C	4.34987922297325	14.98771618319902	5.78594322490851
H	5.67589678537379	16.37717899759643	6.78974348695373
H	4.20246986876183	16.02225066676776	7.69535872054226
H	5.10482602004587	14.38261140012118	5.25024760846210
H	4.07311281417439	15.82475104194827	5.11526627808534
H	2.30564151245591	14.78497826541294	6.48279330368181
H	2.69278032259547	13.78505548236008	5.07615720065238
C	6.83535819316250	6.98748257092655	5.27207677263773
C	9.18316455678008	7.57906708535848	6.14668851412971
C	7.83854052965139	6.89892003854542	6.41651863268715
H	9.96459085296093	7.15242665993278	6.80309810445928
H	9.50246331599745	7.34153927280928	5.10463772851285
H	7.39973341947220	7.34467191354665	7.32731689419764
H	8.01546405241810	5.82208330597853	6.62357968134896
H	7.27393129472640	6.49191137612735	4.37482486299768
H	5.94287822329239	6.37644030726945	5.52177687504846
H	-0.10955263298925	10.95520108669709	10.46487530541465
H	0.07558603664006	12.31442482766538	9.27796125733831
H	1.12750767841878	12.22849499057270	10.72334256763941

H	1.72018714239977	9.43335140026142	7.48614252569239
H	0.40941934208967	10.64909484971882	7.36994021356973
H	0.25556694034815	9.26026119648295	8.51071208167924
H	3.27139530953412	9.44257550286634	9.49812558661342
H	1.80954815468162	9.14790689113379	10.53645774556752
H	2.92830287535391	10.51422185437188	10.86878358392007
H	2.74930977625032	11.69396628846563	2.50142921692239
H	4.52854019185833	11.88626255585315	2.69129586271498
H	3.51612550919083	11.70521940315869	4.13081126994078
H	3.14874219866281	9.68739483854816	0.94889893550802
H	4.16457254999777	8.31697753377683	1.54217164746721
H	4.91562585098461	9.89479795645116	1.14884502196152
H	1.67593566773913	9.42940892061758	3.09011447171110
H	2.47304100362093	9.49309908296075	4.69218347943052
H	2.73927314206248	8.07422347258224	3.62916741309616
C	6.50687036593261	13.58826123182430	11.03420202960196
C	11.01068835295641	11.59948513027391	7.94549111726875
C	11.27424024102489	10.93453567128876	9.30976887271956
C	10.34295189766974	12.96524197687581	8.14053788350735
C	12.31354273110854	11.74628390416127	7.13642838651664
C	4.99595815781408	13.34833433071397	11.17827235602059
C	6.98990252730168	14.68987031303864	11.99922905951544
C	7.26991613456447	12.27939653327589	11.26280276412080
H	6.49026729559253	15.63344675354275	11.73809101307629
H	8.07941168670087	14.82818285898032	11.88903970709478
H	6.77760471077223	14.41199306871807	13.05013753256257
H	6.95532379624760	11.53333776195791	10.51155955654438
H	7.08015060324615	11.89309320535515	12.28187970619645
H	8.35345948226193	12.44755362532638	11.14684868818834
H	4.44688213213091	14.28870957852426	11.01806928699392
H	4.76024724422486	12.96280610394982	12.18749230382840
H	4.66564213520227	12.61460004580606	10.42735853130443
H	10.32051067011282	10.82363316336590	9.84856153676165
H	11.95269464375796	11.56105025904582	9.91852895830971
H	11.71649787599014	9.94045271630794	9.15508285122356
H	9.38817069008967	12.85829053248276	8.67476006603174
H	10.11497942588042	13.40674690236236	7.15973253256133
H	11.00612091701344	13.64362307738832	8.70740346963775
H	12.73320375983108	10.74876010152175	6.94484590258018
H	13.04575820700474	12.36851372355939	7.68492341199669
H	12.09221509579620	12.23553044902563	6.17431610856466
C	8.25317512249512	15.15322643059919	1.93682652658992
C	8.13504409014286	13.95414127087131	1.15673287959944
C	8.36967866874563	16.38835701453358	1.26772141607520
C	8.39580434968077	16.45865569947483	-0.12961401940198
C	8.30262205755957	15.28944816061235	-0.88947598292126
C	8.16885589202755	14.05341191312731	-0.24673325868626
H	8.11387165621103	13.12352601521166	-0.81056203480525
H	8.46704413662252	17.27691477048285	1.88931713375918
H	8.49103273226881	17.43619686982284	-0.61733246784746
H	8.32563999715473	15.32961953995621	-1.98496130380717

N	8.25634990815409	15.05315005821357	3.32426782539274
N	7.99234762378924	12.72787223318075	1.80297756848643
C	8.42669218024428	11.48741696811790	1.33402293916345
N	8.24160373411924	10.50328813032347	2.25338372875471
C	8.82954113109460	9.19037703449757	2.06789727915125
C	7.94987052793058	8.21957657837223	1.27475509406337
H	9.02637355326733	8.78455260247792	3.07098125990665
H	9.79390371995983	9.31884416191977	1.54616884606759
H	7.01839790287249	7.98942707139642	1.81266690813954
H	8.49145838769416	7.26923544287459	1.10866940469893
H	7.70370818673293	8.65397731834616	0.29222630140807
O	8.93598279867605	11.29758498317519	0.22062299886502
C	8.60413861451113	16.02666381466886	4.25744847873150
O	8.91274989655474	17.19594125968165	3.98388909054770
N	8.58217522670331	15.53728595291805	5.52825647424835
C	8.72005977221492	16.42579067825093	6.66613498510789
C	10.17556743331912	16.81260384719110	6.95689083027513
H	8.27531062801962	15.91029811757985	7.52868698722197
H	8.13473852451258	17.34314279454172	6.48100076395455
H	10.77673474621873	15.92262691012011	7.19862281229360
H	10.22885600875656	17.50783877346456	7.81490547776960
H	10.61170881513686	17.30870424756962	6.07574488040136
H	7.85802520013338	10.75407084519754	3.17583014649568
H	7.64396192835441	12.70487560373930	2.78574399499170
H	7.98458182117317	14.15054490140312	3.76241859130357
H	8.20831964645112	14.58318724331844	5.67719040994631

X-ray crystallographic, H-atom optimized structure of $[Et_4N]_4[Fe_2Se_2(SPh)_4]^{2+}$.

Fe	11.32645219418401	8.94817170756782	8.92943056485124
Fe	11.32547125738002	6.86488977335226	7.06598242767772
Se	11.32987632938147	6.66289942680146	9.38333182001034
Se	11.33156711730488	9.15015668688780	6.61208216525857
S	9.39987932886465	9.78786895154927	9.85296315980213
S	13.16662204484474	10.04823268932299	9.80215335184034
C	9.10189729276102	11.40567937781782	9.22101074836823
C	10.06895880162531	12.17203483628340	8.55564747080704
C	9.77428191790141	13.42772786304022	8.02609139344542
C	8.42876353674191	13.91711266694492	8.16189988514383
C	7.50491999311683	13.16338248936645	8.81926709673064
C	7.79254272562295	11.91718323384360	9.34402202170921
C	13.04827824521372	10.06577728747713	11.56810028419170
C	13.95618548622800	10.95240635548363	12.26877554989363
C	13.92609746798770	11.03470454534027	13.65721878805639
C	13.03130497110020	10.20506059346610	14.37379238406931
C	12.17543769120878	9.32631408230394	13.71630219743829
C	12.18701871503231	9.26298532844736	12.30545617866055
S	9.39814477463015	6.02736573010502	6.14204899535273
S	13.16458079972540	5.76275406056003	6.19364231761421
C	9.09820692221441	4.40989246993741	6.77393922018841
C	13.04658464031194	5.74534273452940	4.42767080473513
C	10.06426510381214	3.64244692771713	7.43950356654521

C	7.78830194264650	3.89987560846845	6.65065551854704
C	13.95363710393073	4.85769022004794	3.72718431043540
C	12.18638444133010	6.54909541274735	3.69013586505525
C	9.76806207517564	2.38708709354873	7.96899818265715
C	7.49916476866169	2.65399159198899	7.17535044677397
C	13.92374512276740	4.77542584801117	2.33872482505796
C	12.17502548350602	6.48578960440889	2.27928747104039
C	8.42202090145866	1.89922005946235	7.83290973613104
C	13.03003792801375	5.60607834060475	1.62197521405424
N	6.99720303927728	9.70200960894599	4.54043705075864
C	5.56662861020238	9.40236148693911	4.20599159261626
C	5.11105273197922	9.78838627572611	2.79667718109263
C	7.97326307746163	9.13847346088766	3.50562346595460
C	7.68141643117082	7.62215150079357	3.13616005826407
C	7.16826689447944	11.21522316955212	4.53559806788229
C	8.54248517000703	11.69043948015822	5.01559998348733
C	7.31773277338513	9.10099870338381	5.90015694727487
C	6.50744261849553	9.61542662075690	7.05496999748810
N	15.81620161540256	9.69703659213528	4.54135434272608
C	14.38562719451071	9.39738849868430	4.20690880967195
C	13.93005138281663	9.78341332376902	2.79759438455040
C	16.79226162624087	9.13350047743678	3.50654070889375
C	16.50041496112928	7.61717851744615	3.13707730375249
C	15.98726541797596	11.21025016161187	4.53651531309242
C	17.36148368754597	11.68546650278882	5.01651722809008
C	16.13673133685727	9.09602570015561	5.90107421578792
C	15.32644117379626	9.61045361595961	7.05588725248238
N	6.99446179858778	6.11593537005920	11.45407518806273
C	5.56415668943923	6.41719667261629	11.78822318063860
C	5.10785268282454	6.03168604565786	13.19744276571213
C	7.97094147517116	6.67837048550535	12.48909188122494
C	7.68072816787658	8.19501066524781	12.85849470056077
C	7.16381794031654	4.60252984514941	11.45894959484440
C	8.53759921079008	4.12576393848452	10.97923349482740
C	7.31595197857393	6.71658423996311	10.09442207635117
C	6.50532242685867	6.20307035268104	8.93944044239892
N	15.81346035616296	6.11096238034717	11.45499241814720
C	14.38315524797734	6.41222371141693	11.78914039670535
C	13.92685122115148	6.02671309452634	13.19835998056772
C	16.78994001825383	6.67339746424780	12.49000913205072
C	16.49972677849831	8.19003764522960	12.85941199572753
C	15.98281644493956	4.59755684891323	11.45986686431171
C	17.35659771443479	4.12079091648058	10.98015077014973
C	16.13495053183801	6.71161123717865	10.09533931994130
C	15.32432095780303	6.19809734989296	8.94035769173660
H	6.71570280952832	8.31646219541028	13.36421386247615
H	7.72992147456498	8.83707567363015	11.96923745493078
H	8.47731000377798	8.50940165290441	13.54750384158149
H	8.96974375764347	6.58153351000212	12.05046812459749
H	7.89434194538816	6.04063267508705	13.37593688016528
H	7.73889645941984	6.97646974111251	4.02233589706411

H	8.47215217729355	7.31035168163672	2.43917377529257
H	6.71300564663507	7.50199921645586	2.63652219692027
H	7.89806262909141	9.77582358848697	2.61829741625601
H	8.97199892887326	9.23424418403199	3.94475073905375
H	17.79335482402504	9.23658372100772	3.93496002366633
H	16.70672710893037	9.76669838267062	2.61660915807093
H	16.52663733401593	6.97280506961745	4.02538756837594
H	17.29818457368243	7.29636666943097	2.45337394241210
H	15.53637912134822	7.49566515919432	2.62931023860081
H	17.79120217016076	6.56899132585102	12.06228002010003
H	16.70269614653643	6.04036584745538	13.37976304303786
H	16.53403140981720	8.83524278857029	11.97183764160185
H	17.29398749257627	8.50762056880354	13.54872565202223
H	15.53287342984903	8.31383472040747	13.36126052206962
H	7.02118277937308	4.48876957318367	6.14463706631421
H	11.07592239124701	4.04676223240440	7.52978185650651
H	10.52969176238187	1.80197572823117	8.48757551674341
H	6.47858624407526	2.27108810249263	7.06984231962287
H	8.15371727969415	0.92537525660931	8.24920807621720
H	14.63929550917372	4.24115224177955	4.31262355077506
H	14.59376622940542	4.09687282657546	1.80623185119172
H	13.01183965730338	5.55190823568300	0.52993319954652
H	11.08011080759496	11.76653021797162	8.46528428075603
H	6.48474029659093	13.54739581281834	8.92463163290640
H	7.02479160924615	11.32909425887202	9.85003325461097
H	10.53659226174931	14.01184280118794	7.50738226873972
H	8.16164098563079	14.89110729644093	7.74519321992754
H	12.86895176730394	6.31308670981481	13.27907253489871
H	14.47731043928388	6.56029029764151	13.98382037650280
H	13.99512597772271	4.94589793987019	13.38173488460979
H	14.64284085833615	11.56805783049925	11.68355127982165
H	13.01286317630006	10.25929807681730	15.46582966082944
H	14.59652373617516	11.71276143819787	14.18979131618550
H	11.49500767741374	8.68663942983374	14.28340384958563
H	11.51630675952542	8.57696315583629	11.78280576454844
H	11.51646915792199	7.23595799051188	4.21270872367919
H	11.49558726876957	7.12627575086973	1.71192353616796
H	5.43100082056571	8.32586511278430	4.37208556178765
H	4.96453723806647	9.93105812477916	4.95366403356763
H	5.70514643624547	9.30214341362561	2.01219194739731
H	5.12635309683892	10.87462926052711	2.63471319137507
H	4.07143300337424	9.44633886653920	2.69157467145279
H	6.37070619893573	11.62055726376052	5.16992820610675
H	6.98236082010463	11.53315970003456	3.50413458150749
H	8.72849090433388	11.45251700865419	6.07106461284050
H	8.56326863561590	12.78501175433984	4.91606605576554
H	9.36175552890789	11.28414927921394	4.40803566862717
H	8.38887744896240	9.28064394096691	6.06660487698493
H	7.19427898172780	8.01826583161746	5.77897646842845
H	6.56157330486313	10.70775148131811	7.15421618346557
H	6.95672848426797	9.19851347715132	7.96799816545677

H	5.45377353204743	9.30694579944072	7.01581065396339
H	14.24099331322291	8.32259756189808	4.37691410861368
H	13.78014705897935	9.92200721825316	4.95536182726644
H	14.47947829660528	9.24788448691128	2.01278404201075
H	14.00177314100980	10.86383725433018	2.61335199164287
H	12.87140754877473	9.49987839173372	2.71694622717951
H	15.18805233912355	11.61494257806483	5.16921383287112
H	15.80414421344857	11.52809443388242	3.50485038031870
H	17.52913381801268	11.46855983189009	6.08017358137883
H	17.39330938674976	12.77695265267616	4.88695504225476
H	18.18172229145943	11.25698411684992	4.42590727539083
H	17.20856575986003	9.27040543975516	6.05523786480046
H	15.98794717022676	8.01536235008520	5.77968671788486
H	15.41049801621813	10.69872007789732	7.18529307089441
H	15.72502324433310	9.14938347964993	7.96947211272109
H	14.26429864870483	9.33418561243186	6.99201051994971
H	4.96162407963932	5.88995551018128	11.03989646842544
H	5.43058891068729	7.49397428138186	11.62259656506073
H	5.11548940181016	4.94500038426121	13.35718885367894
H	4.07074674986822	6.38068820167192	13.30459128892152
H	5.70622173995044	6.51178286214759	13.98256442073084
H	6.97720731588567	4.28450258290806	12.49029613536418
H	6.36600564534246	4.19825698846573	10.82428133731008
H	9.35761414013759	4.53432024504745	11.58420715089849
H	8.72254502206928	4.35955515773337	9.92265886827358
H	8.55872581385210	3.03155501206566	11.08285538756883
H	7.19386442183174	7.79946188709317	10.21509282365182
H	8.38688559139037	6.53522489315483	9.92841338563002
H	5.45451022215749	6.52192764411073	8.97305783958037
H	6.54981113578871	5.10993395498927	8.84509855995456
H	6.96161652123448	6.61252412767901	8.02639943277498
H	13.77716331793964	5.88825627733931	11.04068460693370
H	14.23899058612563	7.48695918660369	11.61843106438089
H	15.79942354465332	4.27981808512329	12.49164344391030
H	15.18339948298270	4.19351642976832	10.82694808763027
H	18.17715879625589	4.54792312786350	11.57116396395521
H	17.52475215637529	4.33801005052416	9.91663237003115
H	17.38694053925878	3.02920008116102	11.10919081006514
H	15.98599533513631	7.79222116278888	10.21727565216211
H	17.20702007207444	6.53759744092606	9.94194748086638
H	14.26208784252238	6.47319444883706	9.00862110248752
H	15.40909060620191	5.11026082297816	8.80820063797246
H	15.71944974294940	6.66261621806059	8.02705100892457

Structure of selenocystine

Se	-0.86336116561576	-3.15192896821279	0.87365072174076
Se	0.78210309711509	-2.43809771689479	2.35307383285443
C	2.37319695190093	-2.32978005618402	1.18960780232719
C	2.76177164154988	-0.89348482187483	0.85326098063875
H	2.13275202497637	-2.90737228352551	0.28822267240264
H	3.17415391400163	-2.83143009012538	1.74572214906731

C	4.02840451887350	-0.88748179092421	0.00096691149037
C	-1.58703457107952	-1.53889182457224	0.01380345865214
C	-2.47505324508504	-0.65770360581799	0.91551048896868
H	-2.17986477154160	-1.98853841715504	-0.79802375365007
H	-0.75591687701167	-0.97316202080971	-0.42839222814377
C	-3.18317228194794	0.35552973477435	0.02290979341975
H	-3.24533611526204	-1.29886086630223	1.36960051548650
N	-1.78304551508187	0.07761147990066	1.97127198858023
N	1.66985941511230	-0.19786130705015	0.16304249906164
H	3.06132368961389	-0.38346299423971	1.79228357578325
O	4.83579037312674	-1.79759416099743	-0.04525261502803
O	4.17161434866322	0.27026281452692	-0.65725341262878
C	5.37991051376299	0.41634544233170	-1.44487696220518
H	6.25830117436492	0.37266077438381	-0.78775489947644
H	5.29750503828001	1.39922149315095	-1.92049899760973
H	5.43346173688477	-0.37792371541275	-2.20036081562722
O	-2.83250654033127	1.51373515766577	-0.10984279118977
O	-4.21518956376906	-0.19744592656668	-0.62673656537473
C	-4.92575847222947	0.66935610422435	-1.54706802634780
H	-4.22968384387256	1.07910901787069	-2.29020696097311
H	-5.40540623341975	1.48449441894549	-0.98946303961802
H	-5.67583582123326	0.03073303817691	-2.02471335601523
H	0.89428201596568	-0.12479580825980	0.82037307298398
H	1.95281624231159	0.75909233073195	-0.03792153077090
H	-1.22248862552789	0.81914143924171	1.55319394207459
H	-1.13705305349484	-0.54307687100000	2.45598154912658

References

1. Lipman, J. G., Experiments on the transformation and fixation of nitrogen by bacteria. *Rep. N. J. St. Agric. Exp. Stn.* **1903,** *1903*, 217–285.
2. Spatzal, T. Ph.D. Thesis, Universitaet Freiburg, Freiburg, Germany, 2012.
3. Wolle, D.; Kim, C.; Dean, D.; Howard, J. B., Ionic interactions in the nitrogenase complex. Properties of Fe-protein containing substitutions for Arg-100. *Journal of Biological Chemistry* **1992,** *267* (6), 3667-3673.
4. Yang, K.-Y.; Haynes, C. A.; Spatzal, T.; Rees, D. C.; Howard, J. B., Turnover-Dependent Inactivation of the Nitrogenase MoFe-Protein at High pH. *Biochemistry* **2014,** *53* (2), 333-343.
5. Perez, K. A. Ph.D. Thesis, California Institute of Technology, Pasadena, California, 2016.
6. Spatzal, T.; Perez, K. A.; Howard, J. B.; Rees, D. C., Catalysis-dependent selenium incorporation and migration in the nitrogenase active site iron-molybdenum cofactor. *eLife* **2015,** *4*, e11620.
7. Spatzal, T.; Perez, K. A.; Einsle, O.; Howard, J. B.; Rees, D. C., Ligand binding to the FeMo-cofactor: Structures of CO-bound and reactivated nitrogenase. *Science* **2014,** *345* (6204), 1620-1623.
8. Spatzal, T.; Aksoyoglu, M.; Zhang, L.; Andrade, S. L. A.; Schleicher, E.; Weber, S.; Rees, D. C.; Einsle, O., Evidence for Interstitial Carbon in Nitrogenase FeMo Cofactor. *Science* **2011,** *334* (6058), 940.
9. Yu, S. B.; Papaefthymiou, G. C.; Holm, R. H., Comprehensive iron-selenium-thiolate cluster chemistry. *Inorganic Chemistry* **1991,** *30* (18), 3476-3485.
10. Kabsch, W., Integration, scaling, space-group assignment and post-refinement. *Acta Crystallographica Section D* **2010,** *66* (2), 133-144.
11. Leslie, A., The integration of macromolecular diffraction data. *Acta Crystallographica Section D* **2006,** *62* (1), 48-57.
12. Winn, M. D.; Ballard, C. C.; Cowtan, K. D.; Dodson, E. J.; Emsley, P.; Evans, P. R.; Keegan, R. M.; Krissinel, E. B.; Leslie, A. G. W.; McCoy, A.; McNicholas, S. J.; Murshudov, G. N.; Pannu, N. S.; Potterton, E. A.; Powell, H. R.; Read, R. J.; Vagin, A.; Wilson, K. S., Overview of the CCP4 suite and current developments. *Acta Crystallographica Section D* **2011,** *67* (4), 235-242.
13. Emsley, P.; Lohkamp, B.; Scott, W. G.; Cowtan, K., Features and development of Coot. *Acta Crystallographica Section D* **2010,** *66* (4), 486-501.
14. Murshudov, G. N.; Vagin, A. A.; Dodson, E. J., Refinement of Macromolecular Structures by the Maximum-Likelihood Method. *Acta Crystallographica Section D* **1997,** *53* (3), 240-255.
15. Kleywegt, G. J.; Jones, T. A., xdlMAPMAN and xdlDATAMAN - Programs for Reformatting, Analysis and Manipulation of Biomacromolecular Electron-Density Maps and Reflection Data Sets. *Acta Crystallographica Section D* **1996,** *52* (4), 826-828.
16. Davis, L. C.; Henzl, M. T.; Burris, R. H.; Orme-Johnson, W. H., Iron-sulfur clusters in the molybdenum-iron protein component of nitrogenase. Electron paramagnetic resonance of the carbon monoxide inhibited state. *Biochemistry* **1979,** *18* (22), 4860-4869.
17. Kowalska, J. K.; Hahn, A. W.; Albers, A.; Schiewer, C. E.; Bjornsson, R.; Lima, F. A.; Meyer, F.; DeBeer, S., X-ray Absorption and Emission Spectroscopic Studies of [L2Fe2S2]n

Model Complexes: Implications for the Experimental Evaluation of Redox States in Iron–Sulfur Clusters. *Inorganic Chemistry* **2016,** *55* (9), 4485-4497.
18. Glaser, T.; Rose, K.; Shadle, S. E.; Hedman, B.; Hodgson, K. O.; Solomon, E. I., S K-edge X-ray Absorption Studies of Tetranuclear Iron−Sulfur Clusters: μ-Sulfide Bonding and Its Contribution to Electron Delocalization. *Journal of the American Chemical Society* **2001,** *123* (3), 442-454.